

**EVALUATION OF THE POTENTIAL OF MONOVALENT/DIVALENT SALTS
AND SURFACTANTS FOR IMPROVED OIL RECOVERY FROM
UNCONVENTIONAL LIQUID RESERVOIRS**

A Thesis

by

MANOJ KUMAR VALLURI

Submitted to the Office of Graduate and Professional Studies of
Texas A&M University
in partial fulfillment of the requirements for the degree of

MASTER OF SCIENCE

Chair of Committee,	David S. Schechter
Committee Members,	Hisham A. Nasr-El-Din
	Yuefeng Sun
Head of Department,	A. Daniel Hill

May 2016

Major Subject: Petroleum Engineering

Copyright 2016 Manoj Kumar Valluri

ABSTRACT

Wettability alteration to water-wet and interfacial tension (IFT) reduction were found to play a major role in determining the rate of penetration of imbibing fluids into low permeability and porosity rocks where capillary imbibition dominates and is favored by a water wet rock nature and moderate to high IFT values. This study aims to investigate the effect of brines containing monovalent sodium and divalent calcium ions as well as of three types of surfactants; anionic, nonionic and a complex nanofluid, on alteration of the wettability and oil-water IFT of an unconventional liquid reservoir (ULR) with ultra-low permeability and porosity values and improvement of the resulting oil recovery from imbibition.

Contact angle and IFT measurements were conducted on sidewall cored rock samples obtained from a liquid rich shale play in South Texas which were followed by zeta potential measurements to analyze the stability of aqueous films on the ULR rock surface and understand the observed contact angle trends. IFT was measured using the pendant drop technique using the oil obtained from the same well. Spontaneous imbibition experiments were conducted and monitored periodically for fluid penetration and oil recovery. Salt concentrations varied from 1 wt% to 15 wt% while surfactant concentrations examined were 0.2 gpt, 1 gpt and 2 gpt, where gpt stands for gallons per thousand gallons.

Experimental results suggest that both salts and surfactants were able to alter wettability of samples from intermediate-wet to water-wet. Zeta potential results for salts

suggest an optimum salinity where maximum water wetness is observed. Zeta potential results for surfactants validated the observed contact angle results as all the surfactants produced stable wetting films. Increasing surfactant concentration resulted in significant reduction of IFT, while increase in salt concentration lowered the crude oil/brine IFT marginally. Spontaneous imbibition suggests that wettability alteration is a more important factor than IFT reduction, as moderate to high IFT values favored imbibition in the ultra-low permeability rocks examined. This could be verified from the higher recoveries observed for sodium chloride and nonionic surfactant, both of which were able to alter wettability to water wet while producing high to moderate IFT values.

DEDICATION

This work is the product of many factors that played a key role in shaping my progress technically and professionally. Through this dedication, I would like to remember and thank my family who made countless sacrifices to impart the best education and provide for me as well as instill the noblest of values and principles that guide my actions. I also would like to dedicate this work to my friends at Texas A&M University who are my extended family and have supported me during tough times and being there whenever I needed them. Finally, I dedicate my work to the all the petroleum engineers who, despite the uncertainty and dynamism of the industry, sweat it on or off field to make lives of people better.

ACKNOWLEDGEMENTS

I would like to thank my advisor Dr. David Schechter, who placed his trust in me and provided an opportunity to be a part of cutting edge high profile research. I have always seen him as a constant source of inspiration and will always do. I thank him for supporting me financially as well as morally during tough times while inculcating a strong and independent work ethic. I would also like to thank Johannes Alvarez who has been a great friend and mentor guiding me at every step of my research. I also extend my gratitude to the members of Reservoir Technology group at ConocoPhillips who supported me during the course of this study.

I would also thank my committee members Dr. Nasr-El-Din and Dr. Sun, for being supportive and helping me whenever needed throughout the course of my research.

I would also like to thank my mates in RICH 801 for supporting and putting up with me during the good and bad times.

Finally, I thank the head of department Dr. Daniel Hill, faculty, student workers and staff of the Harold Vance Department of Petroleum Engineering for providing facilities that aided and fostered research of the highest order.

NOMENCLATURE

ASTM	American Society for Testing and Materials
cc	Cubic centimeters
CT	Computed tomography
Deg.	Degrees
DLVO	Derjaguin Landau Verwey and Overbeek theory
DSA	Drop Shape Analyzer
EIA	Energy Information Administration
°F	Degree Fahrenheit
g/mol	grams per mole
gpt	gallons per thousand gallons
IFT	Interfacial tension
mD	Millidarcies
nD	Nanodarcies
N_B	Bond number
N_B^{-1}	Inverse Bond number
mg	milligrams
mN/m	Milli-Newton per meter
mV	Millivolts
μL	Microliter
OOIP	Oil originally in place

TOC	Total organic carbon
TVD	True vertical depth
USBM	United States Bureau of Mines

TABLE OF CONTENTS

	Page
ABSTRACT	ii
DEDICATION	iv
ACKNOWLEDGEMENTS	v
NOMENCLATURE	vi
TABLE OF CONTENTS	viii
LIST OF FIGURES	xi
LIST OF TABLES	xvii
1. INTRODUCTION	1
1.1. Objectives of research and thesis overview	7
2. LITERATURE REVIEW	9
2.1. Wettability	9
2.1.1. Reservoir factors affecting wettability	10
2.1.1.1. Surface charge of the rock	10
2.1.1.2. Surface active agents in crude oil	11
2.1.1.3. Brine composition	12
2.1.1.4. Temperature	13
2.1.2. Wettability measurements	13
2.1.2.1. Contact angles	14
2.1.2.2. Amott-Harvey index	15
2.1.2.3. United States Bureau of Mines	17
2.1.3. Wettability trends in shale reservoirs	18
2.2. Wettability alteration for improved oil recovery	19
2.2.1. Surfactants	21
2.2.1.1. Introduction to surfactants	21
2.2.1.2. Reduction of interfacial tension	23
2.2.1.3. Wettability alteration by surfactants	24
2.2.1.3.1. Ion-pair formation	25
2.2.1.3.2. Adsorption	26
2.2.2. Effect of brine composition on wettability and interfacial tension	27
2.2.2.1. Impact of ions on interfacial tension of crude oil/brine systems	27

2.2.2.2.	Impact of ions on wettability	30
2.2.2.3.	Mechanisms of wettability change by monovalent/divalent ions	32
2.2.2.3.1.	Double layer expansion.....	34
2.2.2.3.2.	Multivalent ion exchange.....	36
2.2.2.4.	Impact of brine composition and salinity on shale rock wettability ...	37
2.3.	Spontaneous imbibition experiments in shale	37
2.3.1.	Imbibition and its types	38
2.3.1.1.	Factors affecting imbibition rate and recovery	39
2.3.2.	Imbibition experiments on shale samples	40
2.3.2.1.	Brine imbibition in shale.....	41
2.3.2.2.	Surfactant aided imbibition in shale.....	42
2.4.	Computed Tomography techniques for imbibition monitoring	43
2.4.1.	Theory of CT imaging.....	44
2.4.2.	Computed tomography for analysis of imbibition studies	46
3.	EXPERIMENTS	48
3.1.	Reservoir description.....	48
3.2.	Materials description	50
3.2.1.	Core samples	50
3.2.1.1.	Aging and preparation.....	51
3.2.2.	Oil sample	53
3.2.3.	Brines	56
3.2.4.	Surfactants.....	58
3.3.	Contact angle experiments	59
3.3.1.	Experimental setup.....	59
3.3.2.	Measurement method	60
3.3.3.	Measurement procedure	61
3.3.4.	Results and discussion.....	64
3.3.4.1.	Brine results	64
3.3.4.2.	Surfactant results.....	71
3.4.	Interfacial tension measurements	83
3.4.1.	Experimental setup.....	83
3.4.2.	Measurement method	84
3.4.3.	Measurement procedure	85
3.4.4.	Results and discussion.....	87
3.4.4.1.	Brine results	87
3.4.4.2.	Surfactant results.....	90
3.5.	Zeta potential measurements.....	93
3.5.1.	Experimental setup.....	94
3.5.2.	Measurement method	96
3.5.3.	Measurement procedure	97
3.5.4.	Results and discussion.....	101
3.5.4.1.	Brine results	101

3.5.4.2.	Surfactant results.....	105
3.6.	Spontaneous imbibition experiments	108
3.6.1.	Experimental setup.....	109
3.6.2.	Measurement method	111
3.6.3.	Measurement procedure	112
3.6.3.1.	Core sample preparation	113
3.6.3.2.	Amott cell setup	114
3.6.3.3.	CT scanning and data acquisition	116
3.6.4.	Results and discussion.....	117
3.6.4.1.	Impact of aging process	117
3.6.4.2.	Imbibition results	120
3.6.4.2.1.	Distilled water	120
3.6.4.2.2.	Brines	123
3.6.4.2.3.	Surfactants.....	132
4.	CONCLUSIONS AND RECOMMENDATIONS.....	139
4.1.	Conclusions	139
4.2.	Recommendations	142
	REFERENCES.....	144

LIST OF FIGURES

	Page
Figure 1. Horizontal and vertical well completions (Source: API, 2009).....	2
Figure 2. Fractured and non-fractured wellbores (Source: API, 2009).....	3
Figure 3. Crude oil production trends from major shale plays in the United States (Source: EIA).....	4
Figure 4. Natural gas production trends from major shale plays in the United States (Source: EIA).....	4
Figure 5. Cost per well drilled with progression of time (Fitzgerald, 2013).....	5
Figure 6. Contact angle measurement.....	14
Figure 7. Capillary pressure changes during Amott Harvey test (Waed Abdallah et al., Schlumberger, 2007).....	17
Figure 8. Structure and types of surfactants (nonionic, anionic, cationic, amphoteric)....	22
Figure 9. Forces at the interface between two immiscible fluids a and b.....	24
Figure 10. Wettability alteration by surfactants through ion-pair formation. The circles represent ionic heads of ionic surfactant while the squares denote the oppositely charged components of the surface active agents in crude oil (Salehi, Johnson and Liang, 2008).....	26
Figure 11. Wettability alteration by surfactants through adsorption. The circles represent ionic heads of ionic surfactant while the squares denote the oppositely charged components of the surface active agents in crude oil (Salehi, Johnson and Liang, 2008).....	27
Figure 12. Double Layer Expansion due to repulsive forces (black arrows) between rock/fluid and oil/fluid interface.....	35
Figure 13. Map of United States showing various shale gas and oil play locations (U.S. Energy Information Administration, updated May, 2011).....	48
Figure 14. Trends of hydrocarbon and reservoir properties across Eagle Ford (Bruce Matsutsuyu, 2011).....	49

Figure 15. Preserved core sample as received from the company.....	51
Figure 16. Trim samples as received from the company.....	51
Figure 17. Chips cut from core trims used for contact angle measurement.....	52
Figure 18. Aging of core chips in Eagle Ford oil.....	52
Figure 19. Core samples being aged in the Yamato DX 400 oven at 180°F.....	53
Figure 20. Gas chromatography results for the received oil sample.....	54
Figure 21. Oil sample received from well SW-1.....	55
Figure 22. Oil-water contrast.....	55
Figure 23. Anton Paar DM 4100 M density meter.....	56
Figure 24. Salts used for preparing brine solutions.....	57
Figure 25. Mettler Toledo MS weighing balance.....	57
Figure 26. Surfactants used in this study.....	59
Figure 27. Contact angle measurement apparatus (OCA 15 Pro).....	60
Figure 28. Cuvette and dispensing needle arrangement.....	63
Figure 29. Contact angle measurement using oil the captive bubble method.....	63
Figure 30. Contact angle results for S1-1 with NaCl brine.....	66
Figure 31. Contact angle results for S1-1 with CaCl ₂ brine.....	66
Figure 32. Contact angle results for S1-3 with NaCl brine.....	67
Figure 33. Contact angle results for S1-3 with CaCl ₂ brine.....	67
Figure 34. Comparison of the effect of sodium and calcium chloride on the wettability of S1-1.....	68
Figure 35. Comparison of the effect of sodium and calcium chloride on the wettability of S1-3.....	69

Figure 36. Changes in contact angle with increasing NaCl concentration for both samples.....	69
Figure 37. Changes in contact angle with increasing CaCl ₂ concentration for both samples.....	70
Figure 38. Contact angles for SW-1 with distilled water.....	73
Figure 39. Contact angles for S-1 with distilled water.....	73
Figure 40. Contact angle results for SW-1 with surfactant A1.....	74
Figure 41. Contact angle results for SW-1 with surfactant N1.....	75
Figure 42. Contact angle results for SW-1 with surfactant C1.....	75
Figure 43. Contact angle results for S-1 with surfactant A1.....	76
Figure 44. Contact angle results for S-1 with surfactant N1.....	76
Figure 45. Contact angle results for S-1 with surfactant C1.....	77
Figure 46. Contact angles with surfactants for SW-1 sample 1.....	77
Figure 47. Contact angle results with surfactants for SW-1 sample 2.....	78
Figure 48. Contact angle results with surfactants for SW-1 sample 3.....	78
Figure 49. Contact angle results with surfactants for SW-1 sample 4.....	79
Figure 50. Contact angle results with surfactants for S-1 sample 1.....	79
Figure 51. Contact angle results with surfactants for S-1 sample 2.....	80
Figure 52. Contact angle results with surfactants for S-1 sample 3.....	80
Figure 53. Contact angle results with surfactants for S-1 sample 4.....	81
Figure 54. Reduction in contact angle for SW-1 at 2 gpt surfactant concentration.....	82
Figure 55. Reduction in contact angle for S-1 at 2 gpt surfactant concentration.....	82
Figure 56. IFT measurement using the pendant drop technique.....	85

Figure 57. Variation in crude-brine IFT with increasing ion concentration.....	88
Figure 58. Crude oil – brine IFT results for various sodium salt concentrations.....	89
Figure 59. Crude oil - brine IFT for various calcium salt concentrations.....	89
Figure 60. Crude oil - aqueous phase IFT for various surfactants.....	91
Figure 61. Variation in crude oil - aqueous phase IFT with various surfactants.....	92
Figure 62. Reduction in crude oil - aqueous phase IFT with various surfactants.....	92
Figure 63. Electrical double layer showing various regions around a charged particle and corresponding electric potentials (Hunter, 2001).....	93
Figure 64. NanoBrook ZetaPALS machine for measuring zeta potential.....	95
Figure 65. Electrode used for measuring zeta potential.....	95
Figure 66. QSonica sonicator probe with controller.....	99
Figure 67. Crushed rock and triple filtered solution for zeta potential determination.....	101
Figure 68. Zeta potential results for S1-1 with various brine concentrations.....	102
Figure 69. Zeta potential results for S1-3 for varying brine concentrations.....	102
Figure 70. Zeta potential results for crude oil - brine system.....	103
Figure 71. Zeta potential results for S1-1 with various surfactants.....	105
Figure 72. Zeta potential results for S1-3 with various surfactants.....	106
Figure 73. Zeta potential results for the crude oil-surfactant system.....	106
Figure 74. Summary of surfactant tests.....	108
Figure 75. Summary of brine tests.....	108
Figure 76. Amott cell for spontaneous imbibition.....	109
Figure 77. Amott cells placed in the oven at a fixed temperature of 180°F.....	110
Figure 78. CT scanner with the Amott cell to be scanned.....	111

Figure 79. Release of air/gas bubbles during aging process.....	119
Figure 80. Contact angles measured before and after imbibition with water (values in the braces are the contact angles in degrees).....	121
Figure 81. Penetration curve for distilled water.....	122
Figure 82. CT scans for distilled water imbibition (color scale for CT number shown to the right).....	122
Figure 83. Oil recovery from distilled water imbibition.....	123
Figure 84. Contact angles measured before and after imbibition with sodium chloride (values in the braces are the contact angles in degrees).....	125
Figure 85. Contact angles measured before and after imbibition with calcium chloride (values in the braces are the contact angles in degrees).....	125
Figure 86. Penetration curves for brine and distilled water.....	126
Figure 87. CT scans for sodium chloride brine imbibition (color scale for CT number shown to the right).....	127
Figure 88. CT scans for calcium chloride brine imbibition (color scale for CT number shown to the right).....	127
Figure 89. Oil recovery for brine and distilled water from imbibition experiments.....	128
Figure 90. Oil recovered from sodium chloride (left) and calcium chloride (right) brine imbibition.....	129
Figure 91. Gas chromatograph of oil recovered from sodium chloride brine imbibition.....	130
Figure 92. Gas chromatograph of oil recovered from calcium chloride brine imbibition.....	130
Figure 93. Oil recovery curves for brine imbibition without dopant addition.....	132
Figure 94. Contact angles measured before and after imbibition with surfactant A1 (values in the braces are the contact angles in degrees).....	133
Figure 95. Contact angles measured before and after imbibition with surfactant N1 (values in the braces are the contact angles in degrees).....	134

Figure 96. Contact angles measured before and after imbibition with surfactant C1 (values in the braces are the contact angles in degrees).....	134
Figure 97. Penetration curves for surfactants and distilled water.....	135
Figure 98. CT scans for Surfactant A1 imbibition (color scale for CT number shown to the right).....	136
Figure 99. CT scans for Surfactant N1 imbibition (color scale for CT number shown to the right).....	136
Figure 100. CT scans for Surfactant C1 imbibition (color scale for CT number shown to the right).....	136
Figure 101. Oil recovery for surfactants and distilled water from imbibition experiments.....	137
Figure 102. Oil recovered from surfactant A1 (left), N1 (middle) and C1 (right) brine imbibition.....	138

LIST OF TABLES

	Page
Table 1. Gas chromatographic analysis of Eagle Ford oil sample	54
Table 2. Oil properties at room ambient and testing temperature and atmospheric pressure.....	56
Table 3. List of surfactants, composition and properties	58
Table 4. Properties of rock samples for brine experiments.....	64
Table 5. Contact angle results for brines with S1-1 and S1-3.....	65
Table 6. Rock sample details for surfactant tests	72
Table 7. Contact angle results for surfactants with SW-1 and S-1	72
Table 8. IFT results for oil-brine interface	87
Table 9. IFT results for oil-surfactant solution interface.....	91
Table 10. Properties of core samples used for spontaneous imbibition experiments	114
Table 11. Solutions prepared for spontaneous imbibition experiments	115
Table 12. Effect of aging process on core samples used for spontaneous imbibition....	118
Table 13. Initial oil saturations of the core samples prior to imbibition	119
Table 14. Results for imbibition test with distilled water	120
Table 15. Results for brine imbibition tests	124
Table 16. Results for surfactant imbibition tests.....	133

1. INTRODUCTION

The focus on unconventional resources for oil and gas production has grown rapidly over the past decade owing to the discovery of a large supply of oil and gas reserves in these formations. Unconventional formations refer to fine grained sedimentary rocks that are rich in organic content. Most of these rocks serve as source rocks to conventional reservoirs. Shale is one such unconventional resource that has been commercially exploited in the United States. Technical advances in drilling, hydraulic fracturing and horizontal well completions have led to the explorations of numerous shale plays in the United States. The shale plays are found at depth below 6000 feet (Nguyen, 2010) and vary in lithology based on their silica/carbonate/clay content. The major difference between these unconventional and conventional resources is the pore scale properties such as porosity and permeability, which are very low in the case of unconventional rocks. Porosity for shale rocks typically varies from 5% in plays like Barnett to 15% in Eagle Ford. Permeabilities are usually a few orders of magnitude lower than those of conventional plays. It is common to find permeabilities reported in the nano Darcy scale for most of these rocks. These ultra-low porosity and permeabilities render conventional stimulation and production techniques less useful. Hence developed were the concepts of hydraulic fracturing and horizontal completions designed to communicate with a large volume of the reservoir.

Hydraulic fracturing refers to the stimulation of a tight reservoir by creating pressure induced fractures through pumping a pre-designed fluid that came into operation

commercially in the late 1940s (Nguyen, 2010). The fluid typically has higher viscosity than water and is designed to transport a proppant that helps keep the induced fracture open for production. The fluid is pumped at a pressure higher than the fracture pressure of the formation rock as the direction and magnitude of the fracture depend on the in situ stress field in the rock. The pumping is usually done in two stages – a clean fluid/pad to create fractures followed by pumping a proppant to avoid closure of the fractures.

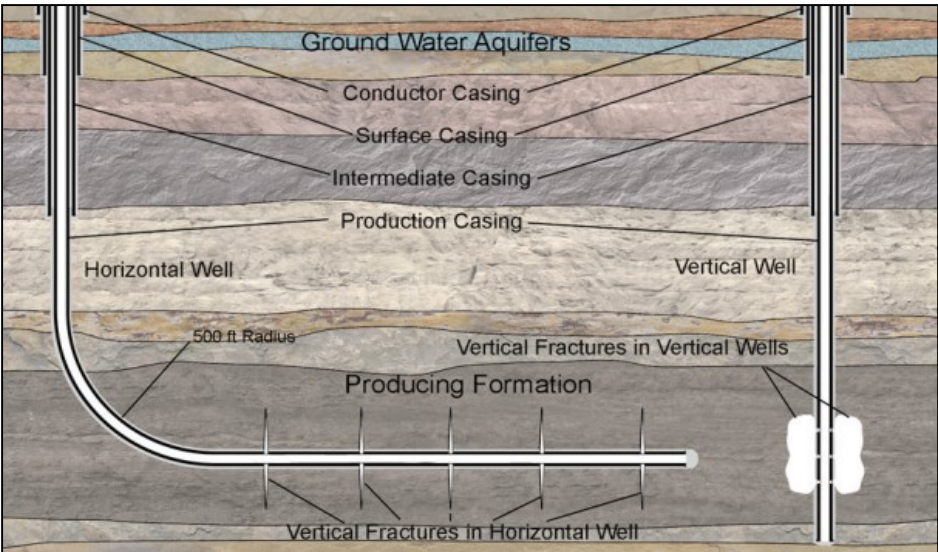


Figure 1. Horizontal and vertical well completions (Source: API, 2009)

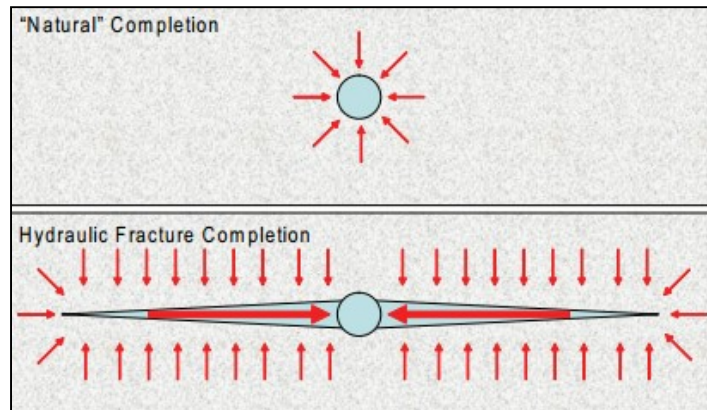


Figure 2. Fractured and non-fractured wellbores (Source: API, 2009)

The effect of hydraulic fracturing and horizontal well drilling on the oil and gas production can be observed from **Figures 3 and 4**. These graphs represent the production of crude oil and natural gas from the major shale plays across the United States. It can be clearly understood that the production has ramped up since 2009 with more wells being drilled. This shale boom led to production of almost 9 million barrels of oil per day, which was last met during the 1970s. However, the cost of these completions and treatments are also much higher compared to conventional techniques thereby demanding a complete economic evaluation before investing into these unconventional assets. For instance, the cost per a Bakken well is around 8 million USD out of which 1.5 – 2.5 million USD accounts for fracturing (Fitzgerald, 2013). The figure below pictorially represents the trend in cost per well drilled over the years.

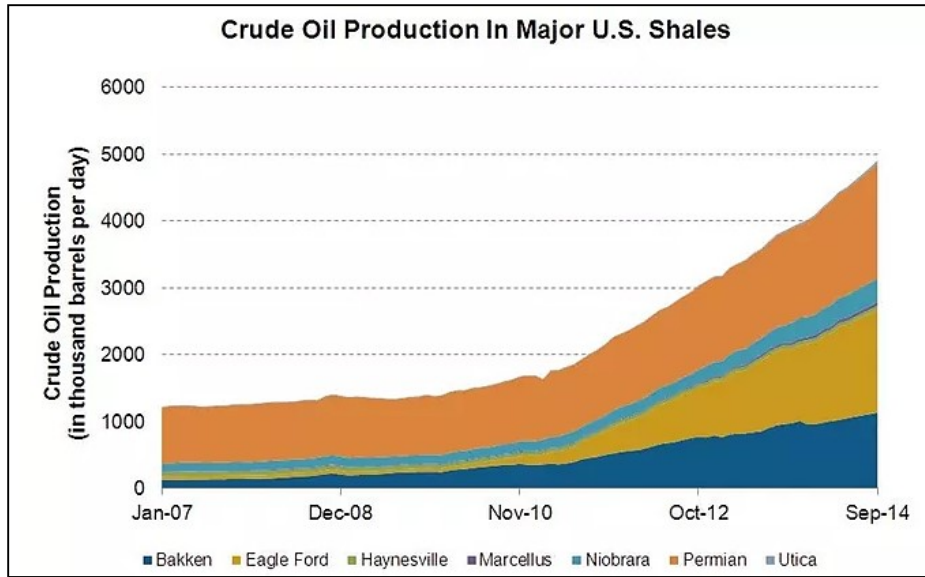


Figure 3. Crude oil production trends from major shale plays in the United States

(Source: EIA)

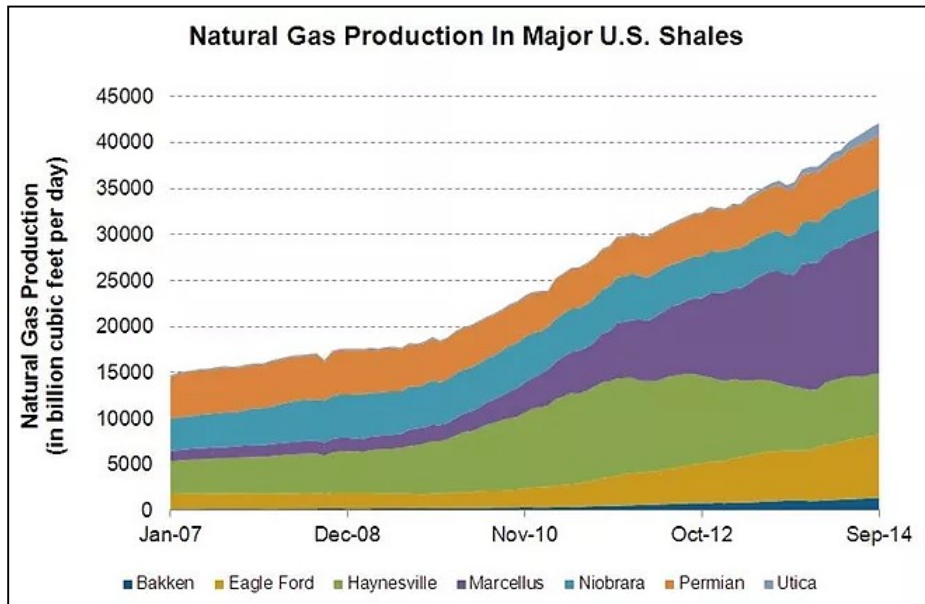


Figure 4. Natural gas production trends from major shale plays in the United States

(Source: EIA)

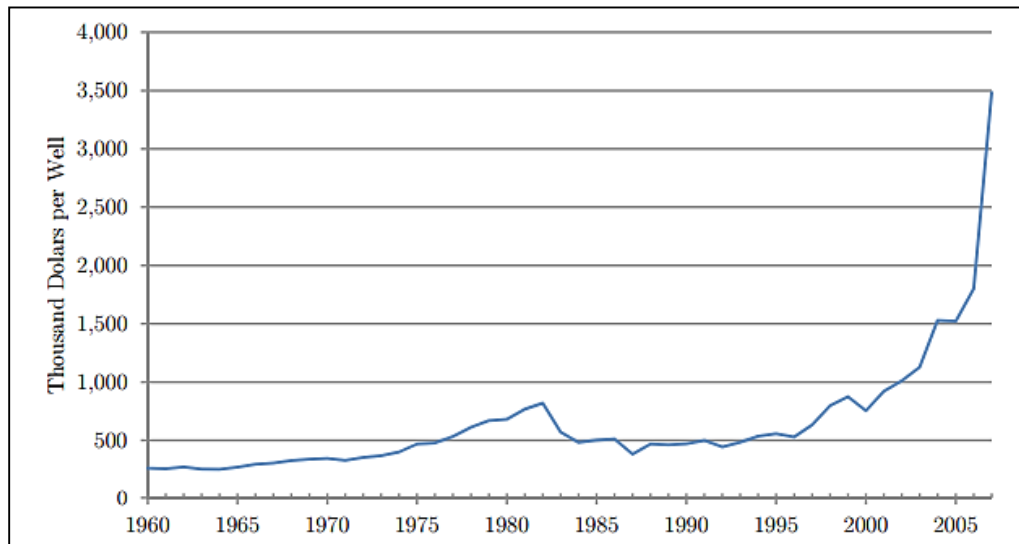


Figure 5. Cost per well drilled with progression of time (Fitzgerald, 2013)

Thus, maximizing the return on investment is a major economic attribute that decides the profitability from such huge investments. This requires optimizing the production per stage which leads to higher produced volumes per treatment. This forms the core of this study as it investigates the addition of salts and surfactants to stimulating fluids to improve oil recovery based on wettability alteration and reduction of oil-stimulating fluid interfacial tension, which were found to have a significant effect on the productivity from a tight rock matrix (Babadagli, 2003). Salts were previously examined for wettability alteration studies in sandstone and carbonate formations (AlShaikh and Mahadevan, 2014; Quan *et al*, 2012; Martavatlzi *et al*, 2012). Most of these studies aimed at evaluating the potential of low salinity waterflooding for enhanced oil recovery. Sodium chloride and calcium chloride are salts that are simple and economically available. Hence, these salts were chosen to be examined apart from the objective of understanding the

difference in interaction of monovalent and divalent ions with the shale rock surface with complex lithology.

In addition, the surfactants were also examined to analyze their ability in mobilizing trapped oil from these tight nanodarcy rocks. Surfactant flooding was found to have a positive effect on carbonate reservoirs in the West Texas basin which led to higher tertiary recovery by mobilizing trapped oil (Adams and Scheivelbein, 1987). Further studies on carbonate cores from the San Andres formation in the Permian Basin in Texas showed suggested that surfactant flooding is not always beneficial for improving oil recovery as its efficiency depends on rock mineralogy, porosity, permeability and pore heterogeneity (Weiss and Xie, 2007). Lohne and Fjelde (2012) have pointed out that the efficiency of a surfactant flood in heterogeneous formations depends on the IFT reduction in the pore throats which may be beneficial or detrimental to oil recovery. A more widely investigated effect of surfactant flooding is wettability alteration of the rock from a native oil/intermediate wet state to water wet state. Seethepalli, Adibhatla and Mohanty (2004) verified this effect on carbonate mineral surfaces and suggested that anionic surfactant has a better impact than cationic surfactants on these type of rocks. This makes the study of surfactants in tight unconventional reservoirs particularly interesting owing to the ability of the surfactants to mobilize oil and flow it through the nanoscale pores. This in conjunction with promoting a water wet state which leads to better imbibition of water based fracturing fluids and release of adsorbed oil drops is believed to improve oil recovery. Studies conducted on shale samples confirmed this as anionic and nonionic surfactant solutions were able to imbibe into the core samples and produce oil as opposed

to distilled water and brine that could not imbibe into the rock as effectively as surfactant solutions (Wang *et al*, 2011; Alvarez *et al*, 2014).

These studies serve as a starting point to understand the changes in wettability and IFT in tight unconventional rocks and their interplay in recovering higher volumes of liquid hydrocarbons, which is the objective of this study. Laboratory investigations were aimed at examining the effect of adding salts and surfactants to stimulating fluids by understanding the surface level changes with both types of fluids that impact wettability and thereby the imbibition of stimulating fluid into tight unconventional liquid reservoirs.

1.1. Objectives of research and thesis overview

The objective of this research study is to examine the potential of adding monovalent/divalent salt as well as three different types of surfactants by understanding their interaction with rock samples that are heterogeneous in lithological composition and the crude oil of the associated formation and tying these changes to the oil recovery from representative core samples. In a bigger scheme of things, the results of this study should help estimate the effect of adding various salts or surfactants to stimulating fluids and the interplay of associated changes in tight heterogeneous unconventional rocks. The objectives could specifically be listed into characterizing the following:

- Wettability alteration by monovalent sodium and divalent calcium ions as well as three types of surfactants (anionic, nonionic and complex) and their interaction with shale rock surface

- Interfacial tension changes at the crude oil – brine interface associated with the addition of salts and surfactants
- Imbibing fluid penetration into the matrix upon addition of salts and surfactants
- Interplay of wettability alteration and IFT reduction on oil recovery from ultra-low permeability rocks

This work has been divided into four major sections. The first section introduces the research by analyzing its importance, previous work and objectives in brief. The second section entails a detailed literature survey on wettability and its alteration for improved oil recovery, imbibition in shale and computed tomography for fluid penetration studies. Experiments conducted are dealt with in section three which includes the description of reservoir, rock and oil samples as well as the experimental setup, theory, procedure, results and their discussion associated with contact angle, IFT and zeta potential measurements as well as spontaneous imbibition. The fourth and final section concludes the work by analyzing the results and corresponding trends and providing recommendations based on experimental evidence in this study.

2. LITERATURE REVIEW

This section deals with literature survey conducted on the key concepts this focuses on as well as the experimentation methods adopted.

2.1. Wettability

Wettability can be defined as the tendency of one fluid to spread on or adhere to a solid surface in the presence of other immiscible fluids (Craig, 1971). A surface is said to be wet by a fluid when it is preferentially wet by that fluid when an immiscible mixture of two fluids interacts with the solid surface. A rock can be either water wet, oil wet or neutrally wet depends on the chemical and electrostatic nature of its surface. In a water wet state, majority of the rock is in contact with water, which also occupies small pore throats. In an oil wet case, this situation is reversed and oil is in contact with a major portion of the rock in addition to occupying small pores. The non-wetting phase usually occupies the central portion of larger pores, forming globules that extend to other pores (Anderson, 1986). In a neutrally wet state, the rock has no preference for the fluid in contact with it. In addition to these states, there is also a fractional wettability wherein the rock has oil wet as well as water wet portions. A water wet core saturated with oil imbibes water spontaneously while an oil wet core may not do so (Anderson, 1986). Similarly, the water present in an oil wet rock can be spontaneously displaced by immersing the rock in oil as the rock surface prefers to stay in contact with oil phase than the water phase. It is

important to understand that the rock is in contact with both wetting and non-wetting phases despite its preference to stay in contact with the wetting phase.

Historically, majority of the reservoirs were assumed to be water wet. However, later investigations suggested that majority of the carbonate reservoirs are predominantly oil wet (Treiber, Archer, Owens, 1972). Out of the 55 reservoirs examined their study, 27 percent were found to be water wet, 7 percent exhibited intermediate wettability while 66 percent were oil wet, which were majorly carbonate reservoirs. Contact angles were used to determine the wettability of the samples where 0° to 75° was considered water wet, 75° to 105° was considered intermediate wet and 105° to 180° was termed oil wet. The concept of contact angle shall be discussed in the upcoming sections. Thus, studying the wettability has since been an important aspect of reservoir characterization owing to its ability to affect flow of fluids through porous channels and the effect of pumped fluids on the formation.

2.1.1. Reservoir factors affecting wettability

2.1.1.1. Surface charge of the rock

Nature of the rock surface plays an important role in shaping the native state wettability of the rock. Sandstone rocks, in an unaltered state, tend to be negatively charged and are weakly acidic when in contact with water of neutral pH and attract basic compounds while carbonate rocks tend to be basic when in contact with water without any salinity and attract acidic compounds such as carboxylic acids from the crude (Somasundaran, 1975). This was illustrated by various experiments conducted (Morrow, Cram and McCaffery, 1973) on quartz, calcite and dolomitic surfaces with various basic

and acidic components derived from crude. Their results suggested that oxygen containing compounds gave higher contact angles on dolomite than quartz implying their ability to make carbonate surfaces more oil wet.

2.1.1.2. Surface active agents in crude oil

A rock can be oil wet either due to a depositional bitumen coating on the rock by crude oil or due to the adsorption of surface active agents present in oil. These surface active agents contain a polar component which adsorbs on the rock surface and a hydrocarbon part which is exposed to the bulk fluid phase in the pores. This exposed hydrocarbon component makes the surface oil wet (Anderson, 1986). Such surface active compounds include carboxylic acids (Seifert and Howells, 1969), asphaltenes (Johansen and Dunning, 1959), porphyrins and other high molecular weight aromatic compounds (Jennings, 1957). Further studies on the effect of various acidic and basic compounds on sandstone and carbonate rocks confirmed that not all surface active compounds are capable of altering the wettability of host rocks. Cuiec (1984) found out that sandstone wettability did not change despite using different acidic and basic solutions and test conditions. Similar effect was observed with limestone wherein no compound except octanoic acid was effect in transforming the surface from water-wet to oil-wet. It was also concluded that compounds with high molecular weight impacted the wetting nature of the rocks (Cuiec, 1984; Denekas, Mattax and Davis, 1960). However, the impact of these surface active agents largely applies to limestone type rocks as sandstone wettability remained unaltered in examinations conducted by Denekas, Mattax and Davis (1959), who

concluded that concentration of these surfactants may be key to altering sandstone wettability as opposed to limestone, which is sensitive to basic, nitrogenous surface active compounds.

2.1.1.3. Brine composition

Brine salinity and pH play a key role in shaping the surface charge of the rock, which affects the ability of a surfactant to interact with the surface. Positively charged surfaces attract anionic surfactants and vice versa. As Anderson (1986) noted, at low pH values, calcitic and siliceous surfaces are positively charged, while silica becomes negatively charged at pH values from 2 to 3.7 and calcite at pH values 8 to 9.5 (Somasundaran, 1975; Strumm and Morgan, 1970; Somasundaran, 1967). Thus it can be inferred that cationic surfactants have a greater effect in calcite surfaces at pH values higher than 9 than those below. The metal ions in brine can affect the solubility of surface active agents present in the crude oil, thereby promoting their adsorption on the rock surface promoting oil-wet nature. Brown and Neustader (1980) found out that multivalent ions such as Ca^{+2} and Mg^{+2} can promote oil wet nature on silica rocks by interacting with specific components of crude oil such as carboxylic acids. This effect was observed even at concentrations as low as 1 ppm. The possible explanation for the oil wetting enhancement of divalent ions is that these ions reduce the solubility of surface active compounds in crude and brine, which drives them to the rock surface where they are adsorbed, thereby promoting oil wetness. In addition to this, divalent ions can also act as bridging agents between rock and surfactants (Anderson 1986). Hence, altering the

composition of the brine that is in contact with the rock may alter the native state wettability, which would be dealt in later sections.

2.1.1.4. Temperature

The effect of temperature on wettability can be understood by measuring contact angles at various conditions. Earlier studies in this direction were conducted on calcite and quartz surfaces (Wang and Gupta, 1995) using corresponding crude oils which led to the conclusion that for a sandstone system, the contact angles increased with increasing pressure and temperature while for a carbonate system, the contact angles decreased with increasing temperature. They assumed contact angles less than 60° to indicate water wetness and angles greater than 120° to indicate oil wetness. The solubility of wettability altering compounds in crude oil increases with increasing temperature. Increasing temperature also reduces the interfacial tension of crude oil-brine system, thereby reducing the oil wet nature of the rock as it tends to be more soluble in the aqueous phase. However, this trend may not be consistent with all types of crude oil-brine systems as investigations by Wang and Gupta (1995) and Okasha and Abdul-Jalil (2010) reported an increase in IFT with increasing temperature. Thus the effect of temperature is not consistent and needs to be established for different each crude oil-brine system.

2.1.2. Wettability measurements

Major techniques for measuring the wettability of rock surfaces are:

- Contact angles
- Amott-Harvey Index

- United States Bureau of Mines

2.1.2.1. Contact angles

Contact angles measurement is the most widely used wettability characterization technique that includes placing an oil drop on the rock surface and measuring the angle at the interface. **Figure 6** illustrates contact angle of an oil droplet on a rock surface in the presence of water/brine. The angle “ θ_o ” is the contact angle with respect to oil in this case. It can be understood that the value of θ_o is smaller when the droplet has a near spherical shape and tends to increase as the droplet disperses or spreads on the rock surface. Hence, contact angles are smaller for water wet surfaces and larger for oil wet surfaces. However, as literature is based on contact angle with respect to water on rock surface, the measured value of θ_o needs to be subtracted from 180° to get the value of contact angle w.r.t water on rock surface, θ .

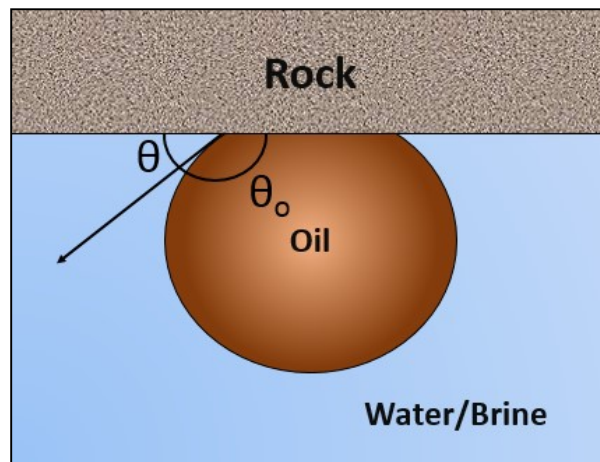


Figure 6. Contact angle measurement

Various methods to measure contact angles include tilting plate method, sessile or pendant drop method, vertical method, tensiometric method, cylinder method and capillary rise method (Wang and Gupta, 1995). Sessile or pendant drop method uses a microscopic optical system which is illuminated by artificial lighting and is a commonly employed technique to measure contact angles, which could be advancing or receding contact angles. Advancing contact angles are measured by advancing the tip of an oil droplet towards the rock surface and receding contact angles are measured by retreating the droplet away from it.

The choice of ranges of contact angles denoting water wet, intermediate wet and oil wet behavior hasn't been consistent as various researchers assumed different ranges for analysis. Treiber, Archer and Owens (1972) assumed water wetness from 0° to 75° , intermediate wetness from 75° to 105° and 105° to 180° to be indicative of oil wetness. Wang and Gupta (1995) used 0° to 60° , 60° to 120° and 120° to 180° for water, intermediate and oil wet nature respectively. Adejare, Nasralla and Nasr-El-Din (2012) considered angles below 70° to be water wet and those above 110° to be oil wet. Hence values around the range of 60° to 75° can be considered upper limit of water wetness and 105° to 120° can be considered the lower limit of oil wetness.

2.1.2.2. Amott-Harvey index

Amott Harvey index uses spontaneous and forced imbibition experiments on core samples to determine the wetting nature of the rock. A core with an initial oil saturation is placed in an Amott Harvey cell containing an imbibing fluid, usually a brine, and the

corresponding imbibed brine and expelled oil volumes are noted after a pre-determined period of time (greater than 10 days) (Abdallah *et al.*, 2007). The subsequent core with imbibed brine is forced to imbibe additional fluid by means of a coreflood or centrifuge and the corresponding volumes of brine and oil are measured. Similar process is followed with oil imbibing spontaneously and forcibly and the corresponding volumes are measured. The Amott Harvey indices are then calculated as follows:

$$I = I_w - I_o = \frac{S_2 - S_1}{S_4 - S_1} - \frac{S_4 - S_3}{S_4 - S_1} \text{ (Eq. 1)}$$

where

I – Amott Harvey wettability Index

I_w – Water Imbibition Index

I_o – Oil Imbibition Index

$S_2 - S_1$ = Volume of oil recovered by spontaneous imbibition

$S_4 - S_1$ = Total volume of oil recovered

$S_4 - S_3$ = Volume of water recovered by spontaneous imbibition

$S_4 - S_1$ = Total volume of water recovered

Saturation S_1 , S_2 , S_3 and S_4 correspond to the points as shown in **Figure 7**.

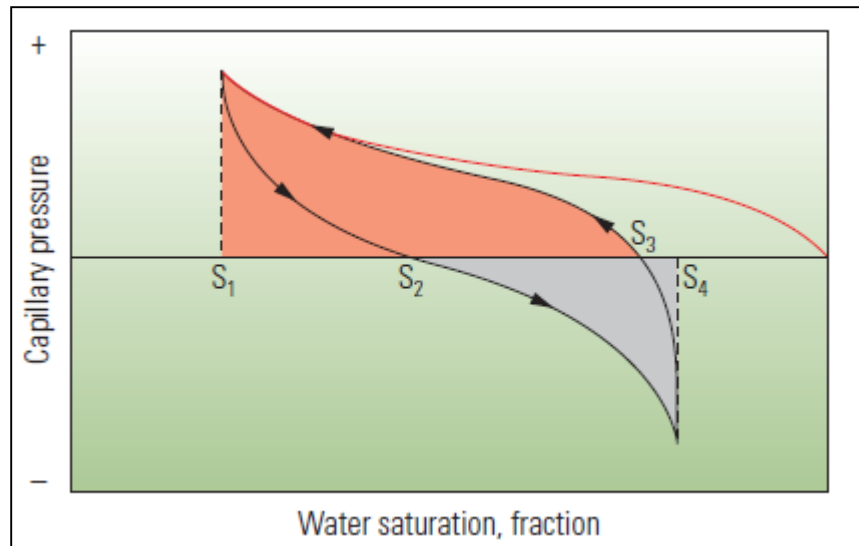


Figure 7. Capillary pressure changes during Amott Harvey test (Waed Abdallah et al., Schlumberger, 2007)

Amott Harvey indices vary between +1 and -1, the former corresponding to strong water wetness and the latter to strong oil wetness. The analysis can be further refined considering I values between 0.3 to 1 to be water wet, -0.3 to 0.3 to be neutrally wet and -0.3 to -1 being oil wet (Cuiec, 1984).

2.1.2.3. United States Bureau of Mines

A United States Bureau of Mines (USBM) test includes placing a core at residual water saturation and an initial oil saturation in a centrifuge containing water/brine and measuring the oil volumes at periods to construct the curve from S_1 to S_4 . The fluid in the centrifuge is then replaced with oil and curve from S_4 to S_1 is constructed. Plot areas

between the saturation curves and the zero capillary line, both above (A_1) and below (A_2), are calculated. USBM index is then calculated by:

$$I_{\text{USBM}} = \log \frac{A_1}{A_2} \text{ (Eq. 2)}$$

Though the measurement range is from $-\infty$ to $+\infty$, measurements usually range between +1 (water wet) to -1 (oil wet). Both Amott Harvey and USBM methods give a qualitative indication of wettability but are not as accurate as the contact angle technique. Amott Harvey method works better in the neutral wettability region than the USBM method (Glover, 2001) and is a widely accepted industry procedure while the contact angle technique requires pure fluids and artificial rock surface samples (Abe, 2005).

2.1.3. Wettability trends in shale reservoirs

Shale reservoirs constitute a major unconventional source of hydrocarbons that are characterized by low porosity and permeability values. Measuring the wettability of these reservoirs is fundamental to designing a hydro fracturing treatment. Traditional techniques for measuring wettability such as Amott Harvey test and USBM are difficult to characterize shale rocks due to their low permeability and porosity. Other techniques for characterizing wettability include quantitative methods such as Nuclear Magnetic Resonance (NMR), chromatographic techniques and qualitative methods such as interfacial tension, capillary pressure measurements (Thyne, 2013). Passey *et al.* estimated shale reservoirs to be water wet presuming they originated as organic rich mud deposits

in marine environments. However, the organic content plays a major role in this regard as it is predominantly oil wet, making the wettability characterization of shale complex. Mineralogy of the shale, especially the content of clays, quartz and carbonate also play a key role in this regard. Odusina, Sondergeld and Rai (2011) considered rock samples from Eagle Ford, Barnett, Floyd and Woodford shale formations and conducted imbibition studies using brine and dodecane, which is the oil phase, and measured the bulk relaxation times using NMR spectroscopy to estimate the volume of fluids imbibed. The corresponding results suggested that both brine and dodecane wetted the shales similarly suggesting a mixed wettability. TOC was found to have the highest impact on the intake of dodecane. Experiments on the middle member of Bakken shale suggested that the wettability for this formation varied between neutral to weakly oil wet (Wang *et al.*, 2012). Contact angle measurements conducted by Alvarez *et al.* (2014) on carbonate and siliceous shale liquid rich reservoirs ranged between 70° and 102° , which suggests a weakly oil wet nature. Hence it can be understood that shale tends to be neutral to weakly oil wet, which largely depends on the organic content that promotes an oil wetting state.

2.2. Wettability alteration for improved oil recovery

Altering the wettability of the rock to a water wet state helps recover additional oil by mobilizing oil trapped in fine channels after primary recovery, which is a strong motivation behind the research of enhanced recovery techniques (Kathel and Mohanty, 2013). Various ways to alter wettability include thermal applications (Wang and Gupta, 1995), surfactants and low salinity brines with divalent ions. Dong, Hong and Rui (2006)

experimented on Berea sandstone whose wettability was initially altered to an oil wet state and tested the efficiency of an alkaline surfactant polymer flood with varying wetting conditions. It was found that the recovery efficiency of the flood was highest for a water wet and oil wet conditions while water flooding was found to be successful for neutral wetting conditions. Thus it can be inferred that the efficiency of a recovery process largely depends on the wetting state of the reservoir, which needs to be altered if needed to improve oil recovery. Nasralla, Bataweel and Nasr-El-Din (2011) investigated the effect of low salinity brines on wettability of mica surfaces and concluded that a water wet state was favored owing to repulsive forces oil/brine and brine/rock interfaces. It was also noted that wettability alteration depended on the oil composition. Weiss and Xie (2007) tested the efficiency of anionic, nonionic and amphoteric surfactants on altering the wettability carbonate reservoir rock and concluded that surfactants improve the recovery efficiency of a water flood by creating a water wet state and improving the imbibition profile. Salts and surfactants have been found to alter the wettability of rock surface as the above studies suggest. Hence it is important to understand the underlying mechanisms by which this change can be achieved. The following sub sections deal with analyzing the theory behind wettability alteration by surfactants and salts.

2.2.1. Surfactants

2.2.1.1. Introduction to surfactants

Before understanding the mechanisms by which surfactants can alter the wettability of a rock oil system, it is important to understand what constitutes these molecules. A surface active agent or surfactant is a molecule which has the ability to adsorb at the interface between two immiscible fluids and reduce the interfacial free energy between the molecules of the two fluids. Surfactants have a structure that contains two groups, a lyophilic group that has a strong attraction for the solvent phase and a lyophobic group that tends to repel the solvent phase molecules. The surfactants used in oil-water systems generally consist a hydrophilic head that is an ion bearing positive (cationic surfactants) or negative charged (anionic surfactants) or a neutral molecule (nonionic surfactants), and a hydrophobic tail composed of chained or unchained hydrocarbon groups. Some surfactants consist of hydrophilic heads bearing both positive and negative charges and are characterized as amphoteric or zwitterionic surfactants. The following schematic shows various types of surfactant as discussed above:

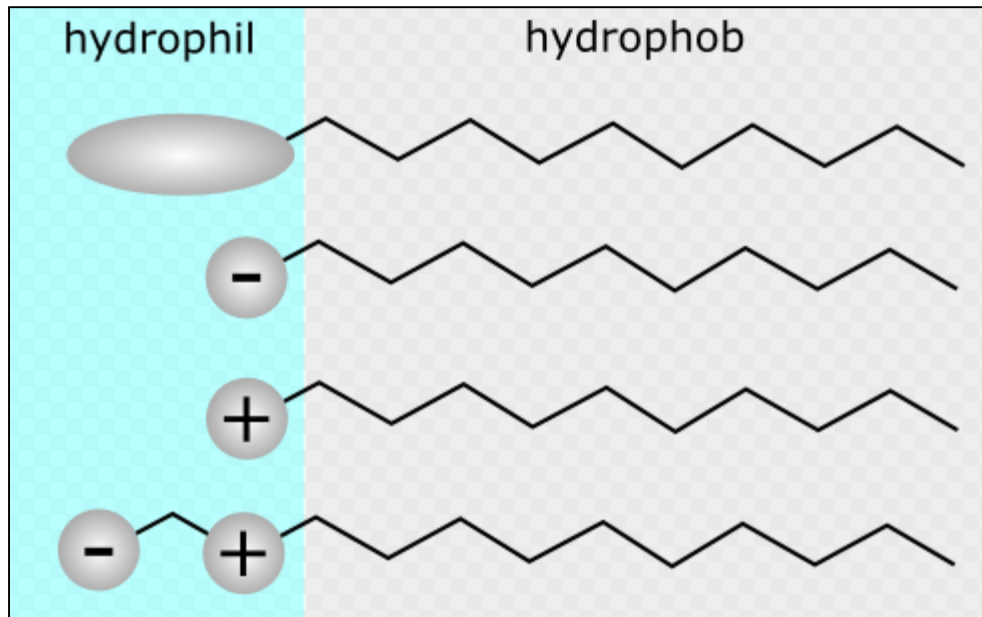


Figure 8. Structure and types of surfactants (nonionic, anionic, cationic, amphoteric)

Some examples of different types of surfactants are as follows:

- Anionic: Carboxylates, sulfates, sulfonates
- Nonionic: Alcohols, polyoxyethylenated chains
- Cationic: Quarternary ammonium salts
- Zwitterionic: Aminocarboxylic acids

Surfactants are primarily used in the oil industry for the following applications:

- Drilling mud: To stabilize various components of a complex mixture of chemicals
- Enhanced Oil Recovery: In alkaline surfactant polymer flooding to recover additional oil or to generate foams to control the mobility of injected fluids in porous media

- Fracture fluid additives: As thickeners to improve fluid viscosity and prevent corrosion of casing and tubing

This study also focuses on the effect of surfactants in reducing the interfacial tension between oil and aqueous phases and altering the native wetting state of the reservoir rock towards a preferentially water wetting condition, which shall be dealt with in the forthcoming sections.

2.2.1.2. Reduction of interfacial tension

One of the major application of surfactants is the reduction of interfacial tension between two immiscible phases that can dissolve either part of the surfactant molecule. Reducing interfacial tension helps improve gravity-driven drainage process, which was proven by previous studies (Seethepalli, Adibhatla and Mohanty, 2004). To understand the mechanism of IFT reduction, let us consider the following schematic in **Figure 9** where a and b are two immiscible fluids and A_{aa} denotes the force of interaction between two molecules of a and A_{ab} denotes that between a molecule of a and one of b. Similar explanation applies to A_{bb} and A_{ba} w.r.t. fluid b. The difference is the potential energy needed to bring a molecule from interior of b to a. This energy is characterized by interfacial tension value between b and a.

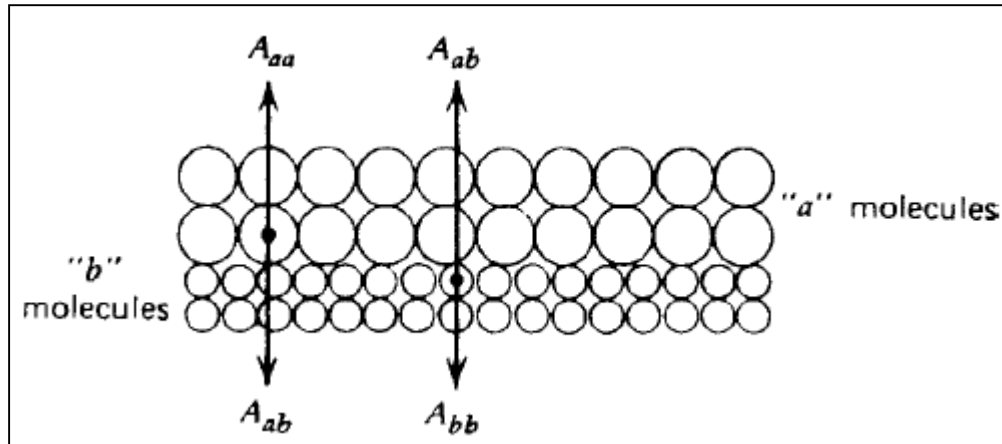


Figure 9. Forces at the interface between two immiscible fluids a and b

Now consider adding to this system a surfactant that has components soluble in both a fluids. These surfactant molecules adsorb at the interface formed by the fluids and replace the molecules from b and a. The resulting interaction of the molecules in bulk phases of both fluids is with the surfactant, which facilitates the transport of molecules from one bulk phase to the other as the difference between A_{aa} and A_{ab} (and between A_{bb} and A_{ba}) is reduced. IFT reduction depends on various factors such as the polarity difference between the fluid phases, lyophilic-lyophobic balance of the surfactant molecule and temperature of operation.

2.2.1.3. Wettability alteration by surfactants

Stadness and Austad (2000) made some of the early attempts to study wettability alteration in chalk samples using surfactants. They tested fourteen different water soluble cationic and anionic surfactants on low permeability chalk samples and concluded that

both the types of surfactants were able to alter the wettability to a water wet state and displace oil through spontaneous imbibition with cationic surfactants yielding superior results. Similar experiments conducted on oil-wet carbonate rocks (Seethepalli, Adibhatla and Mohanty, 2004) suggested that anionic surfactants were effective in promoting water wetness. To understand what effect a surfactant can have on the rock wettability, it is paramount to understand the underlying mechanism of wettability alteration by surfactants.

Surfactants have the ability to alter the wetting nature of the rock via two major mechanisms – adsorption and ion-pair formation with surface active components of crude (Salehi, Johnson and Liang).

2.2.1.3.1. Ion-pair formation

As previous studies suggest (Stadness and Austad, 2000; Salehi, Johnson and Liang, 2008), the charged heads of ionic surfactants tend to form ionic pairs with oppositely charged surface active components of crude oil that adheres to the rock surface, thereby displacing the oil molecules from the rock surface and opening the rock to wetting by aqueous phase. This can be observed with cationic surfactants in carbonates and anionic surfactants in sandstone. The carbonates are positively charged owing to which they interact with acidic components of crude (e.g. carboxylates). Introducing a cationic surface means the positive head interacts with the negatively charged surface active molecules of the oil and forms an ion-pair as shown in the schematic below. Similar explanation holds

true for anionic surfactants that react with basic components of crude in negatively charged sandstone rocks.

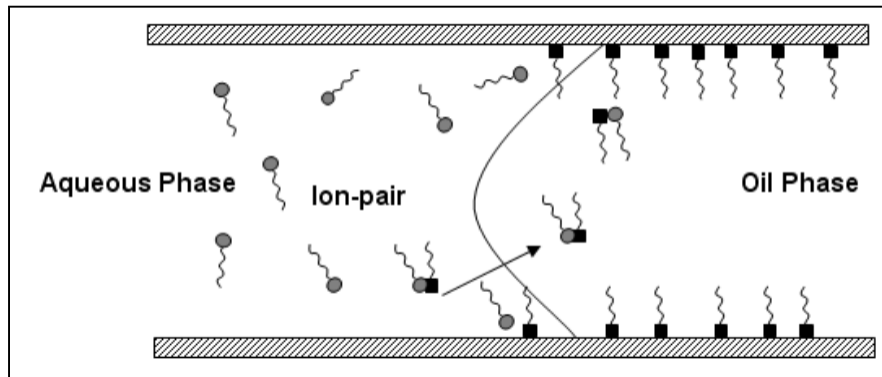


Figure 10. Wettability alteration by surfactants through ion-pair formation. The circles represent ionic heads of ionic surfactant while the squares denote the oppositely charged components of the surface active agents in crude oil (Salehi, Johnson and Liang, 2008)

2.2.1.3.2. Adsorption

Stadness and Austad (2000) noted that anionic surfactants improved imbibition in carbonate rocks despite those not effective at forming ion-pairs as the anionic heads and acidic surface active agents of crude bear charges of repulsive nature. Hence, they suspected there is another mechanism by which surfactants alter the wettability of rocks. They predicted the formation of a surfactant-oil monolayer via hydrophobic interaction of the alkyl chains of the surfactant and those of crude oil, which leads to the hydrophilic ionic heads of the surfactants pointing towards the bulk fluid phase as illustrated in the figure below. This layer is weak and can be reversed due to the weak hydrophobic interaction that is not as strong as an ion-pair. This was further verified by Salehi, Johnson

and Liang (2008) who analyzed the wettability through Amott-Harvey tests and concluded that the rock became more oil wet after a second imbibition cycle due to the reduced strength of the monolayer.

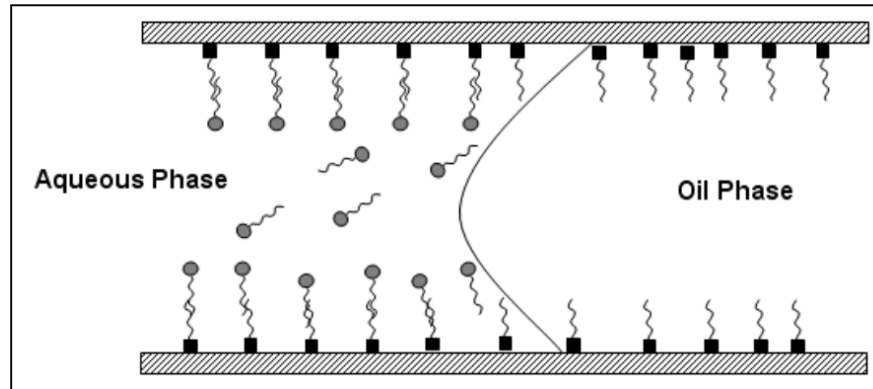


Figure 11. Wettability alteration by surfactants through adsorption. The circles represent ionic heads of ionic surfactant while the squares denote the oppositely charged components of the surface active agents in crude oil (Salehi, Johnson and Liang, 2008)

2.2.2. Effect of brine composition on wettability and interfacial tension

This section aims at understanding the effect of salinity and compositions of brine solutions on the interfacial tension of crude oil/brine systems and the changes in wettability associated with manipulating the ionic composition and content of the brine.

2.2.2.1. Impact of ions on interfacial tension of crude oil/brine systems

Literature contains various studies that examine the effect of brine salinity and type of salts in the brine on interfacial tension of hydrocarbon/brine interface. However, a fixed

trend has not been established as majority of them suggest an increase in IFT with increasing salinity (Cai *et al.*, 1996) while some of them conclude IFT does not necessarily increase with salinity (Abdel-Wali, 1996; Vijapurapu and Rao, 2003; Alotaibi and Nasr-El-Din, 2009).

Cai *et al.* (1996) measured the interfacial tensions of 10 normal alkane + water/brine systems using the pendant drop technique. The salts that were used in their study included NaCl, CaCl₂, and MgCl₂. Their results suggested that IFT increased with increasing salt concentration. However, the increase was insensitive to the salts used. Serrano-Seldana *et al.* (2004) examined the impact of aqueous phase ionic strength on the advancing contact angles and IFT of glass/brine/n-dodecane, and polyacrylonitrile/brine/n-dodecane systems. The ionic strength varied between 0-1.5 M NaCl with the testing conditions remaining constant at 77⁰F and atmospheric pressure. Fluctuating IFT values were observed as the salinity NaCl concentration was increased which couldn't be explained.

Abdel-Wali (1996) measured the IFT of crude oil samples from Safinya formation in Saudi Arabia for various crude compositions by varying oleic acid and octadecylamine concentrations in the crude and different brine salinities by varying the NaCl concentration from 0 to 200,000 ppm. His results suggested that there was an optimum salt concentration that corresponded to the lowest IFT for a given oleic acid/octadecyl amine concentration until which the IFT decreased due the increased activity of the surface active compounds. Beyond this concentration, the IFT increased suggesting higher salt concentrations were detrimental to IFT reduction. This could probably be due to the salting out effect in which

increasing salt concentration leads to water molecules surrounding the salt ions thereby reducing the solubility of crude and other non-polar components in water as less water is available for solubilization.

Vijapurapu and Rao (2003) conducted tests with Yates crude oil and brine where they diluted the brine with deionized water to observe its effect on IFT and wettability. Their results indicated that the lowest IFT was obtained at 50% dilution of the brine. Alotaibi and Nasr-El-Din (2009) measured the IFT of a brine/n-dodecane system by varying the NaCl concentration in the brine. It was observed that IFT values were time dependant and different trends were noticed at different periods of time. It was also concluded that IFT reduced upon lowering the NaCl concentration and there exists an optimum salinity to maximize oil recovery. Lashkarbolooki and Ayatollahi (2014) investigated the effect of chloride and sulfate salts of sodium, calcium and magnesium on the interfacial tension of acidic asphaltenic crude/carbonate rock/brine systems and found out that chloride salts were more effective at decreasing the IFT between crude and brine with high salinities reducing IFT. IFT was also found to be higher for monovalent salts such as NaCl and KCl.

Various trends have been observed though a conclusion of the impact of salts on crude/brine IFT hasn't been reached. Various phenomena have been attributed to the impact of salts on IFT. Price (1976) argued that solubility of hydrocarbon species reduces with increasing salinity due to salting out effect while Bai *et al.* (2010) suggest salts can also accelerate the diffusion of surface active agents in crude from the bulk solution to the interface, thereby improving their activity. The effect of salts on IFT also depends on the

type and the amount of surface active components present in the crude oil/brine system (Moeini *et al.*, 2014).

2.2.2.2. *Impact of ions on wettability*

Carbonate rocks have been the focus of experimental work to study the effect of brine composition on wettability alteration. Martavaltzi *et al.* (2012) performed experiments on limestone outcrop samples to analyze the change in wettability with various brine solutions. It was found that ion concentration of calcium, magnesium and sulfate has a significant impact on wettability as the surface charges were altered, leading to the release of adsorbed organic acids and changing the behavior of the rock from oil wet to water wet. Ca^{+2} was found to influence the wettability of rock significantly as Mg^{+2} was found to have little effects on the rocks examined. Studies have also shown that SO_4^{-2} has the most effect on changing the wetness of source rock to water wet in the presence of Ca^{+2} and Mg^{+2} ions (Kwak, Yousef and Al-Saleh, 2014). In alkaline conditions, sulfate was found to change the surface charge of carbonates from positive to negative (Zhang and Austad, 2005). This reversal of polarity results in more water molecules adhering to the rock surface and hence the wettability change. Besides sulfate ions, chloride salts were also found to improve oil expulsion by reducing the oil wetness. AlShaikh and Mahadevan (2014) studied the effect of chloride and sulfate salts of sodium, magnesium and calcium on wettability on aged calcite mineral surfaces and concluded that chloride salts have the maximum impact on changing the contact angle to the surface to water wet state.

Standal *et al.* (1999) investigated the contact angles of isooctane oil phase and water solutions consisting of NaCl and CaCl₂ on silicate glass and α -alumina as solid phases. Their results saw an increase in the contact angle of the oil/brine/rock system with increasing salinity. They inferred from these results that as the salt concentration increases, the concentration of surface active molecules in the aqueous phase decreases, thereby causing them to be adsorbed on the solid-liquid or liquid-liquid interface and promote oil wetness and decrease interfacial tension. This effect was found to be more pronounced for divalent (Ca⁺²) ions as the IFT reduced to lower values than those obtained by NaCl while the contact angles were higher. Zekhri, Ghannam and Almehaideb (2003) measured the contact angles of oil/rock samples obtained from UAE oilfields at 0, 1,000, 10,000 and 50,000 ppm salinities of NaCl and found out that the maximum reduction in contact angle, hence maximum water wetness, was achieved at 10,000 ppm (1 wt%) as the contact angle decreased from 48° to 29°. This helped them conclude there is an optimum salinity which is different than the formation salinity that would change the contact angle of a flooded area during water injection.

Quan *et al.* (2012) used kaolinite, montmorillonite, illite, chlorite and quartz surfaces as solid phases and crude oil samples from the Changqing oilfield in China that were tested with aqueous phases containing various concentrations of NaCl, CaCl₂, MgCl₂ and Na₂SO₄. Zeta potential and contact angle measurements suggested that NaCl altered wettability towards water wet better than CaCl₂ and MgCl₂ solutions. Zeta potential results suggested that the interface of oil/NaCl solution was more negative compared to those with CaCl₂ and MgCl₂ with higher negative values observed at lower salinities. Also the

clay/NaCl interfaces showed more negative zeta potentials compared to those with CaCl₂ and MgCl₂. The contact angle results were consistent with zeta potential results suggesting improved water wetness by NaCl as compared to CaCl₂ and MgCl₂. The reason for this is that a more stable water film is formed in the case of NaCl due to the repulsion between brine/oil and brine/rock interface hence promoting water wetting.

Thus the impact of divalent ions on wettability alteration was found to be significant and is worth examining in tight reservoirs with rock lithology similar to that of carbonates such as Eagle ford shale which is also composed of significant proportions of clays and quartz. However, it is essential to analyze some of the major theories that explain wettability change to analyze trends observed in experimental results, which is the subject of the following sections.

2.2.2.3. Mechanisms of wettability change by monovalent/divalent ions

Prior to understanding the mechanisms of wettability change and trends in zeta potential, it is imperative to understand the surface chemistry of rock-brine and oil-brine interactions as these shape the wetting nature of the rock. A thin double layer exists between these two interfaces which is filled with brine/aqueous phase which acts as a medium for crude-rock interactions.

An electrical layer formed when around a particle is surrounded by oppositely charged ions in solutions is governed by various surface forces that include van der Waals and Coloumbic electrostatic interactions (Hirasaki, 1991). Surface charges at these interfaces define how thick and stable an aqueous film on a rock surface is. The thickness

of this film is important as it is proportional to the water wetness of the rock which means a thick and stable film promotes water wetness. The stability of this film also depends on the sequence of wetting alteration. An initially water wet rock may form a metastable film on the surface as the oil forces itself into the pore space. Whereas if the oil adsorbs onto the rock surface when there exists no aqueous film on its surface, a much stable film is formed as compared to the previous case. Eagle Ford shale is deposited in marine environment which implies the rock was initially in contact with water as further deposition of organic material and cooking of kerogen forced the oil into pore space thereby creating a metastable state. Hence the intermediate values of wettability exist for Eagle Ford shale.

Hirasaki (1991) states the electrical field near a surface decays exponentially with a decay length called Debye length that is inversely proportional to the square root of the electrolyte concentration. Hence, as theory suggests, as the salt concentration of an aqueous solution increases, the Debye length should decrease thereby reducing the influence and magnitude of the electric field at a surface. Characterizing the stability of these thin films with salinity changes gives an indication of wetness change and the effect of individual ions on water wetness. One way to do this is by measuring the zeta potential of the brine/rock interface which helps assess stability of the brine film on rock surface.

Myint and Firoozabadi (2015) analyzed the stability of thin films in low salinity flooding and identify four major interactions that affect the thin film stability in sandstones. These are:

- Electrostatic interaction between brine-oil/brine-rock interfaces as explained by the DLVO theory (after Derjaguin and Landau, Verwey and Overbeek).
- Hydrogen bonding between polar functional groups in oil and polar groups on rock surface
- Lewis acid/base interactions between charged groups in oil and oppositely charged groups on the rock
- Formation of organometallic complexes between carboxylic acid (COO^-) groups in oil and divalent ions (Ca^{+2}) adsorbed on rock surface.
- The last three interactions are classified as non-DLVO interactions.

2.2.2.3.1. Double layer expansion

Myint and Firoozabadi (2015) attributed the effect of monovalent and divalent ions on wetting change to double layer expansion and multicomponent ion exchange. Double layer expansion affects the DLVO interaction while multicomponent exchange affects the other three. For lower salinities, as discussed earlier, the Debye length and hence, the film thickness increases due to lower screening of the repulsive forces between negatively charged crude and negatively charged quartz/clay/silica surfaces. This effect is more pronounced with monovalent ions as there is less screening and more repulsion, which is an alternate explanation for the results observed by Quan *et al.* (2012). Similar argument was put forward by Nasralla and Nasr-El-Din (2012) who conducted experiments on Berea sandstone and concluded low salinities of NaCl were favorable to higher oil recovery from

waterflooding due to wettability alteration towards less water wet owing to higher repulsion between the crude oil/brine and rock/brine interfaces.

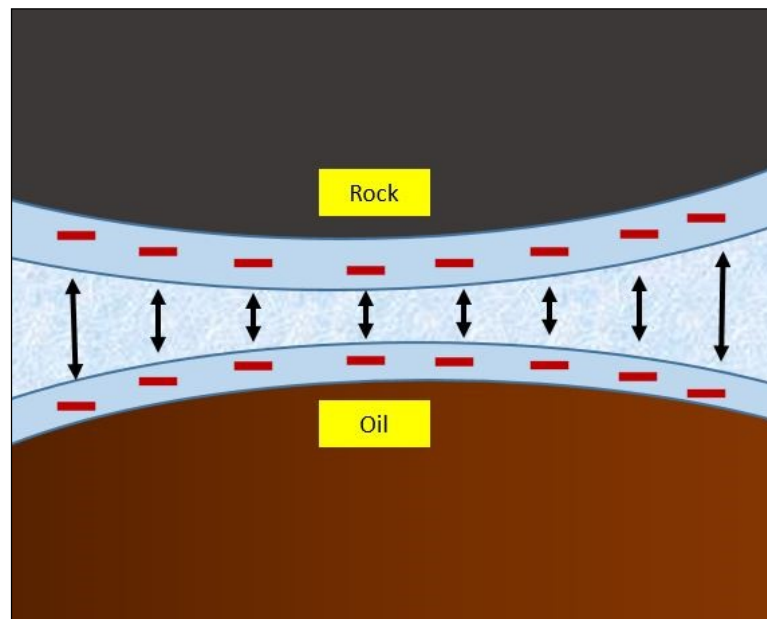


Figure 12. Double Layer Expansion due to repulsive forces (black arrows) between rock/fluid and oil/fluid interfaces

However, the mechanism of double layer expansion may be different for carbonates as they are positively charged in aqueous solutions. It might be possible to assume the zeta potentials of carbonate/brine surfaces be positive as the surface charge is positive. However, experiments conducted by Chen *et al.* (2014) on TP powder, which is 82% calcite and some quartz and clays, with NaCl and CaCl₂ brine suggested that at low salinities, the zeta potential for brine rock interface were negative with dispersions in NaCl having the higher negative values than those of CaCl₂ at same concentrations. One proposed mechanism is due that as carbonate dissolves in the brine, the pH of the solution

increases and drives the zeta potential towards a more negative value (Myint and Firoozabadi, 2015).

2.2.2.3.2. Multivalent ion exchange

Another mechanism of wettability alteration by ions is the multicomponent ion exchange through the thin water film. As stated earlier, divalent ions such as calcium form complexes with the negatively charged/acidic crude components as they are adsorbed onto the negatively charged sites in clays/silica. These complexes can be broken by introducing unbridged monovalent/divalent cations that interact with the negative sites in oil and rock separately as proposed by Lager *et al.* (2008). Besides this mechanism, calcium ions are capable of altering the negative charge on an oil surface to a positive by forming carboxylic acid bonds as suggested by the following reaction proposed by Brady *et al* (2012):



Hence the previously negatively charged oil molecules now bear a positive charge and are repelled from the rock surface making it more water wet. Zeta potential measurements by Zhang *et al* (2007) also suggest calcium is a potential determining ion for carbonate rocks, whose presence can alter the surface charge and thus, the wettability of the rock surface.

2.2.2.4. *Impact of brine composition and salinity on shale rock wettability*

Morsy (2014) conducted numerous imbibition experiments on shale samples from various plays such as Mancos, Barnett, Bakken and Eagle Ford. Experiments on the middle member of the Bakken shale suggested an improved oil recovery with 15% brine compared to 30% brine which led to the conclusion that the recovery factor was higher for lower salinity solutions, opening up the prospects of low salinity water flooding in shale. One possible explanation for this stems from the fact that the middle member of the Bakken has a high carbonate content and low salinity brine were proven to improve oil recovery in carbonate rocks (Nasralla *et al.*, 2014). This was further verified by measuring the contact angles of Bakken rock and oil in formation brine (30% salinity) and low salinity brine (15% salinity), which showed that contact angle was lowered from an initial 81° to 74° , promoting a water wet behavior. Experiments were also conducted on Eagle Ford samples that were initially water wet, which were soaked in alkaline solutions of varying pH. The results suggested that as pH increased, the value of contact angle decreased leading to a more water wet state. Hence pH of the brine may also have an effect towards determining the wettability and hence oil recovery from the shale rock.

2.3. Spontaneous imbibition experiments in shale

This section deals with the concept and mechanism of spontaneous imbibition and its types and reviews some previous attempts of spontaneous imbibition experiments with shale cores.

2.3.1. *Imbibition and its types*

Imbibition is a process wherein a wetting fluid absorbs into the matrix of a rock due to capillary forces and drives out the non-wetting phase. Imbibition plays a major role in determining oil recovery from rock matrix and is largely dependent on capillary forces, wetting nature of the rock, contact angle and hysteresis (Abe, 2005). Imbibition can be classified as spontaneous and forced. Other form of classification is co-current and counter-current. Spontaneous imbibition occurs due to capillary forces in a matrix and is predominant in naturally fractured low permeability reservoirs. Forced imbibition occurs when the wetting phase (usually aqueous phase) is forced into the rock matrix against capillary pressure to push out oil (Buckley, 2001). Countercurrent imbibition occurs when imbibing fluid enters the rock matrix from a face and the non-wetting phase moves out of the matrix through the same face. The relative permeabilities of both the phases are low as the flow of one phase hinders the flow of the other (Schechter *et al.*, 1994). Co-current flow occurs when the imbibing fluid that enters the matrix through one face and the non-wetting phase leaves the matrix through the other face. The relative permeabilities of both phases are higher as compared to countercurrent flow. To understand the dominant type of imbibition and its flow characteristics, it is essential to analyze the interplay between capillary and gravity forces which is given by dimensionless numbers such as the Bond number (N_B) or the inverse bond number (N_B^{-1}). Bond number gives the ratio of gravity forces to capillary forces while inverse bond number gives the ratio of capillary to gravity forces (Schechter *et al.*, 1994).

2.3.1.1. Factors affecting imbibition rate and recovery

As mentioned earlier, imbibition is largely dependent on the capillary forces existing between the two immiscible phases. Low interfacial tensions lead to lower imbibition rates as the driving force i.e. capillary pressure reduces. However, at low IFT values, gravity segregation may play a dominant role as oil recovery may improve as a result of countercurrent imbibition. This trend may not hold true always as observed by Babadagli (2003) and Austad, Matre and Milter (1998). Their experiments suggested that imbibition rates improved as a result of lowering IFT. As Babadagli (2003) states, when the capillary forces are high due to strongly water wet behavior or high IFT values, capillary imbibition dominates recovery as a countercurrent flow pattern may be prevalent whereas gravity may dominate recovery when the matrix is less water wet or the IFT is lowered, leading to a concurrent flow profile.

Schechter *et al* (1994) experimented with sandstone cores with 15 mD, 100 mD, 500 mD and 700 mD permeabilities to study the effect of IFT alteration on imbibition rates and recovery. IFT of the oil phase (iso-octane) was altered by addition of Isopropyl alcohol and 2 wt% calcium chloride was used as the brine phase. The study suggests low IFT (low N_B^{-1}) produces the highest ultimate recovery while the imbibition rate was low. Intermediate values of IFT produced higher recovery rates and good final recovery that was higher than high IFT case but lower than the low IFT case. They were able to conclude that at high values of N_B^{-1} , capillary forces dominated imbibition leading to countercurrent flow and low recovery rates while at low values of N_B^{-1} the rates were higher due to gravity dominated vertical flow. As for intermediate values of N_B^{-1} , both gravity and capillary

components played their role in recovering the non-wetting phase which led to higher recovery rates than both low and high IFT cases. Hence it can be understood that capillary and gravity forces play a significant role in determining the nature of flow and thus the recovery and rate of an imbibition experiment.

Permeability of the rock is another important factor that determines the efficiency of an imbibition process and was found to directly affect the rate of imbibition (Mattax and Kyte, 1962). Low permeability reservoirs have high capillary forces and hence have a strong potential for countercurrent imbibition while there is in gravity dominated flow, the permeability is higher and Darcy flow leads to better recovery. However, experiments on Berea cores by Zhou *et al* (2000) suggested that wettability is a more defining parameter that facilitates imbibition in a wide range of permeabilities. So was found to be the case with initial fluid saturations as experimental investigations confirmed wettability alteration was more decisive than permeability and fluid saturations in impacting imbibition (Zhou *et al*, 2000; Stadness and Austad, 2000).

2.3.2. Imbibition experiments on shale samples

Imbibition of fluids into shale samples is a much more complex process compared to conventional core samples composed of carbonate or sandstone due to their complex lithology and extremely low permeability and porosity values. Imbibition patterns vary for samples from different plays as observed by Morsy (2014), who experimented with samples from Barnett, Eagle Ford and Marcellus. For instance, the author placed the samples in imbibition cells with water and observed cracks along the bedding planes in

Barnett and Marcellus while none in Eagle Ford, which was attributed to the low clay content in these samples. Wang *et al.* (2010) conducted brine imbibition experiments with core samples from Pierre and Bakken shale in North Dakota. Their results suggested that Pierre shale permeability increased possibly due to mineral dissolution and cracking caused by clay swelling, which was encouraging for imbibition in low permeability shale.

2.3.2.1. Brine imbibition in shale

Morsy (2014) evaluated the stability and oil recovery from Mancos and Bakken shale samples when imbibed with NaCl and KCl brines of salinities varying from 5 wt% to 30 wt %. Mancos shale samples were the most sensitive to distilled water and brine solutions as they were observed to be fragmented at salinities lower than that of formation water (13.8 – 21.2 wt% salinity). However, the oil recovery factor went up to as high as 59% at 5 wt% salinity which opens up the prospect of low salinity water flooding in shale. Low salinity brine was also found effective in improving recovery from Bakken shale samples. However, no visible cracks were observed in Bakken at low salinity of 15 wt% and hence clay swelling was not the dominant mechanism here. The increase in recovery was attributed to wettability alteration as was verified by measuring the contact angles at formation brine salinity of 30 wt% and lower salinity of 15 wt% which were 81° and 74° respectively. Morsy (2013) experimented with Eagle Ford shale samples using distilled water and 2 wt% KCl as imbibing fluids. Higher recovery was observed for distilled water which induced cracks due to clay swelling. Clay swelling was absent in 2 wt% KCl imbibition which led to a lower recovery. These studies suggest waterflooding by

imbibition could be a potential secondary recovery method in low permeability and low porosity unconventional reservoirs too, which is the focus of this study.

2.3.2.2. *Surfactant aided imbibition in shale*

Some of the early studies on imbibition experiments in shale with the aid of surfactants was done by Shuler (2010) who improved the oil recovery from Bakken samples using a carbonate reservoir surfactant (CRS) to about 45% OOIP. Wang *et al.* (2011) evaluated the stability of various nonionic, anionic and cationic surfactants in high temperature and high salinity conditions and screened out a nonionic and an anionic surfactant for conducting imbibition studies on Bakken shale. Imbibition studies suggested an increase in the oil recovery from the samples when surfactants were added.

Alvarez *et al* (2014) conducted spontaneous and forced imbibition experiments in tight unconventional liquid reservoir samples using anionic and nonionic surfactants which were found to reduce the contact angle of the rock and interfacial tension of oil/fracture fluid system. Computed Tomography (CT) was employed to visualize the penetration of the imbibing fluids into the rock matrix and defined a parameter known as the penetration magnitude that gave a quantitative indication of penetration. Results suggested that surfactant based fluids had a higher initial and total penetration which was also in coherence with oil recovery that was higher for surfactant based fluids. Anionic surfactant produced the best results followed by nonionic surfactants.

Neog (2014) examined the potential of five surfactants that included nonionic and complex nano-surfactants on enhancing the performance of hydraulic fracturing fluids to

improve recovery from ultra-tight shale reservoirs. His results suggested the complex surfactants were more effective in terms of wettability change though the nonionic species were equally effective in improving oil recovery from spontaneous imbibition, thereby concluding that wettability alteration alone does not contribute to improving oil recovery. Interfacial tension was also found to play a significant role in deciding the ultimate oil recovery. However, a field scale simulation study involving a single well fracture model suggested that wettability alteration might necessarily not improve oil recovery. This was linked to the development of an additional capillary force due to preferential wettability of the rock that reduces the viscous force generated during pressure drawdown. However, the results encouraged the prospect of secondary/tertiary recovery from these reservoirs as lab scale studies were in favor of surfactant aided imbibition in shale.

2.4. Computed Tomography techniques for imbibition monitoring

Computed Tomography (CT) is a non – destructive imaging technique that can be utilized for observing porous interior of a rock as well as the flow of fluids through it. Radiological imaging with computed tomography was first discussed by Hounsfield in the year 1972. CT scanners using the petrographic analysis differ from the conventional X-ray techniques in that they generate cross sectional images of the object by measuring the attenuation of a beam of X-rays as it is rotated around the object at angular increments from a single plane (Akin and Kovscek, 2003). These images are then converted into a cross sectional image using back projection algorithms and Fourier transforms.

2.4.1. Theory of CT imaging

An X-ray source that revolves around the object to be scanned emits X-rays that penetrate a thin volumetric slice of an object at different angles. The reflections from the object are then recorded by a series of detectors that pass on the attenuation data thus received to a software that mathematically reconstructs it into a cross section image. Thus, a parameter called linear attenuation coefficient is of interest and is calculated from Beer's law as follows:

$$I_0/I = \exp(-\mu h) \text{ (Eq. 1)}$$

where

I_0 = Incident X-ray intensity

I = Intensity remaining after an X-ray passes through a thickness, h

μ = Linear attenuation coefficient

This law assumes a monochromatic radiation from source though in reality, the beam is polychromatic with varying photon energies. These facts result in artefacts in images. Once the image reconstruction is complete and the attenuation coefficients are known for each volume element or voxel in the image, this data is converted into CT number using the following equation:

$$CT = 1000 \frac{(\mu - \mu_w)}{\mu_w} \text{ (Eq. 2)}$$

where,

CT = CT number in Hounsfield units

μ = Linear attenuation coefficient

μ_w = Linear attenuation coefficient of water

CT number for air is -1000 and that for water is 0 as water serves as reference for measurement. A decrease in CT number implies the components of the rock matrix are getting lighter or less dense and vice versa.

Important reservoir rock parameters such as porosity and fluid saturations can be computed from these CT numbers as discussed by Akin and Kavscek (2003) as follows:

$$\Phi = \frac{CT_{wr} - CT_{ar}}{CT_w - CT_a} \text{ (Eq. 3)}$$

$$S_o = \frac{CT_{wr} - CT_{wor}}{CT_{wr} - CT_{or}} = \frac{CT_{wr} - CT_{wor}}{\Phi(CT_w - CT_o)} = 1 - S_w \text{ (Eq. 4)}$$

where,

Φ = Porosity

CT_{wr} = CT number of water saturated rock

CT_{ar} = CT number of air saturated rock

CT_{or} = CT number of oil saturated rock

CT_{wor} = CT number of oil + water saturated rock

CT_w = CT number of water

CT_a = CT number of air

CT_o = CT number of oil

S_o = Oil saturation

S_w = Water saturation

2.4.2. *Computed tomography for analysis of imbibition studies*

Various researchers have successfully used CT scan technology to study the movement of fluids and change in the saturation of in situ fluids in rock samples during imbibition tests. Chen *et al* (2000) studied the effect of surfactant solutions on improving recovery from Yates rock samples through CT scan monitored imbibition experiments. CT scans were taken periodically and spatial fluid movement and saturations were characterized for each of these points. The saturations obtained from CT numbers were found to be in agreement with those calculated from material balance conducted based on the oil recovered. CT scan results helped conclude initial recovery was due to capillary dominated radial flow while the recovery at a later time was due to gravity segregation based vertical flow.

Alvarez *et al* (2014) tested the efficiency of surfactant aided imbibition in tight unconventional rocks using CT scan analysis. They defined a parameter named penetration magnitude as follows:

$$\text{Penetration Magnitude} = CT_t - CT_{\text{initial}} \text{ (Eq. 5)}$$

where,

CT_t = CT number of the sample at a time t

CT_{base} = Base CT number which is taken to be the lowest CT number of the sample during the study. This was chosen to be the CT number of the sample before fluid injection.

An initial penetration magnitude (%) was calculated based on the following equation:

$$\text{Initial Penetration Magnitude, \%} = \frac{CT_o - CT_{\text{base}}}{CT_{20} - CT_{\text{base}}} \text{ (Eq. 6)}$$

where

CT_0 = CT number at the start of fluid injection

CT_{20} = CT number after 20 hours of fluid injection (final time)

These parameters were instrumental in quantifying and analyzing the effectiveness of the surfactants based fracture fluids to penetrate into the rock matrix. Results suggested that nonionic and anionic surfactants could penetrate the tight rock matrix much better compared to fracture fluids without these surfactants.

Hence it can be understood that CT scan technology can be instrumental in estimating the effectiveness of fluid penetration as well as characterizing changes in saturation of fluids, which is why the imbibition experiments in this study were conducted in conjunction with periodic CT scan monitoring.

3. EXPERIMENTS

3.1. Reservoir description

The samples received were from two wells namely S-1 and SW-1, both of them from Texas and lie in the liquid rich window of Eagle Ford shale. The Eagle Ford shale is the source rock that fed Austin Chalk and is rich in carbonate content. It overlies Buda Limestone and is overlain by Austin Chalk. It is a unique reservoir that produces hydrocarbons ranging from dry gas to black oil. The play has an acreage of more than 11 million acres and is located geographically as shown in the figure below.

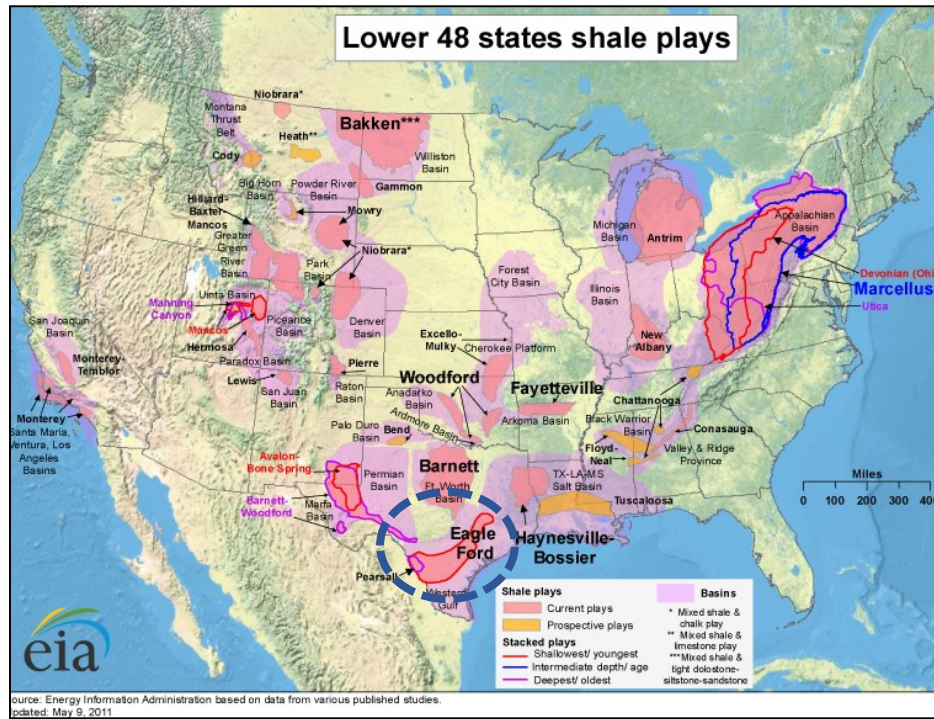


Figure 13. Map of United States showing various shale gas and oil play locations (U.S. Energy Information Administration, updated May, 2011)

Eagle Ford shale is a unique play owing to the spatial variation of rock and fluid properties over its acreage. The pay decreases in depth as we move from southwest to northeast as well as from northwest to southeast. **Figure 14** illustrates the variation of some in situ fluid and rock properties as we move in the northwest – southeast direction.

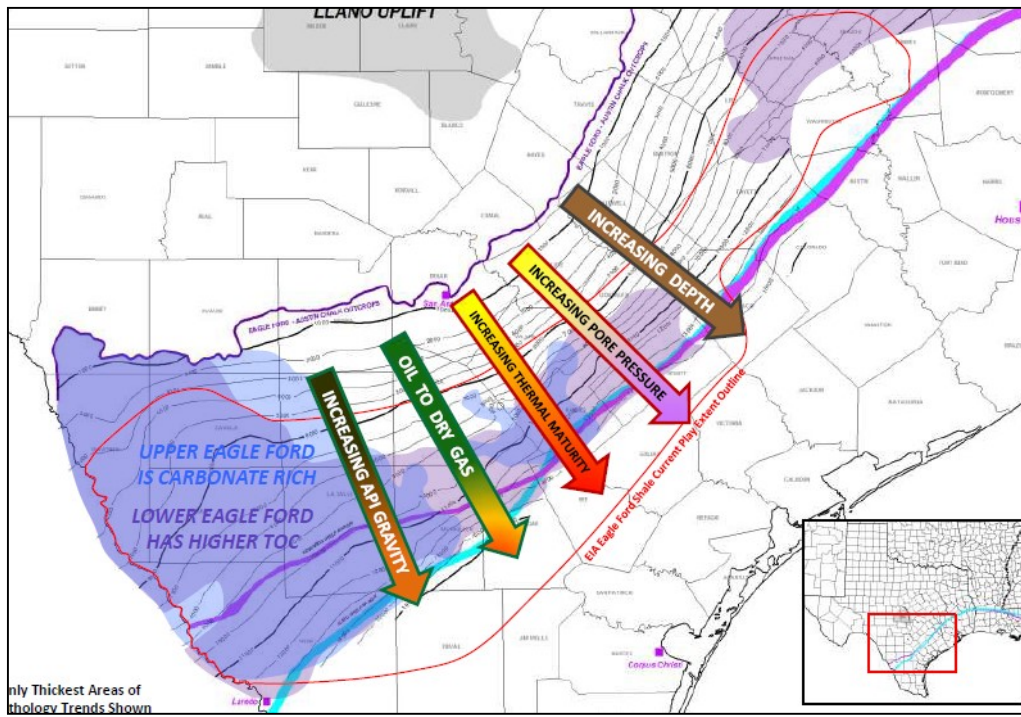


Figure 14. Trends of hydrocarbon and reservoir properties across Eagle Ford (Bruce Matsutsuyu, 2011)

The Eagle Ford play has a variable pay thickness ranging from 40 feet to 450 feet as we move from north east to south west. The total organic content (TOC) ranges between 3-7%, porosity between 6-11% and the true vertical depth (TVD) of wells between 4,500 feet to 11,500 feet (Bruce Matsutsuyu, 2011). In a geological perspective, Eagle Ford was

deposited during an anoxic extinction event that occurred at the Cenomanian/Turanian boundary during which warm seas existed and the high carbon dioxide levels in the atmosphere led to increased organic productivity and high TOC (Li Fan *et al.*, 2011). According to the U.S. Energy Information Administration (EIA), Eagle Ford houses about 3.4 billion barrels of recoverable oil and 20.8 trillion cubic feet of recoverable natural gas. A typical oil well in this play produces 680 barrels of oil per day while a gas well produces 20 Mscf of gas per day (Drilling Productivity Report of the U.S. EIA, March 2015).

3.2. Materials description

3.2.1. Core samples

The samples received were from liquid rich portion of the Eagle Ford play. The samples were taken at different depths from two wells S-1 and SW-1. The cores were received in a preserved state with a thick layer of wax surrounding each core plug. Core trims corresponding to the plugs were also received in an unpreserved state. These trims were aged and used for contact angle measurements. The aging process of this cores shall be dealt with in later sections.



Figure 15. Preserved core sample as received from the company

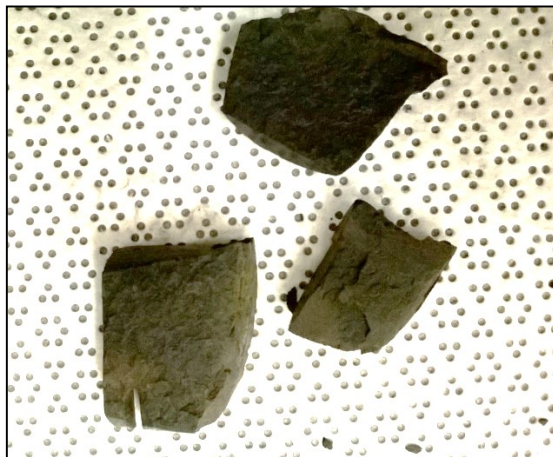


Figure 16. Trim samples as received from the company

3.2.1.1. Aging and preparation

The trims shown above were further cut into smaller pieces, typically measuring 0.25 inches x 0.25 inches. Initial tests on the samples indicated water wetness owing to a prolonged exposure to surface conditions. Hence, the samples were aged in corresponding

crude oil sample at 180⁰F in an attempt to reach the temperature closest to that of the reservoir. The samples were then cleaned to ensure there are no oil droplets on the rock surface with necessary care to ensure the samples aren't over cleaned. An aging time of at least two hours was ensured between successive brine experiments and at least four to six hours for two successive surfactant experiments.

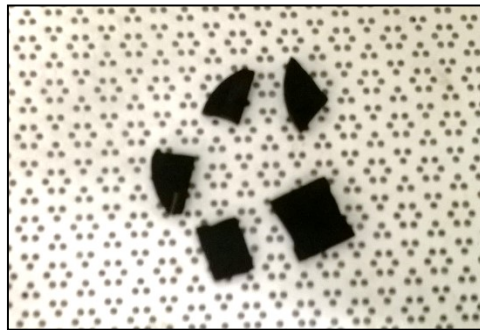


Figure 17. Chips cut from core trims used for contact angle measurement

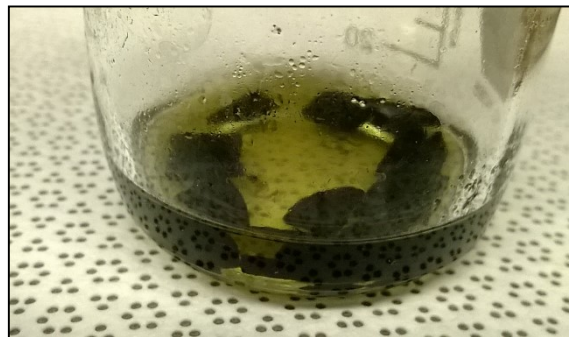


Figure 18. Aging of core chips in Eagle Ford oil



Figure 19. Core samples being aged in the Yamato DX 400 oven at 180°F

3.2.2. Oil sample

Oil samples obtained were taken from Well SW-1 and shipped in a pressurized state. The sample was pale yellow in color and had a vapor phase that contained hydrogen sulfide and carbon dioxide and had a pungent smell to it. Gas chromatography and Mass spectrometry were employed to analyze the composition of the oil sample. The results (**Table 1**) suggest a strange 6.54% Toluene and 12.16% ortho-Xylene presence.

Table 1. Gas chromatographic analysis of Eagle Ford oil sample

S No.	Component	mass %
1)	Hexane, 2-methyl-	4.00%
2)	Hexane, 3-methyl-	2.73%
3)	Heptane	4.38%
4)	Cyclohexane, methyl-	5.46%
5)	Heptane, 2-methyl-	2.49%
6)	Toluene	6.54%
7)	Heptane, 3-methyl-	2.94%
8)	Octane	5.13%
9)	Octane, 2-methyl-	3.56%
10)	o-Xylene	12.16%
11)	Nonane	5.19%
12)	Decane	7.37%
13)	Undecane	5.12%
14)	Dodecane	5.27%
15)	Tridecane	4.50%
16)	Tetradecane	4.18%
17)	Pentadecane	3.84%
18)	Hexadecane	3.52%
19)	Heptadecane	3.13%
20)	Octadecane	2.57%
21)	Nonadecane	2.19%
22)	Eicosane	2.04%
23)	Heneicosane	1.71%
	Total	100.00%

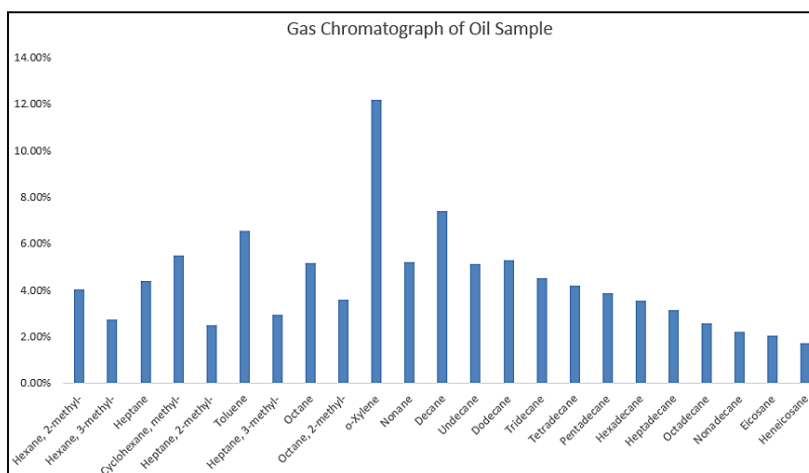


Figure 20. Gas chromatography results for the received oil sample

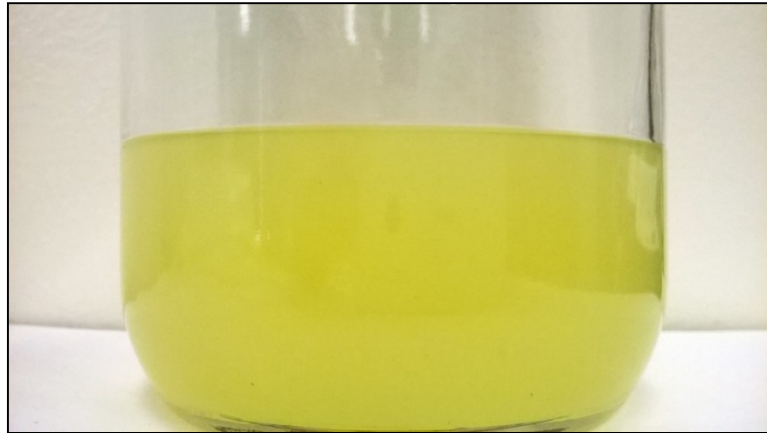


Figure 21. Oil sample received from well SW-1

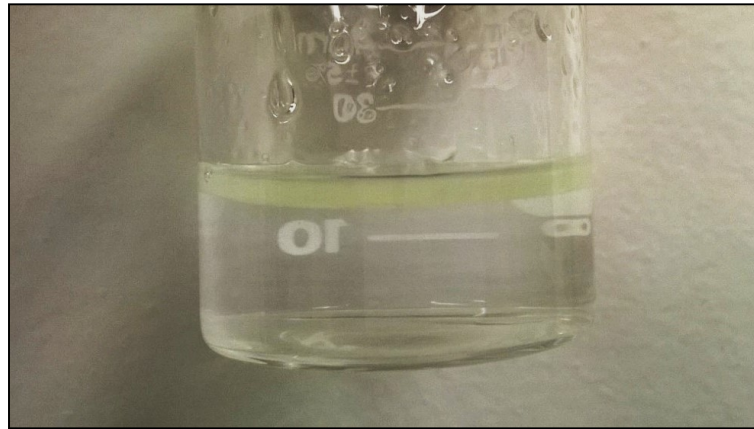


Figure 22. Oil-water contrast

The density of the sample was measured at ambient and testing temperature using Anton Paar DM 4100 M density meter.

Table 2. Oil properties at room ambient and testing temperature and atmospheric pressure

Oil Properties		
Temperature (°F)	Density (g/cc)	°API
77	0.7614	53.19
180	0.7176	52.61



Figure 23. Anton Paar DM 4100 M density meter

3.2.3. *Brines*

The two salts used for preparing brines were sodium chloride and calcium chloride dehydrate with varying concentration of 1, 2, 3, 5, 10 and 15 wt%. The salts were provided by Fischer Scientific. Distilled water marketed by Ozarka Corporation was used as solvent. The salts were weighed using a Mettler Toledo weighing balance that had a readability of 0.01g. The solutions were mixed using a magnetic stirrer until there were

no visible solute particles and were stored by covering them with a plastic film to ensure no contamination and exposure to the atmosphere.



Figure 24. Salts used for preparing brine solutions



Figure 25. Mettler Toledo MS weighing balance

3.2.4. Surfactants

Surfactants used for experiments are listed in the table below:

Table 3. List of surfactants, composition and properties

Surfactant	Type	Primary components	Composition (wt%)	pH	Specific Gravity
N1	Nonionic + Anionic	Methyl alcohol	60-100	6.3 - 7.3	0.8232 - 0.8482
		Proprietary Ethoxylated Alcohols	7 - 13		
		Proprietary Sulfonate	5 - 10		
A1	Anionic + Nonionic	Methyl alcohol	10 - 30	4.74	0.9742 - 0.9992
		Proprietary Sulfonate	7 - 13	- 5.74	
C1	Complex Nanofluid	Isopropyl alcohol	5 - 40	5.0	0.96 - 1.01
		Citrus Terpenes	5 - 15	- 8.0	

Surfactant A1 is predominantly anionic containing both ethoxylated alcohol (nonionic) and an alkyl sulfonate (anionic) components. Surfactant N1 is a mixture of nonionic and anionic components with a dominant nonionic character. C1 is a complex surfactants whose composition is unknown due to proprietary nature of these compounds. However, they are indicated to be composed of citrus terpenes. The use of citrus terpenes and creating micro-emulsions for cleaning purposes was first developed and patented by William A. Williams (1993) where a mixture of d-limeone (terpene), a nonionic surfactant and few other solvent compounds was used for cleaning soil form glass and metal parts.

The solutions were prepared by adding 0.2, 1 and 2 gpt (gallons per thousand gallons) of surfactant to distilled water and mixing the contents using a magnetic stirrer while covering the solutions with plastic film to avoid contamination.

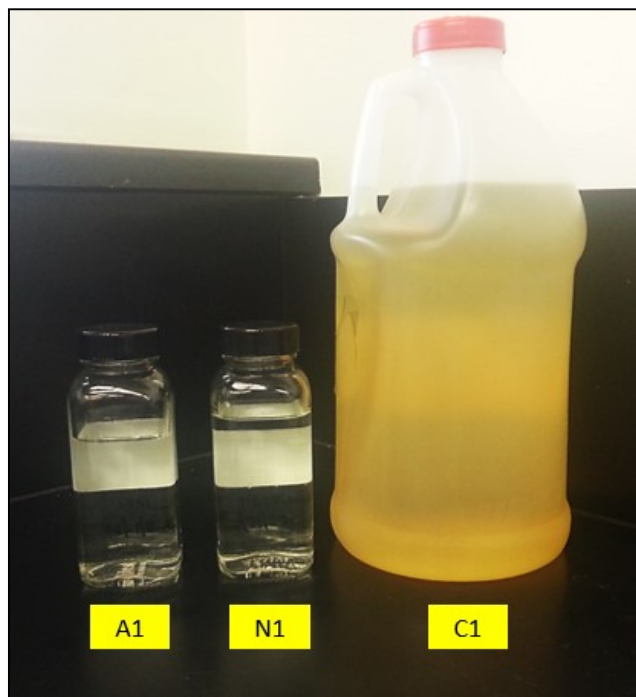


Figure 26. Surfactants used in this study

3.3. Contact angle experiments

3.3.1. *Experimental setup*

Contact angle measurement was performed on Dataphysics OCS 15 pro device that contains a video based optical measurement system. A drop shape analyzer (DSA) software was used to analyze the shape of dispensed droplets and process the results. The

apparatus consists of a magnifying system, a dispensing system and a platform that is heated by a water jacket whose temperature can be controlled through the DSA software. A cuvette containing the surfactant/brine solution is placed on the platform and heated to a set temperature along with the prepared shale trim samples as shown in **Figure 27**. A j-shaped capillary needle is then used to dispense oil onto the rock surface. Illumination and temperature are adjusted using the DSA software.

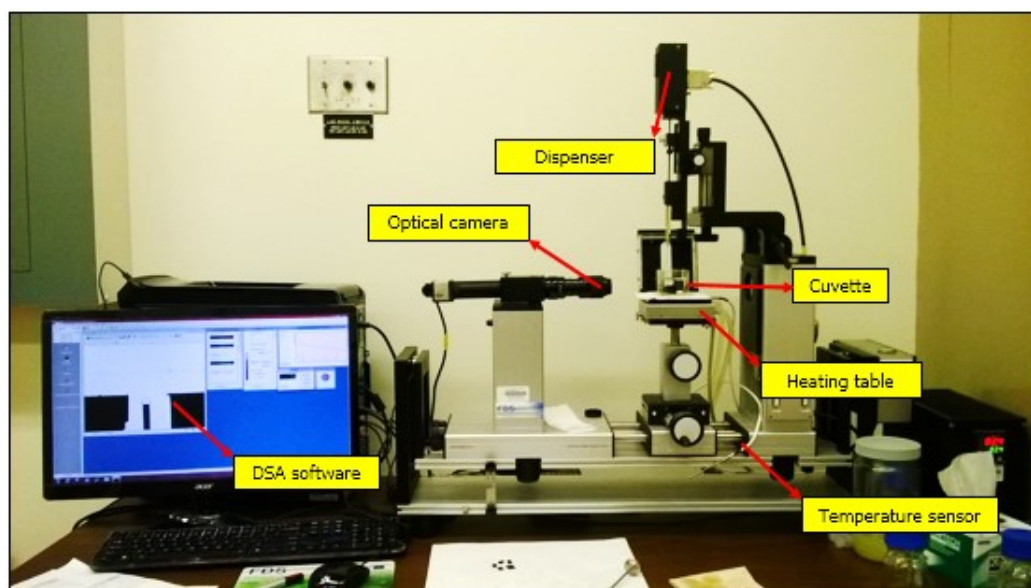


Figure 27. Contact angle measurement apparatus (OCA 15 Pro)

3.3.2. *Measurement method*

The contact angle of oil droplet on the rock surface in the presence of aqueous solutions was measured using the captive bubble method. Captive bubble method measures the contact angle between and liquid and a solid surface using drop shape

analysis. In this case, a drop of crude oil is injected from a needle pointing upwards onto the shale rock surface that is also in contact with the stimulating fluid. The measured contact angle is then subtracted from 180° to yield contact angle on water on the rock surface.

3.3.3. Measurement procedure

The following are the major steps followed in contact angle measurement:

1. The aged trim samples are cleaned and prepared as discussed in previous sections.
2. Surfactant/brine solutions are then prepared with distilled water. Three different surfactant concentrations – 0.2gpt, 1gpt and 2gpt were tested where ‘gpt’ corresponds to gallons of surfactant per thousand gallons of solution. 1gpt is equivalent to 1000 ppm or 0.1 vol%.
3. The solution is then heated in a cuvette along with a stand that holds the rock sample placed on it (**Figure 28**). A temperature sensor was dipped onto the solution to monitor the temperature that was set to 180°F , which is the maximum attainable temperature on the device.
4. Once the solution reaches set temperature, the sensor is removed from the solution and the capillary needle is lowered into the cuvette such that the needle lies between the two adjacent faces of the rock holder.
5. The trim sample is then placed on the holder using prongs and the tip of the needle is brought closer to the rock surface facing it as the oil is dispensed in

small amount, typically 0.1 μL . Care has to be taken such that there are no air bubbles interfering with the contact angle measurement.

6. Once the oil drop is dispensed onto the rock and it spreads, the video recorded by the camera arrangement of the device is used to pick a frame. Once this is done, a baseline is appropriately placed at the rock-oil drop interface and the subsequent angle formed tangential to the baseline and the drop shape is measured using the DSA software.
7. Two contact angle values, CA left and CA right are displayed. CA left is chosen for all measurements while it is important to ensure the two values are as close ($\pm 1^\circ$) as possible implying a symmetrical drop shape has been formed.
8. Four readings were taken per each depth using four different chips and the most repetitive or median value was chosen as the contact angle, which was later subtracted from 180° to yield the required value of contact angle w.r.t water.

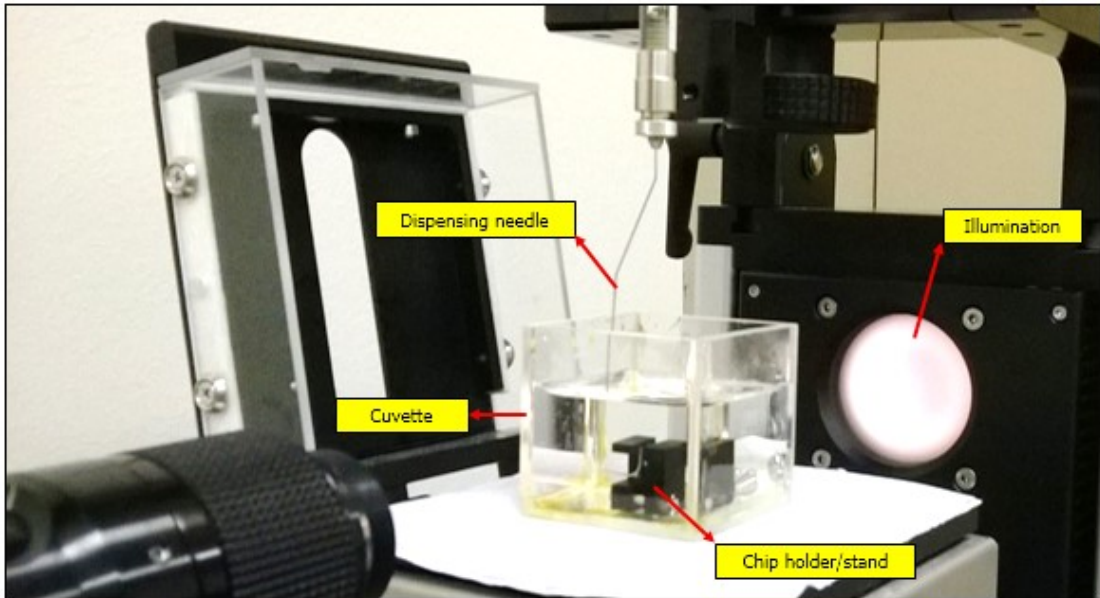


Figure 28. Cuvette and dispensing needle arrangement

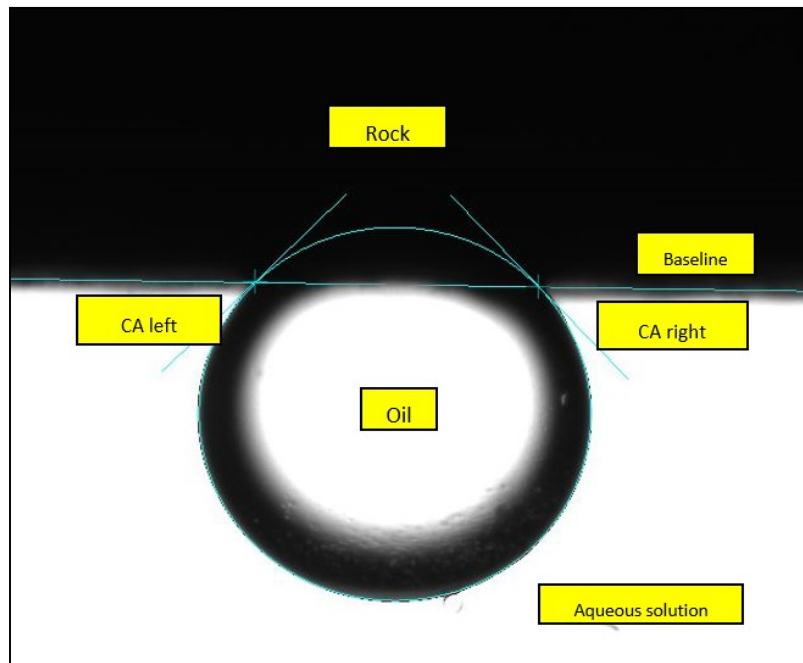


Figure 29. Contact angle measurement using oil the captive bubble method

3.3.4. Results and discussion

Two sets of contact angle experiments were conducted on shale rock samples using brines (NaCl and CaCl₂) and surfactants. The objective of the brine experiments was to understand the impact of monovalent sodium and divalent calcium on the wetting nature of the rock surface while the surfactant tests were conducted to determine if anionic, nonionic or complex surfactant was effective at altering wettability towards more water wet state. To serve as a reference, contact angle values between 0 – 60° were considered water wet, 60 – 120° as intermediate wet and 120 – 180° as oil wet. The two sets of results are presented and discussed as follows:

3.3.4.1. Brine results

The rock samples used for experiments with brine were taken from well S1. Two different depths were chosen to ensure consistency in the results. The composition of the samples are as shown below:

Table 4. Properties of rock samples for brine experiments

Sample	S1-1	S1-3
Calcite %	56.3	60.2
Quartz %	15.3	15.4
Clays %	20.2	15.8
Pyrite %	4.7	4.1
Plagioclase %	2.8	2.6
Marcasite %	0	1.2

The contact angle results obtained for both the samples are presented in **Table 4** as well as illustrated using the following pictures. The first two images (**Figures 30 and 31**) show consolidated results for sample S1-1 with NaCl and CaCl₂ respectively while the next two (**Figures 32 and 33**) represent the corresponding results for sample S1-3. The boxes below each window show the concentration of salt in the brine while the numbers in braces indicate the value of contact angle w.r.t water.

Table 5. Contact angle results for brines with S1-1 and S1-3

Brine	Brine Salinity (wt %)	Cation Content (wt %)	S1-1 (deg.)	S1-3 (deg.)
Distilled Water	-	-	75.7	73.3
NaCl	1	1	45.7	40.7
	2	2	47.4	37
	2.5	2.5	43.7	39.5
	3	3	44.1	41.1
	5	5	59.1	55
	10	10	61.7	59.7
	15	15	69.1	70.6
CaCl₂.2H₂O	1	0.755	59.8	64.4
	2	1.51	55	57.5
	3	2.265	48.6	46.3
	5	3.775	41.8	46.7
	10	7.55	52.8	50.7
	15	11.325	57	54.2
	20	15.1	64.2	58



Figure 30. Contact angle results for S1-1 with NaCl brine



Figure 31. Contact angle results for S1-1 with CaCl₂ brine



Figure 32. Contact angle results for S1-3 with NaCl brine

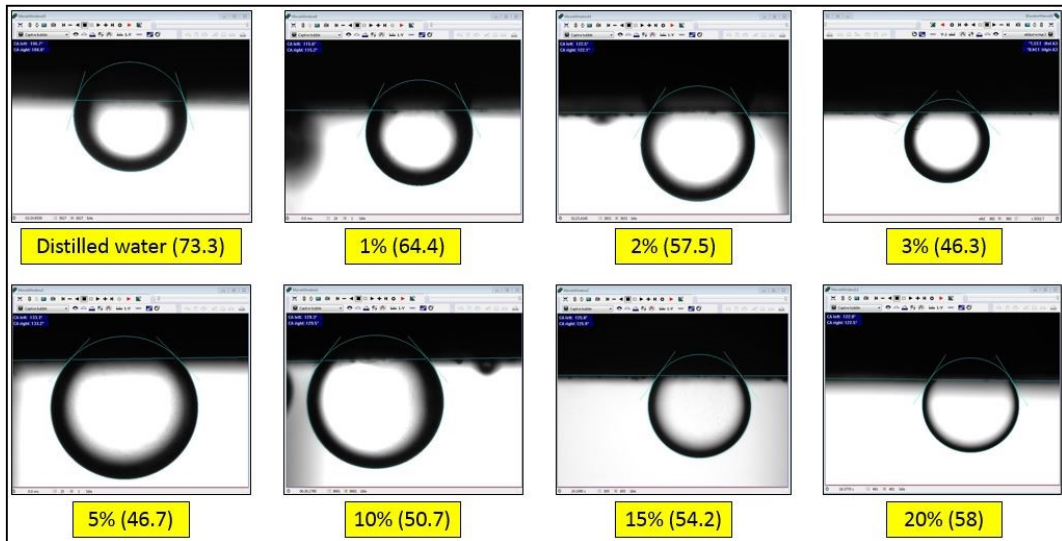


Figure 33. Contact angle results for S1-3 with CaCl₂ brine

Figures 34 and 35 as used to illustrate the comparison of the effect of Na⁺ and Ca²⁺ concentrations in the brine on the wettability of rock for S1-1 and S1-2 respectively

as **Figures 36 and 37** summarize the impact of NaCl and CaCl₂ on altering contact angle and oil-brine interfacial tension. It is important to note that the Calcium ions concentration is different from the salt concentration of calcium chloride dihydrate which contains two parts of water and one part of calcium chloride per molecule of salt. A simple mass balance using the molecular weight of calcium chloride (111 g/mol) and water (18 g/mol) deduces that per every 1 wt% of salt added, there is 0.755 wt% of calcium ions in the solution.

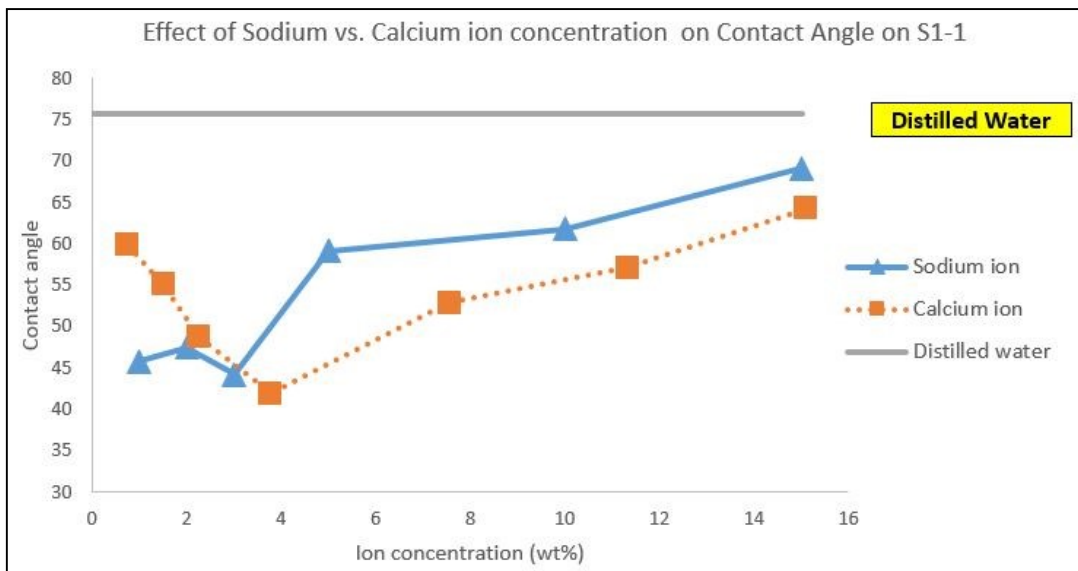


Figure 34. Comparison of the effect of sodium and calcium chloride on the wettability of S1-1

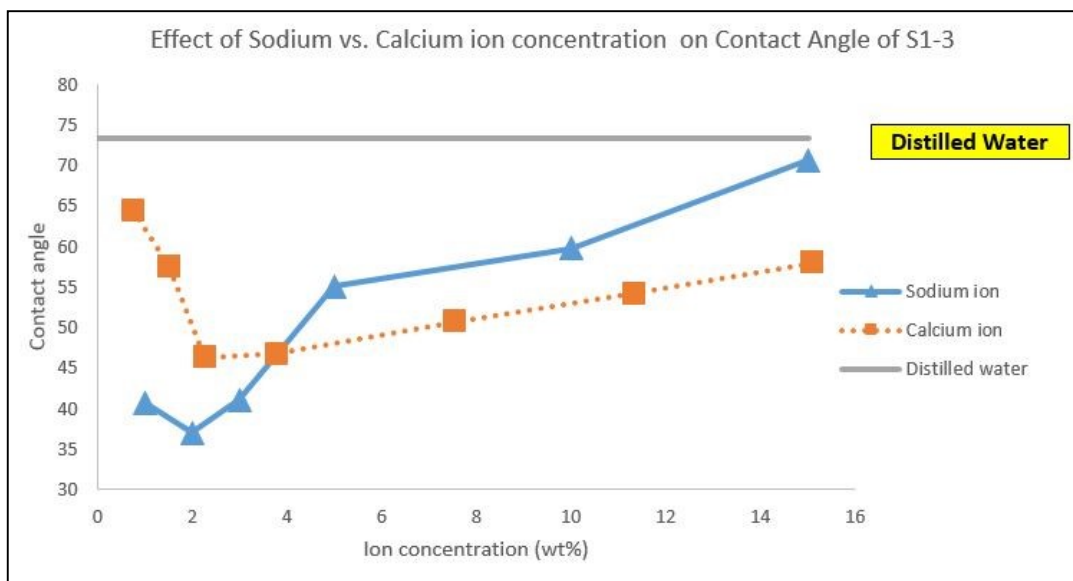


Figure 35. Comparison of the effect of sodium and calcium chloride on the wettability of S1-3

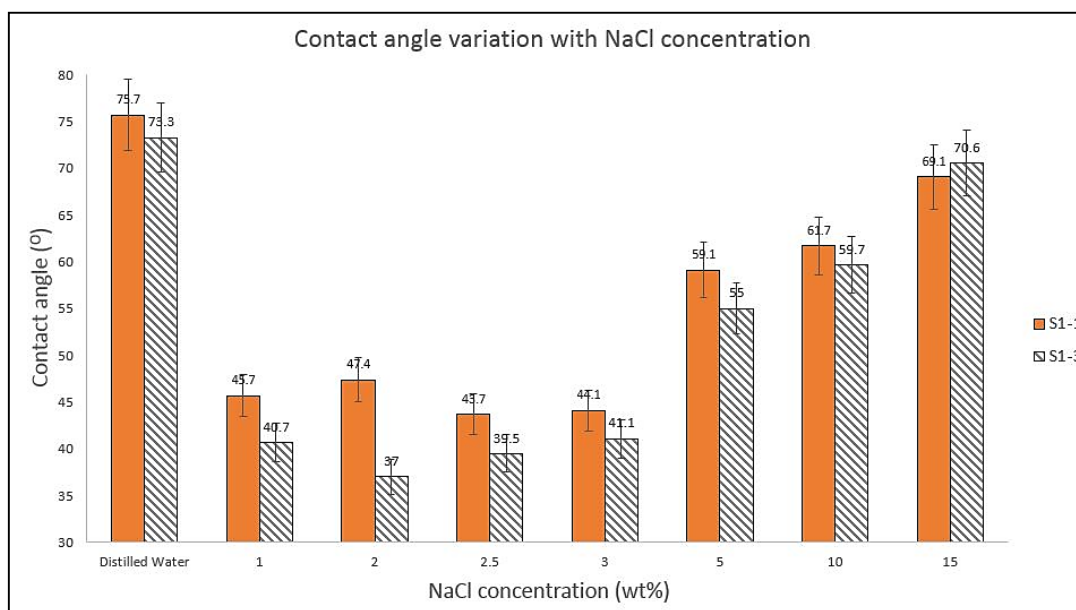


Figure 36. Changes in contact angle with increasing NaCl concentration for both samples

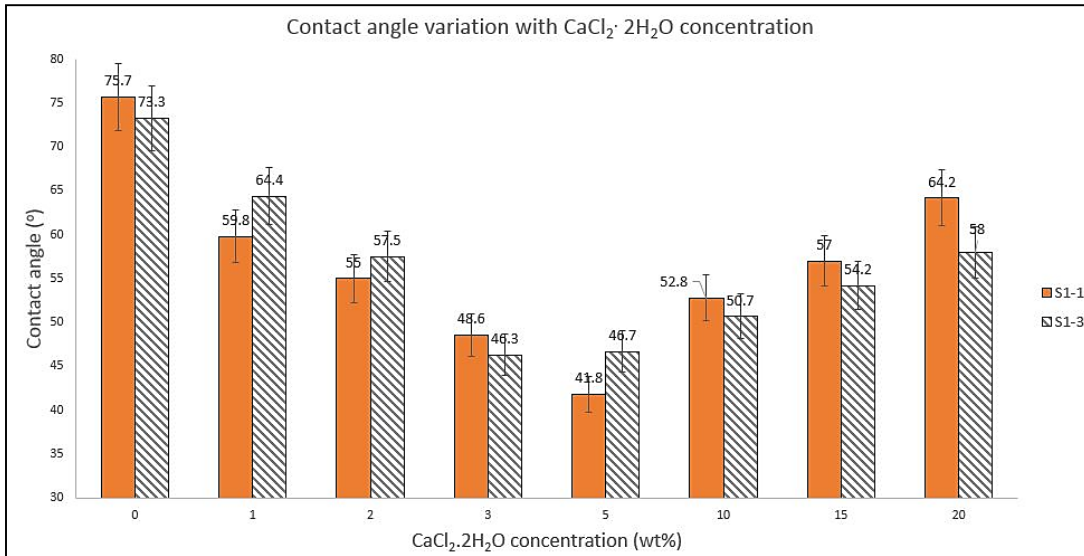


Figure 37. Changes in contact angle with increasing CaCl₂ concentration for both samples

The results from contact angle experiments confirmed that adding monovalent (Na⁺) and divalent ion (Ca⁺²) salts did affect the contact angle of the shale surface. All the contact angles obtained for various concentrations were lesser than that obtained using distilled water which implied the rock was more water when it was in contact with brines. However, the trends observed suggest both the ions had an optimum concentration at which the contact angle was the least. This value was found to be around 2-2.5 wt% for NaCl and 5 wt% for CaCl₂·2H₂O. The reduction in contact angles for the salts can be attributed to (a) double layer expansion by repulsion and (b) multicomponent ion exchange leading to the desorption of adsorbed oil molecules as discussed by Myinth and Firozabadi (2015). The contact angle increased with increasing salt concentration as expected due to salting out effect wherein the salt dehydrates the region around an oil

molecule thereby forcing the polar surface active groups in the oil droplet to spread on the rock surface rather than staying in contact with the aqueous fluid. Also the Debye length, as discussed in the literature review section, decreases with increasing ionic strength thereby reducing the stability of an aqueous film on rock surface.

Comparing the effect of sodium and calcium ions on rock wetting properties, contact angle results from both samples indicated that sodium was more effective than calcium at lower concentrations and produced lesser contact angles while calcium was found to be more effective as the concentration increased. These results suggest that the mechanism by which both the ions affect wettability may be different with one of the two earlier discussed mechanisms being the dominant factor in each case. Further experimentation was needed to verify this.

3.3.4.2. Surfactant results

Samples from two wells namely S-1 and SW-1 were chosen for the study of wettability change with surfactants. Four samples were chosen per well to ensure consistency in the trends observed. The samples for SW-1 had a depth range of 100 feet while those for S-1 had a range of 60 feet. The details of the samples are as follows:

Table 6. Rock sample details for surfactant tests

Well	Sample depth (feet)	Lithology						
		Calcite	Dolomite	Clays	Quartz	Pyrite	Marcasite	Plagioclase
SW-1	1	46.1	1.3	26.4	15.1	4.6	0.4	2.5
	2	54.7	1.0	20.4	11.8	3.0	0.7	4.4
	3	50.3	0.6	22	12.7	4.3	0.8	3.3
	4	50.7	0.5	20.9	13.1	4.4	1.1	3.5
S-1	1	57.9	0.5	18.0	16.2	3.8	1.1	2.6
	2	60.2	0.9	15.8	15.4	4.1	1.0	2.6
	3	53.9	1.1	21.7	14.8	4.4	1.1	3.0
	4	53.9	1.1	21.7	14.8	4.4	1.1	3.0

Contact angle results obtained for surfactants with the rock samples from various depths are presented in **Table 7**.

Table 7. Contact angle results for surfactants with SW-1 and S-1

Well		SW -1 (deg.)				S - 1 (deg.)			
		1	2	3	4	1	2	3	4
Distilled Water	-	96.1	97.5	86.2	99.2	95.1	72.8	82	89.7
C1	0.2 gpt	85.1	85	91	80.5	66.2	66.7	68.9	74.8
	1 gpt	76.3	70.5	80	76	61.3	63.4	67.9	63.6
	2 gpt	66.5	66.8	77.8	69.5	75.9	82.2	76	69.4
N1	0.2 gpt	87.4	73.2	75.1	90.2	78.9	63	60.3	73.6
	1 gpt	63	59.6	61.9	78.9	59.5	54.7	54.1	61.4
	2 gpt	50.3	48.3	53.5	57.8	49.4	49.1	45.6	50.5
A1	0.2 gpt	85.2	82	73.4	83.6	74.9	61.1	64.6	77.7
	1 gpt	54.1	56.6	61.4	59.6	53.7	59.3	58.6	57.2
	2 gpt	44.2	41.7	41.7	42.3	49.1	40.7	44.8	45.6

Initial tests with distilled water suggested all the samples were intermediate wet as indicated by **Figures 38 and 39**.

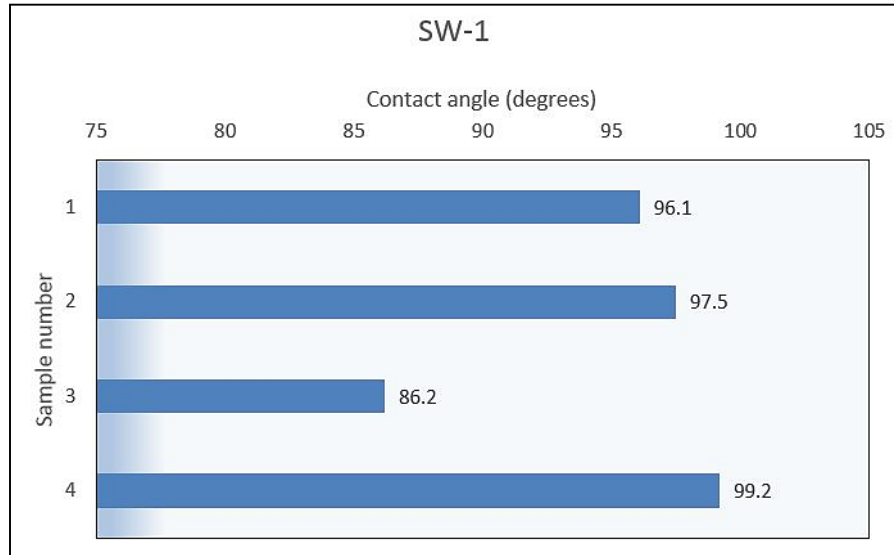


Figure 38. Contact angles for SW-1 with distilled water

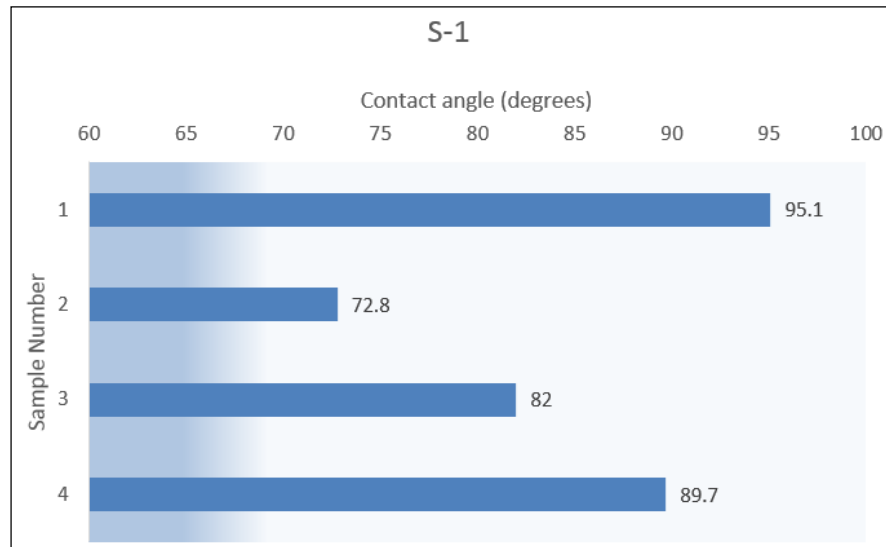


Figure 39. Contact angles for S-1 with distilled water

Results obtained from the contact angle experiments for SW-1 are shown in **Figures 40-42** while those for S-1 are shown in **Figures 43-45** for anionic (A1), nonionic (N1) and complex (C1) surfactants. The sample number and the corresponding contact angle in degrees are indicated in the box below each drop capture image and the concentration of surfactant being indicated by the boxes to the extreme left in each row of images.



Figure 40. Contact angle results for SW-1 with surfactant A1



Figure 41. Contact angle results for SW-1 with surfactant N1



Figure 42. Contact angle results for SW-1 with surfactant C1



Figure 43. Contact angle results for S-1 with surfactant A1



Figure 44. Contact angle results for S-1 with surfactant N1



Figure 45. Contact angle results for S-1 with surfactant C1

Figure 46-49 illustrate the trends in contact angle changes for well SW-1 with the three surfactants namely A1 (anionic), N1 (nonionic) and C1 (complex) for 0.2, 1 and 2 gpt concentrations.

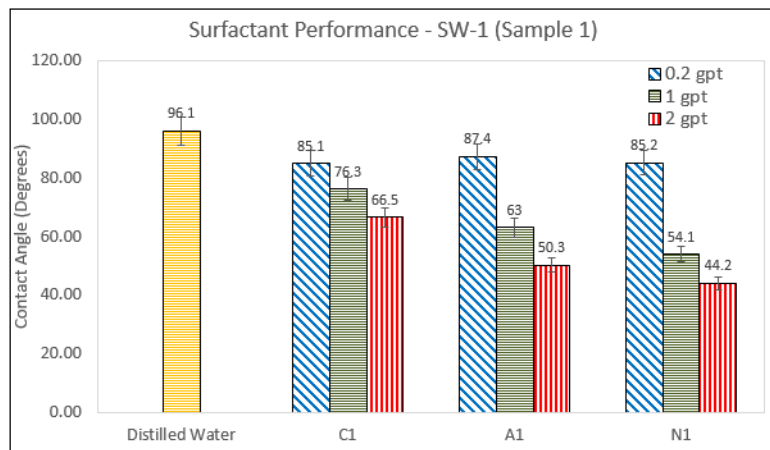


Figure 46. Contact angles with surfactants for SW-1 sample 1

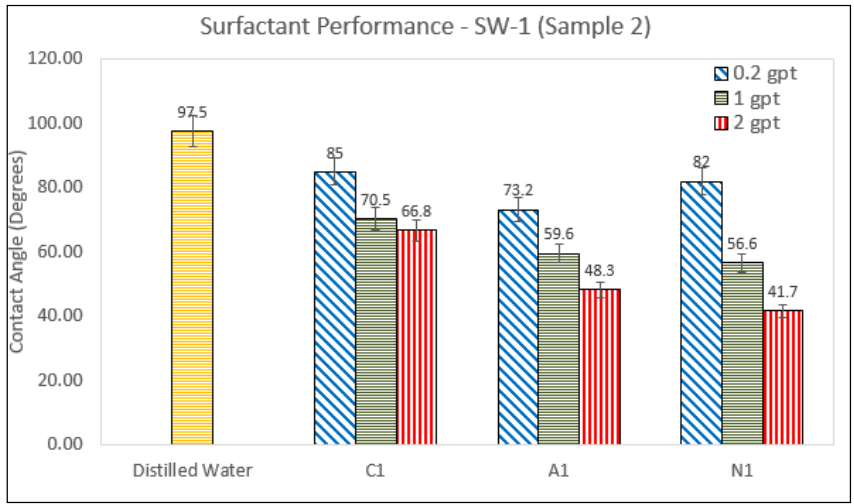


Figure 47. Contact angle results with surfactants for SW-1 sample 2

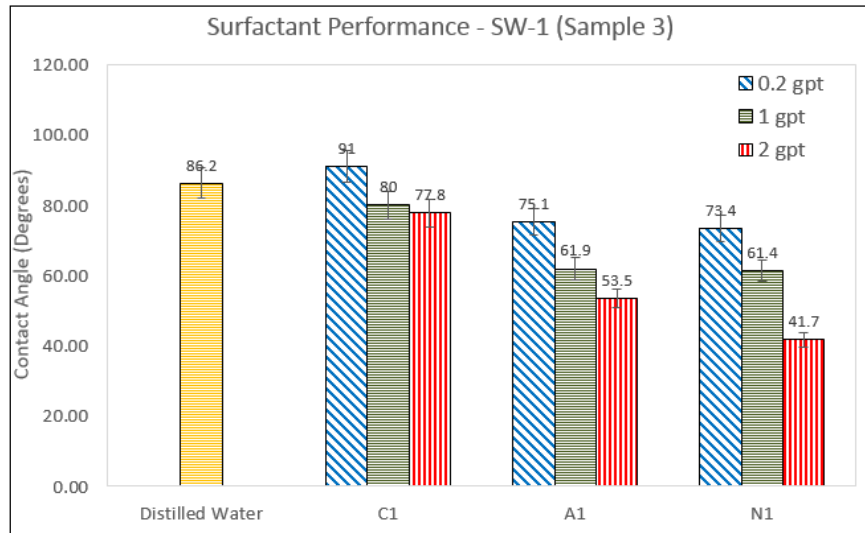


Figure 48. Contact angle results with surfactants for SW-1 sample 3

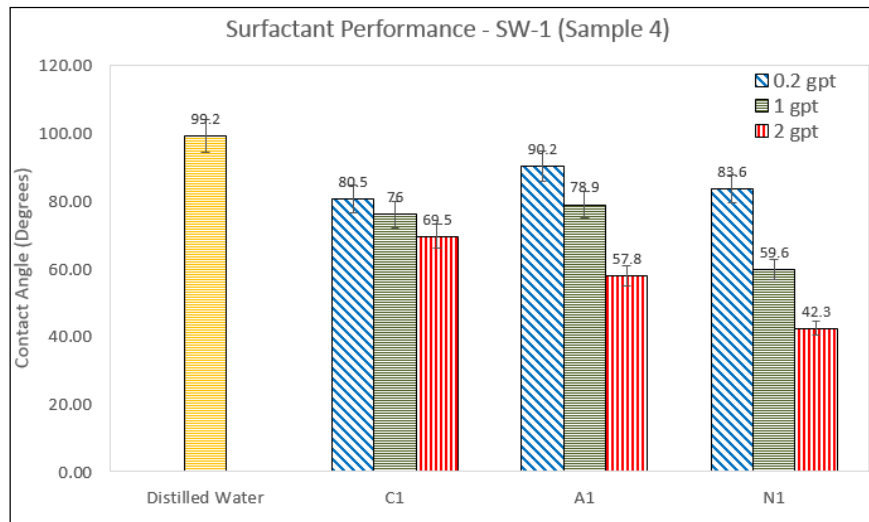


Figure 49. Contact angle results with surfactants for SW-1 sample 4

Figures 50-53 illustrate the changes in contact angles for samples from well S-1 when 0.2, 1 and 2 gpt solutions of the three surfactants were used.

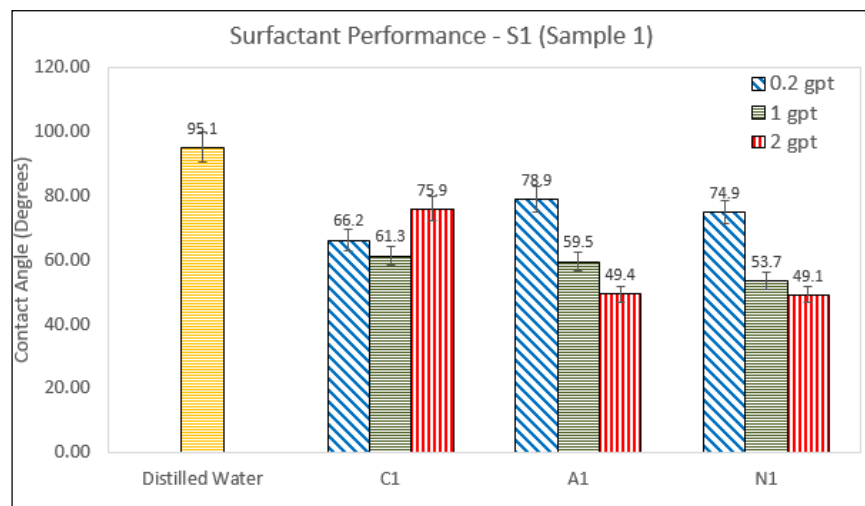


Figure 50. Contact angle results with surfactants for S-1 sample 1

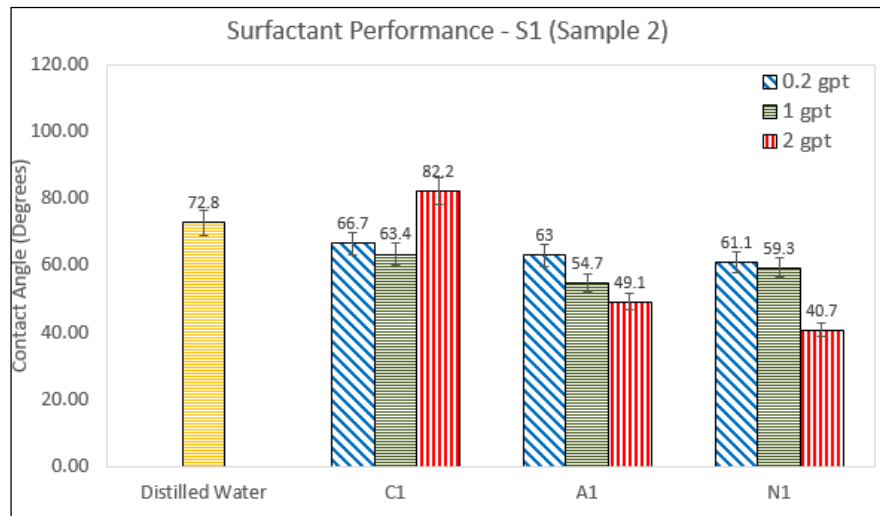


Figure 51. Contact angle results with surfactants for S-1 sample 2

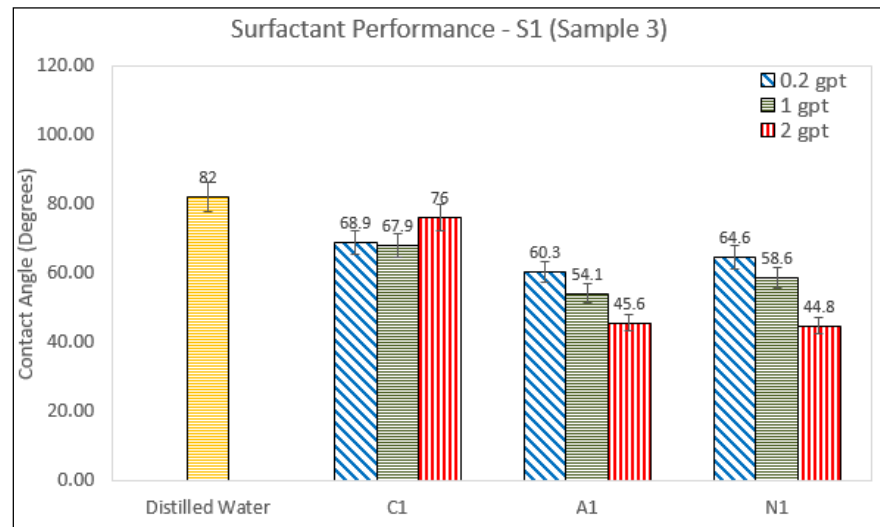


Figure 52. Contact angle results with surfactants for S-1 sample 3

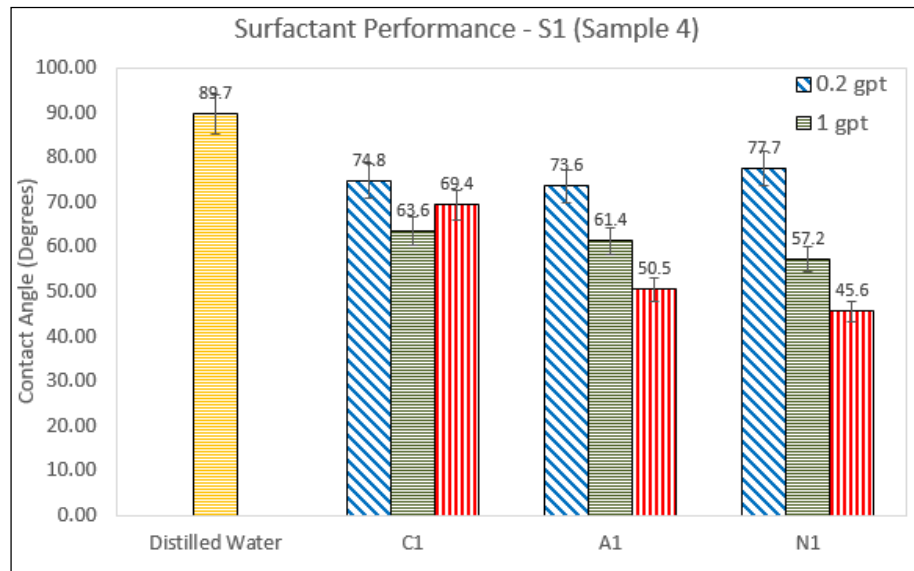


Figure 53. Contact angle results with surfactants for S-1 sample 4

As was observed from the results, all the surfactants were effective in reducing the contact angle and promoting water wetness from an intermediate wetting state of the rock samples. A1 was found to have the highest effect in decreasing the contact angle towards water wet followed by N1. Complex surfactant gave poor results for some sample depths and was not as effective as A1 and N1 though it promoted water wetness in most cases. The contact angle decreased with increasing concentration for all cases for A1 and N1 and in most cases for C1. Thus, 2 gpt was found to be better for promoting water wetness. The results can be better understood by visualizing the reduction in contact angle at 2 gpt of surfactants for both wells as shown in **Figures 54 and 55**.

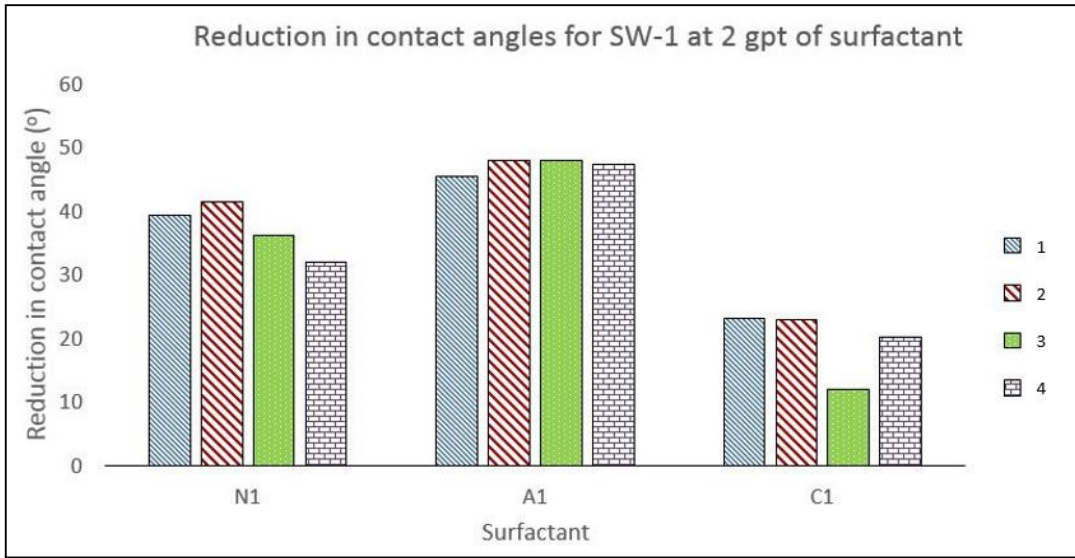


Figure 54. Reduction in contact angle for SW-1 at 2 gpt surfactant concentration

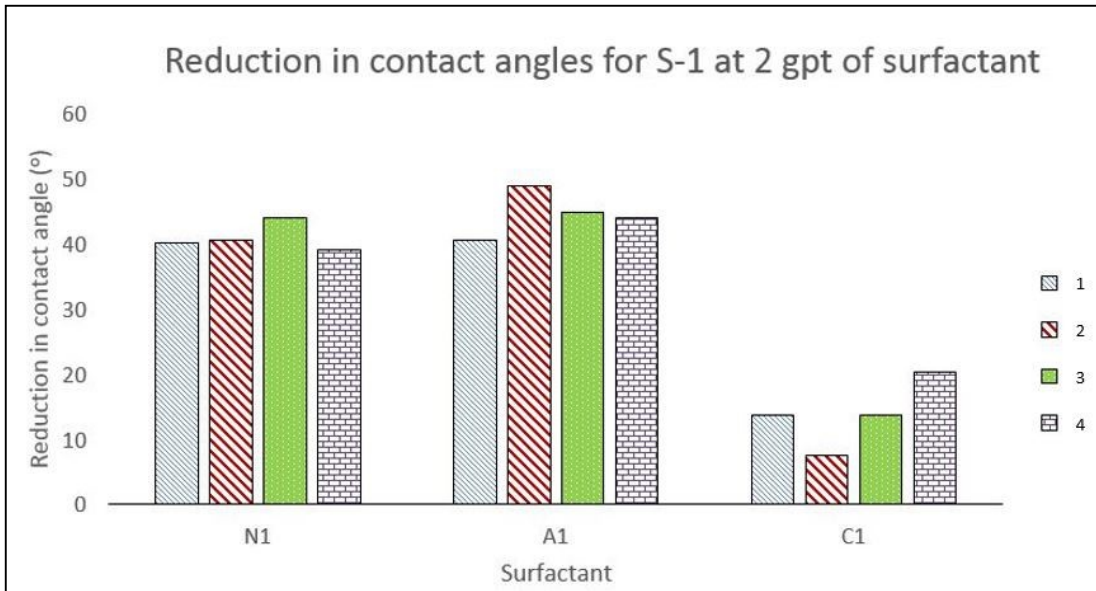


Figure 55. Reduction in contact angle for S-1 at 2 gpt surfactant concentration

As can be observed from the results above, the reduction in contact angle is highest for the predominantly anionic surfactant A1 followed by nonionic surfactant N1 while the complex surfactant was the least of the lot. The performance of anionic surfactant can be related to the fact that its negatively charged heads compete with the negatively charged surface active groups in crude oil to adsorb onto the shale surface which has a high calcite percentage. The reason for the performance of complex surfactant is difficult to comprehend owing to the uncertainty in its composition.

3.4. Interfacial tension measurements

Interfacial tension measurements were conducted using the same apparatus as described in the previous section. An IFT test was performed after each contact angle measurement with surfactants and brine.

3.4.1. Experimental setup

The OCS 15 Pro apparatus described in the previous section was used for IFT measurements with the only modification being the chip/rock holder was not needed to perform the experiment. The J-shaped capillary needle was used to dispense oil and DSA software was employed to analyze the oil drop shape and calculate IFT using the pendant drop method described below.

3.4.2. Measurement method

Drop shape analysis was employed to analyze interfacial tension. Measurements were made using the pendant drop technique with the bottom of the bubble facing upwards and the needle below the bubble. In drop shape analysis, the surface tension is measured by fitting drop shape to the Young Laplace equation. In pendant drop technique, a drop is suspended from a needle in a bulk liquid/gaseous phase as the drop orients itself into a shape resulting from the interaction of interfacial tension and gravity. Once a drop shape has been chosen (**Figure 56**), equation 7 is used to calculate IFT (σ) (Stauffer, 1965):

$$\sigma = \frac{\Delta\rho g D^2}{H} \text{ (Eq. 7)}$$

where,

$\Delta\rho$ = density difference between the two fluids

g = acceleration due to gravity

D = equatorial diameter

H = shape-dependent parameter

H depends on the shape factor of the drop (S) which in turn depends on the equatorial diameter D and the diameter d at a distance D from the top of the drop (Andreas *et al.*, 1938).

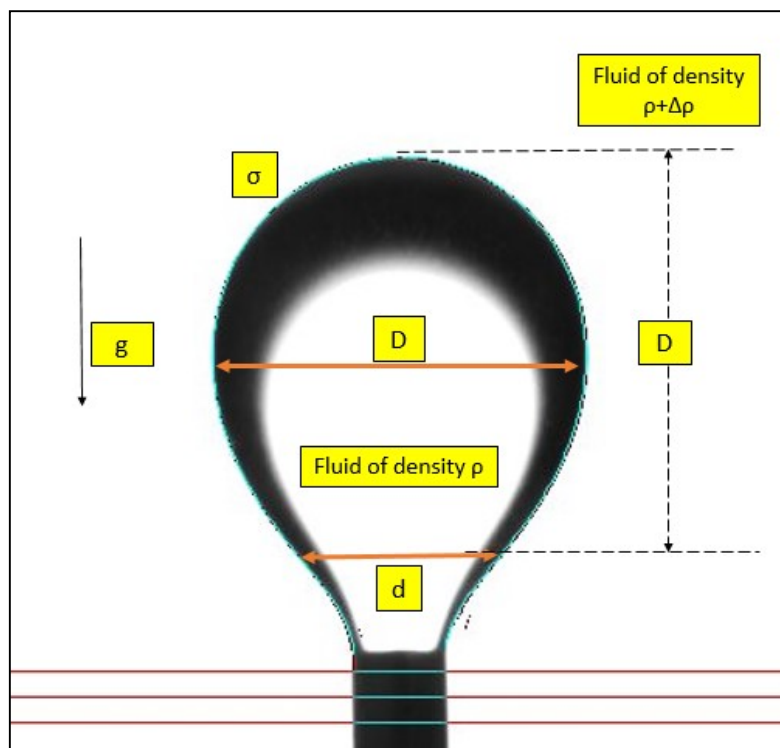


Figure 56. IFT measurement using the pendant drop technique

3.4.3. *Measurement procedure*

The following were the major steps in IFT measurement procedures:

1. Solutions of surfactants/salts were prepared as discussed previously.
2. A clean and clear cuvette was used to hold the solutions. It is important to ensure the cuvette doesn't heat or cool rapidly as thermal effects may lead to brittle failure of the cuvette.
3. The cuvette containing aqueous solution is then placed on the platform that is heated to a previously set temperature by means of a circulatory water bath.

4. A temperature sensor is then placed in the cuvette to monitor the bulk temperature of the solution.
5. Upon reaching the desired temperature, the sensor was taken off from the solution and the J-shaped capillary needle filled with the oil phase is lowered into the solution.
6. Pendant drop (bottom up) technique was chosen in the DSA software as oil was dispensed in small increments. These increments depend on the type of solution in the cuvette. For example, anionic surfactant produced low values of surface tension at 2gpt concentrations owing to which 0.05 μm increments were used to measure IFT. Whereas higher increments ($\sim 2\text{-}5\mu\text{m}$) could be used while measuring IFT of oil in distilled water, which needed high volumes of oil owing to high interfacial tension.
7. Oil was dispensed till the drop left the needle. Care should be taken to ensure the oil droplet is in equilibrium prior to dispensing additional amount. It is also paramount to ensure the droplet leaves the needle purely due to the buoyancy and not due to force exerted by injection.
8. Upon the oil drop leaving the needle, the frames captured by the existing video capture device were analyzed and the frame closest to the moment of detachment of the drop from the needle was chosen to analyze drop shape using DSA software.
9. Upon providing the density values for both fluids and needle diameter, the software provides a value of IFT upon adjusting the baseline accordingly.

3.4.4. Results and discussion

Interfacial tension results for the crude oil/brine and crude oil/surfactant solution systems are presented in the following sections.

3.4.4.1. Brine results

The interfacial tension results obtained for various concentration of Na⁺ and Ca²⁺ ions in solution are as listed in **Table 8**. **Figure 57** represents these results.

Table 8. IFT results for oil-brine interface

Brine	Brine Salinity (wt%)	Cation Content (wt%)	IFT (mN/m)
Distilled Water	-	-	34.03
NaCl	1	1	32.25
	2	2	31.63
	2.5	2.5	31.57
	3	3	31.2
	5	5	30.36
	10	10	29.4
	15	15	28.8
CaCl ₂ .2H ₂ O	1	0.755	31.04
	2	1.51	29.36
	3	2.265	28.15
	5	3.775	29.33
	10	7.55	24.55
	15	11.325	25.3
	20	15.1	23.74

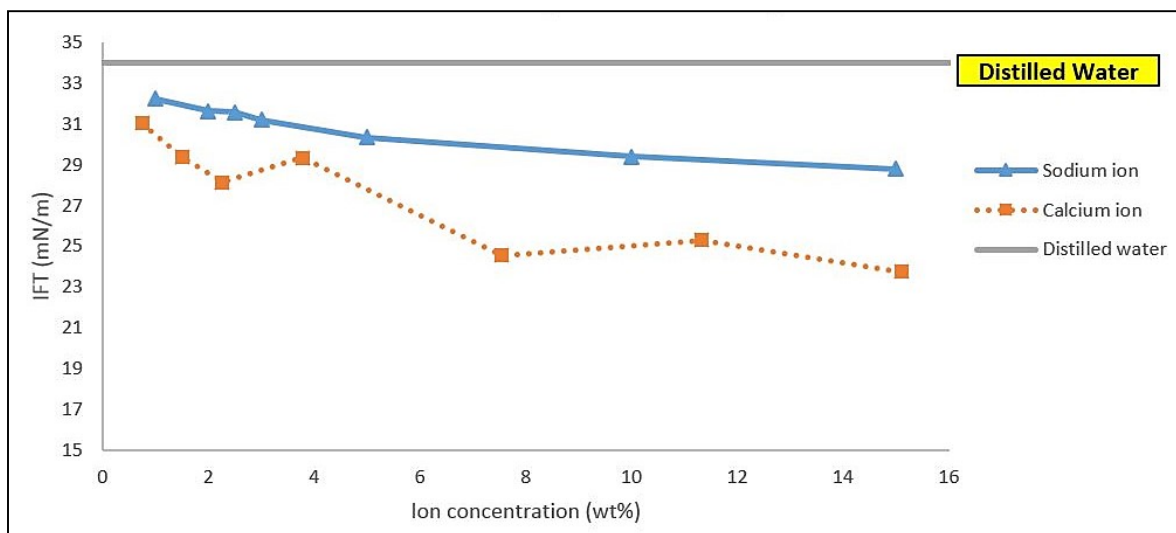


Figure 57. Variation in crude-brine IFT with increasing ion concentration

Figures 58 and 59 show the captured pictures of oil droplets in the brine solution that were used by the drop shape analysis software to calculate the interfacial tension values. The values on the boxes show concentration of the salt added with the corresponding IFT value is shown in braces.

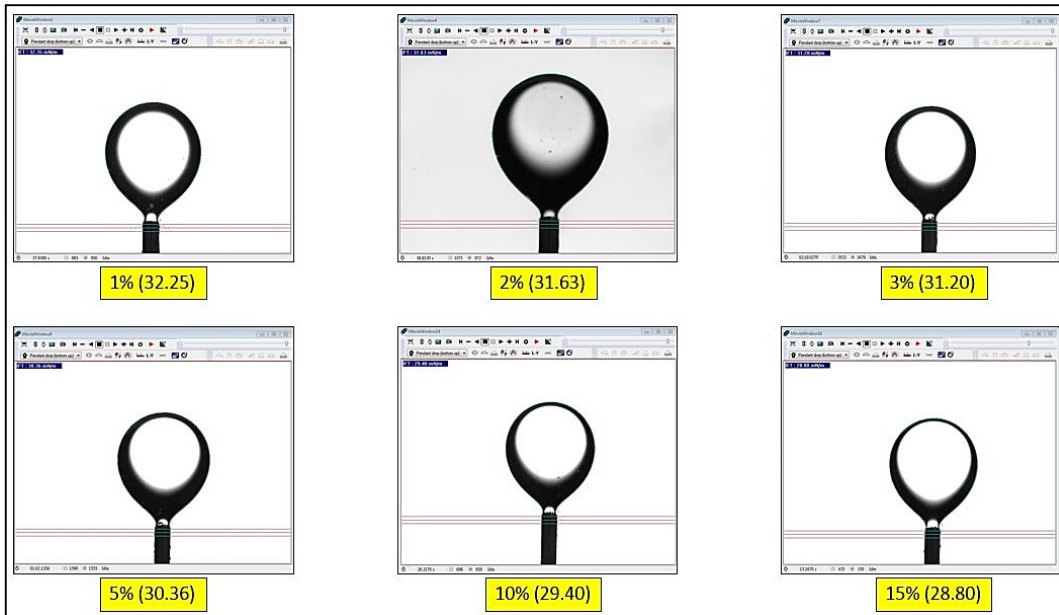


Figure 58. Crude oil – brine IFT results for various sodium salt concentrations

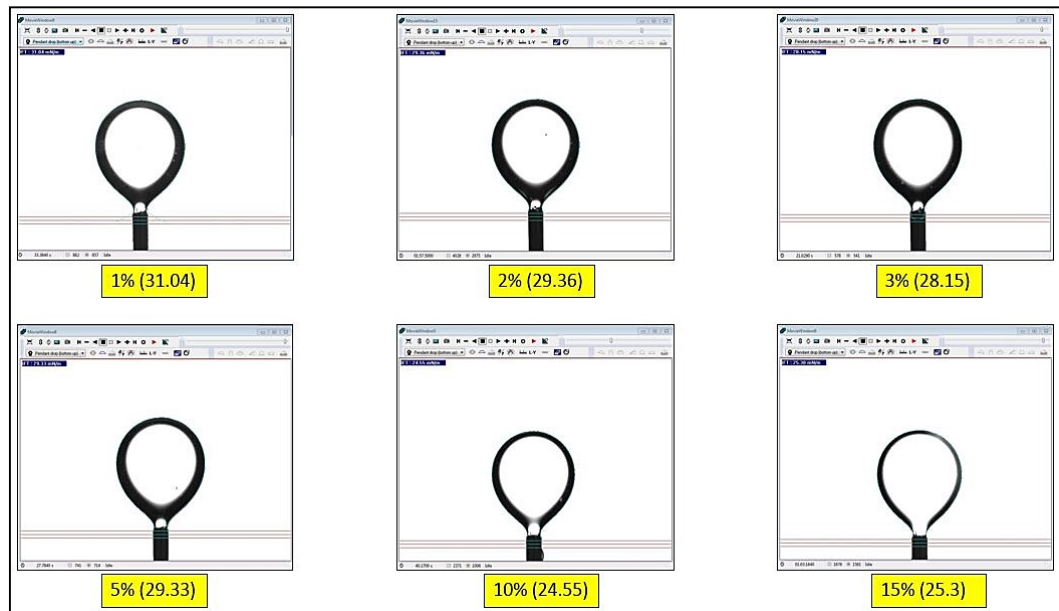


Figure 59. Crude oil - brine IFT for various calcium salt concentrations

Initial crude oil-water interfacial tension was found to be 34.03 mN/m, which is a significant value. Addition of NaCl and CaCl₂ did reduce the IFT but not significantly. NaCl at 15 wt% reduced the IFT to 28.8 mN/m, which is 5.23 mN/m less than the initial value while CaCl₂.2H₂O at 20 wt% (15.1 wt% of CaCl₂) produced an IFT of 23.74 mN/m, which is 10.29 mN/m less than the initial value implying calcium salt was twice as effective as the sodium salt at reducing the IFT. These results suggest that increasing salt concentration also increases the concentration of polar surface active agents of oil near the oil-brine interface, which further improves the solubility of oil in the brine and reduces the associated interfacial tension as suggested by Bai *et al* (2010). Divalent calcium salt was found to be more effective in this regard compared to the monovalent sodium salt. This might have to do with the fact that the cations react with acidic components of the crude thereby reducing their surface concentration, which leads to the diffusion of more surface active molecules to the oil-brine interface. This cationic association with polar components is better in case of divalent ions that bear higher positive charge compared to the monovalent cations as is observed in the results obtained.

3.4.4.2. Surfactant results

IFT measurements were also conducted with surfactant solutions at three different concentrations of 0.2 gpt, 1 gpt and 2 gpt. The results obtained are shown in **Table 9** and **Figure 60**. **Figure 61** shows captured images of oil drop in surfactant solution that were utilized by the drop shape analysis software to compute the interfacial tension using pendant drop technique. **Figure 62** depicts the trends in IFT alteration with surfactant type

and concentration. **Figure 63** is a bar graph showing the reduction in IFT from initial oil – water IFT for the three concentrations of various surfactants.

Table 9. IFT results for oil-surfactant solution interface

Surfactant	Concentration (gpt)	IFT (mN/m)
Distilled Water	-	34.03
C1	0.2	10.26
	1	7.15
	2	7.25
N1	0.2	7.55
	1	5.49
	2	4.48
A1	0.2	6.35
	1	4.57
	2	2.89

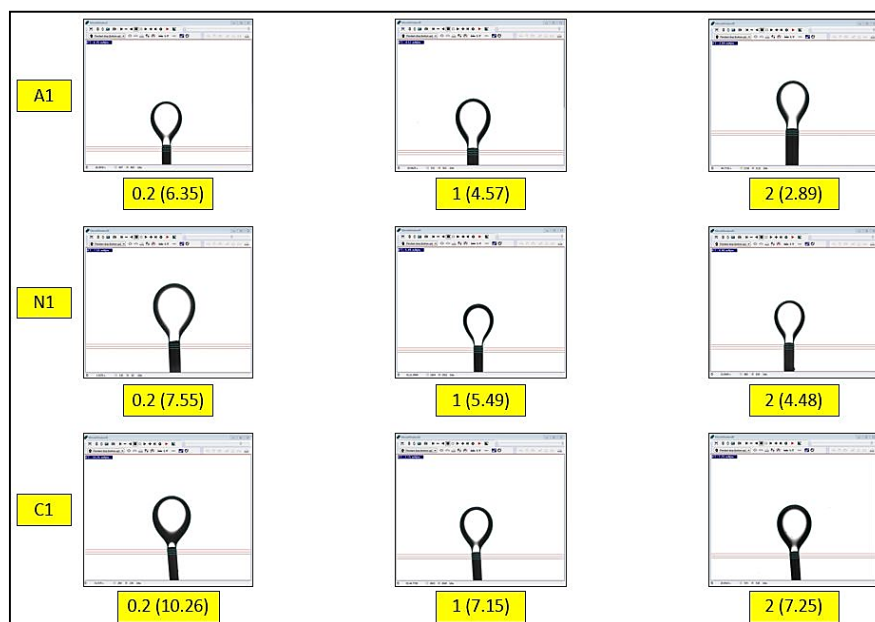


Figure 60. Crude oil - aqueous phase IFT for various surfactants

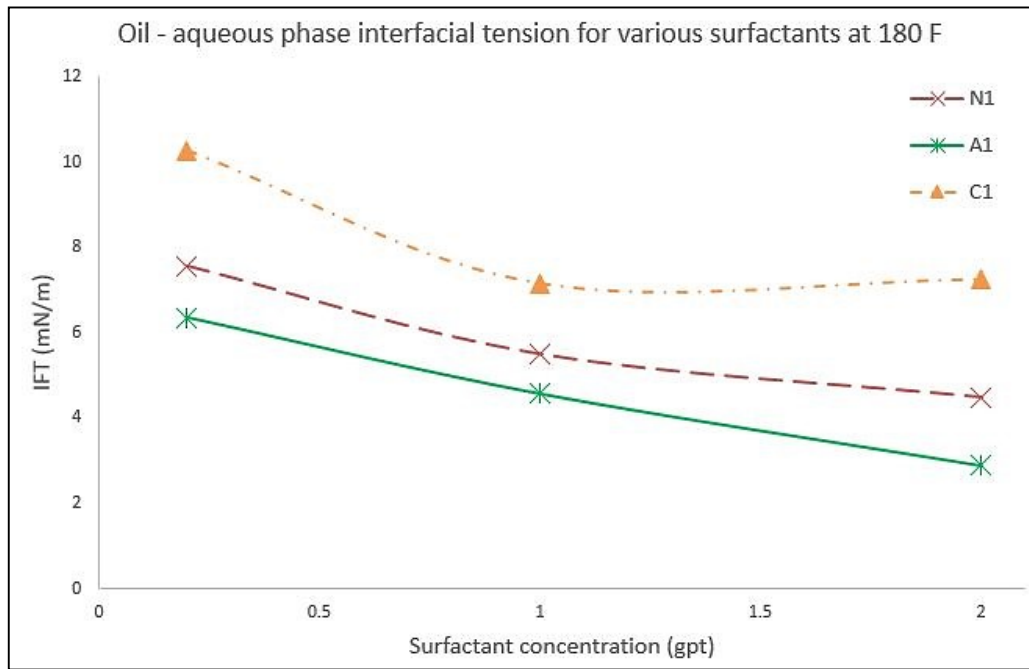


Figure 61. Variation in crude oil - aqueous phase IFT with various surfactants

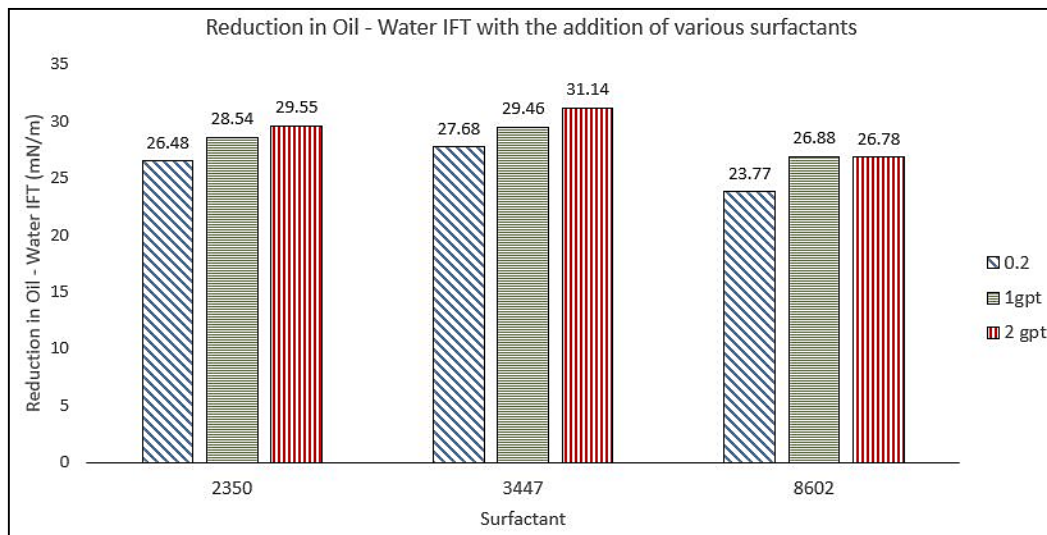


Figure 62. Reduction in crude oil - aqueous phase IFT with various surfactants

As the above figure suggests, all the surfactants were effective at reducing the oil/water IFT which was initially at 34.03 mN/m. Anionic surfactant was the most effective in reducing the IFT followed by nonionic and complex surfactants. Higher concentrations of surfactants were found to reduce the IFT better, which is expected as all these surfactants had critical micellar concentrations higher than the tested concentrations.

3.5. Zeta potential measurements

Zeta potential can be defined as the electric potential between any point in the bulk fluid and the outermost slipping layer called shear plane of counter ions that are attracted to the oppositely charged solute ion. This is better illustrated in the figure below.

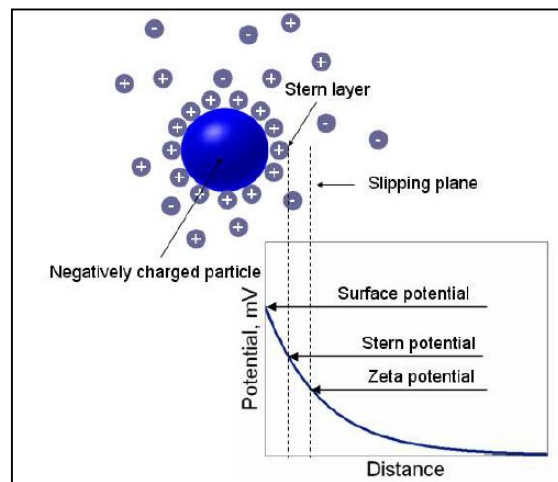


Figure 63. Electrical double layer showing various regions around a charged particle and corresponding electric potentials (Hunter, 2001)

Zeta potential gives an indication of the strength of surface charges on a solute particle as well as the nature of the charge. Higher the zeta potential, stronger is the

stability of solute particles in the colloidal dispersion. In other words, higher zeta potential values for a rock-fluid system imply the fluid forms a stable film on the rock surface. If the zeta potentials for oil-fluid and the rock-fluid interfaces are high and of similar nature, it is safe to say the fluid effectively forms a stable layer between the oil and rock boundaries owing to repulsive interactions of high magnitude between the two interfaces of the double layer. As a convention, zeta potential values (+/-) ranging from 0 – 5 indicate poor stability and rapid flocculation while those above 60 indicate excellent stability. Values around 30 – 40 are considered to be moderately stable while those ranging from 10 to 30 indicate incipient stability.

3.5.1. Experimental setup

The NanoBrook™ ZetaPALS device (**Figure 64**) for zeta potential measurements was manufactured by Brookhaven instruments. The ZetaPALS device has the capability of measuring zeta potential by two different methods namely electrophoretic light scattering (ELS) and phase analytical light scattering (PALS) techniques which are dealt with in the next section. An electrode (**Figure 65**) in contact with the colloidal dispersion whose properties are to be determined is inserted into the device and the NanoBrook™ hardware is initialized for measurements. The system also includes the ParticleSolution™ software which gathers the results from the hardware and analyzes them based on the inputs to yield a complete set of statistical data.



Figure 64. NanoBrook ZetaPALS machine for measuring zeta potential

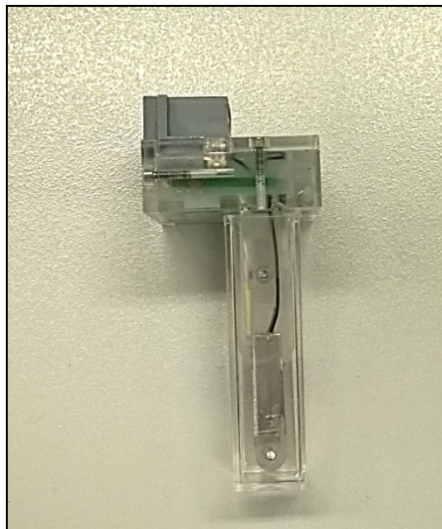


Figure 65. Electrode used for measuring zeta potential

3.5.2. *Measurement method*

The two major methods can be employed to measure zeta potential such as:

- Electrophoretic Light Scattering (ELS)
- Phase Analytical Light Scattering (PALS)

The basic principle of zeta potential measurements is to measure electrophoretic velocity of the particles in the solution, calculate electrophoretic mobility from the electrophoretic viscosity and finally evaluate zeta potential. Equations 8 and 9 illustrate this technique.

$$V_{ep} = \mu_{ep} * E \text{ (Eq. 8)}$$

The relation between electrophoretic mobility and zeta potential is defined by Smoluchowski for Debye lengths very small compared to the ionic radius as:

$$\mu_{ep} = \xi_o \zeta / \eta \text{ (Eq. 9)}$$

where,

V_{ep} = Electrophoretic velocity

μ_{ep} = Electrophoretic mobility

E = Electric field strength

ξ_o = Dielectric constant of the liquid

ζ = Zeta potential

η = Viscosity of the liquid

The electrophoretic velocity is measured by applying a finite potential difference across the suspension. The particles with zeta potential move from one electrode to another at velocities that are calculated by passing a laser beam through the solution and measuring either the Doppler shift or phase shift of the light reaching the detector at an angle of 15°. ELS passes direct current and measures Doppler shift while PALS employs alternating current and measure phase shift. This velocity is then converted into electrophoretic mobility using equation 8, which is further used for calculating the zeta potential using equation 9.

3.5.3. Measurement procedure

Zeta potential measurements are very sensitive to sample preparation and analysis procedures. This sections deals with a sample preparation procedure that has been developed for the rock, brine and surfactant samples that were used in this study which is as follows:

1. The aqueous solution (brine / surfactant) was prepared and stored in a clean container covered with Para-film/cap to ensure negligible interaction with the surroundings and exposure to contaminants like dust.
2. Rock trims and chips were finely crushed using a mortar and pestle and passed through an ASTM 325 sieve with openings no larger than 45 μm and the resulting powder was stored in a vial.
3. A clean 10-20 mL syringe was taken and its plunger removed before attaching a 0.2 μm ACRODISC syringe filter to its tip and filling it with aqueous solution.

4. The plunger is slowly inserted back into the syringe and the solution in it was pushed out, which is collected in a clean vial previously rinsed with deionized water. This is the first pass of filtration.
5. Repeating step 5 two more times by pouring the filtered solution back into the same syringe and filter assembly gave a triple filtered solution.
6. A pinch of crushed rock (typically $< 1\text{mg}$) powder was added to the filtered solution (10ml) in the vial. For oil – brine solutions, 0.1 ml (or less) of crude oil was added to the filtered solution.
7. The contents of the vial were sonicated using QSonica ultrasonic processor probe with its tip at least halfway into the solution. A frequency of 40 Hz was applied for 1 minute. The sonicated solution was left to stabilize by letting it sit for 5-10 minutes so the heavy insoluble particle could settle down. The waiting time was typically 24 hours for oil – brine measurements.
8. The solution from the vial was added to a clean and neatly rinsed cuvette and filled it up to its two thirds.
9. The electrode was inserted completely into the cuvette ensuring there are no air bubbles and the faces of the cuvette were wiped clean using Kim wipes and ensure the outside of the arrangement is completely dry. Any streaks or smudges were washed with deionized water and wiped until the surface is clean.
10. The electrode was now plugged into the device by sliding open the top lid of the ZetaPALS machine and inserting the cuvette-electrode system into the slot provided.

11. The lid was closed and zeta potential measurements were taken by initializing Particle Solutions™ software and selecting the PALS mode of zeta potential measurement. Once the measurement is done, the cuvette was removed and dispensed as it cannot be re-used.
12. Electrode was washed with deionized water and put back into the storage cell. The electrode is the most important and sensitive component of the machine which required proper cleaning and maintenance for better results.

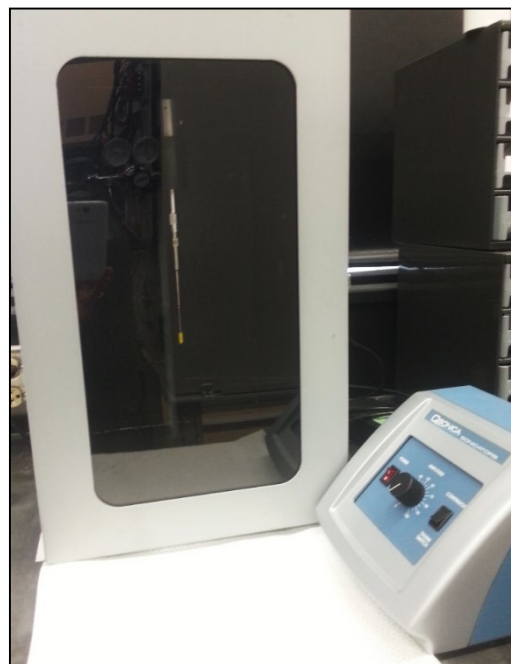


Figure 66. QSonica sonicator probe with controller

The machine was found to produce the cuvettes contained clear solutions. An indication of satisfactory clarity in these solutions is the reference vs. sample count rate

as calculated by the software. Reference and sample count rates infer to the number of photons measured that correlates to the light scattering in the solution. High sample count rates than the reference count rates imply high light scattering and inconsistent results. It was advised to obtain a sample close to half of the reference count rate. Hence the solutions were diluted to adjust the count rate based on the feedback of the previous run. It was also ensured that the standard deviation in zeta potential values was less than 2 mV.

The following precautions were taken to ensure consistent and reliable results:

1. Every container or volumetric equipment was rinsed with distilled water before use
2. The solutions were covered from being exposed to surroundings
3. A clean, dust free environment was chosen for sample preparation. Dust can significantly affect results.
4. The electrode was maintained dry and clean.
5. It was ensured no air bubbles were attached to the electrode before measurement and any bubbles present were shaken off by tapping the electrode – cuvette arrangement gently on a hard surface.
6. The sonic probe was cleaned with distilled water before immersing it into the solution for sonication.
7. Samples prepared were clear to slightly turbid. Samples with higher turbidity were diluted accordingly in the cuvette using the filtered stock solution and made to sit for a while to let any undissolved particles to settle down.



Figure 67. Crushed rock and triple filtered solution for zeta potential determination

3.5.4. Results and discussion

As was the case in previous experiments, two sets of zeta potential measurements were conducted with brine – rock and surfactant – rock samples. Zeta potential of oil-brine and oil-surfactant solutions were also measured and reported. The results are discussed in this section. The rock samples used were from the same well and depths as those used for contact angle measurements with brine samples, S1-1 and S1-3. The reason behind this choice is to maintain consistency in correlating contact angle and zeta potential results.

3.5.4.1. Brine results

Sodium and calcium chloride brines were prepared and filtered as discussed in the previous sections. The sample preparation procedure was followed to prepare 4 rock-brine

and oil-brine mixture samples at 1, 2, 3 and 5 wt% concentrations. **Figures 68-70** depict the zeta potential results obtained for both the rock samples as well as with crude oil.

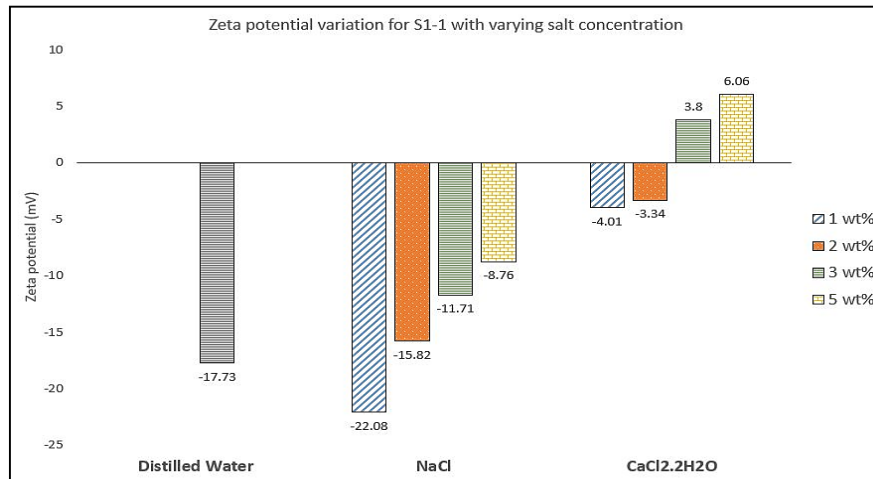


Figure 68. Zeta potential results for S1-1 with various brine concentrations

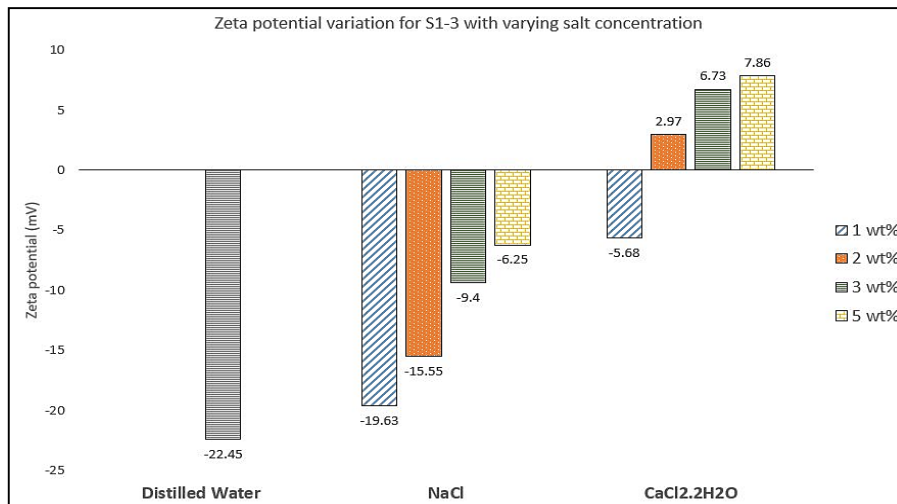


Figure 69. Zeta potential results for S1-3 for varying brine concentrations

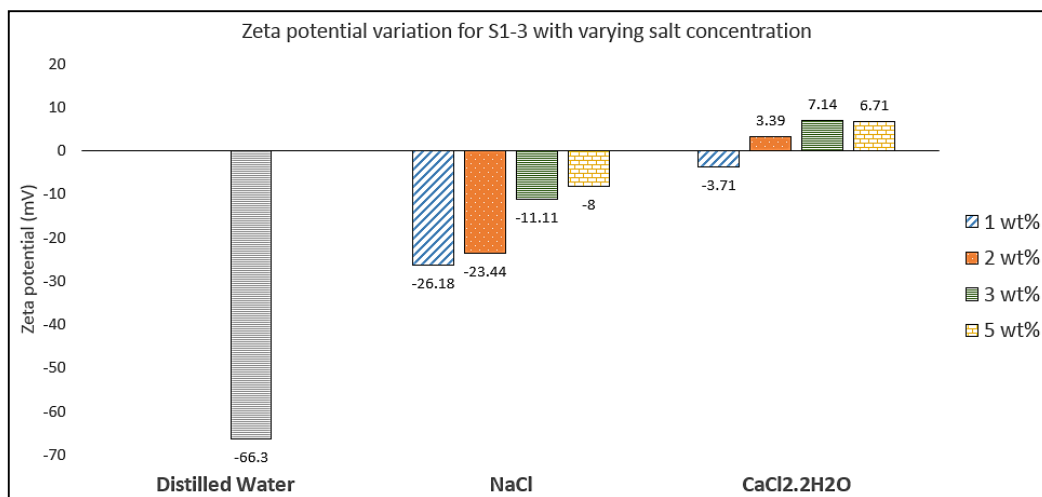


Figure 70. Zeta potential results for crude oil - brine system

It can be inferred from the above results that the zeta potential becomes less negative with increasing salt concentration as more cations surround the rock particles that are initially negatively charged as indicated by zeta potential values with distilled water, which were found to be -17.73 mV and -22.45 mV for S1-1 and S1-3 respectively. Zeta values of +/- 10 mV or above are assumed to be stable and those below are unstable with the stability increasing with increasing magnitude. Hence by this definition, the stability of brine films decreases as more salts are added to solution though NaCl was found to produce better stable film with S1-1 at low salinity (1 wt%) compared to distilled water. Stability of films formed by CaCl₂ were much lower compared to those formed by NaCl at all the concentrations examined. However, the increase in magnitude of the positive zeta potential with increasing Ca⁺² concentration implies an improvement in film stability, which might be a possible explanation for lower contact angles at higher salinities when compared to Na⁺. This stability of NaCl brine films at low salinity is

consistent with results obtained by Quan *et al* (2012) who suggested NaCl formed stable films on silica and clays at low salinities. Similar results were also observed by Shehata and Nasr-El-Din (2015) who tested sandstone, quartz, clays and micas and suggested 0.5 wt% NaCl produced more negative zeta potentials compared to CaCl₂ and MgCl₂ solutions.

Zeta potential results for oil suggest that the most stable film is formed with distilled water. Low salinities of NaCl formed relatively stable films compared to CaCl₂ which could not form a stable film at the salinities examined. The reason for such a huge difference in zeta potentials for the no salt and salt cases might be due to the surface activity induced by adding cations which interact with the surface active agents in the oil molecules thereby hindering the formation of a thick stable film.

The change in zeta potential from negative to positive was observed with changing CaCl₂.2H₂O salinity from 1 to 2 wt% which followed a similar trend as the corresponding rock-brine zeta potential. This suggests as the ionic content of calcium increases, the surface charge at both rock and oil reverses in nature and the repulsive forces between the two films increase with increasing salinity. Low salinities of NaCl form stable films as is observed from the zeta potential results of both brine-rock and brine-oil interfaces that have higher negativity at 1 and 2 wt% compared to 3 and 5 wt%.

The correlation of stability and negativity of NaCl films to the low contact angles at low salinities can be understood by electrical double layer expansion. More negative the zeta potential, more electronic repulsion with oil – brine interface which is usually negatively charged and stable wetting. However, the results obtained for CaCl₂ suggest

double layer expansion/ repulsion is not the only mechanism at play in wettability alteration of the rocks examined as was discussed earlier. These can be cationic adsorption at negatively charged sites and desorption of anionic polar compounds from oil by divalent cations which is the case with Ca^{+2} . Positive zeta potentials of the rock surface with increasing Ca^{+2} also verify this fact as the surface changes its nature and starts to desorb previously adsorbed cationic components from crude. Hence it is understood that a multitude of factors determine the effect of these monovalent/divalent ions in shaping the wettability of shale rock surface.

3.5.4.2. *Surfactant results*

The three surfactant A1, N1 and C1 were used to prepare solutions at 0.2, 1 and 2 gpt concentrations and zeta potentials with samples S1-1 and S1-3 were measured.

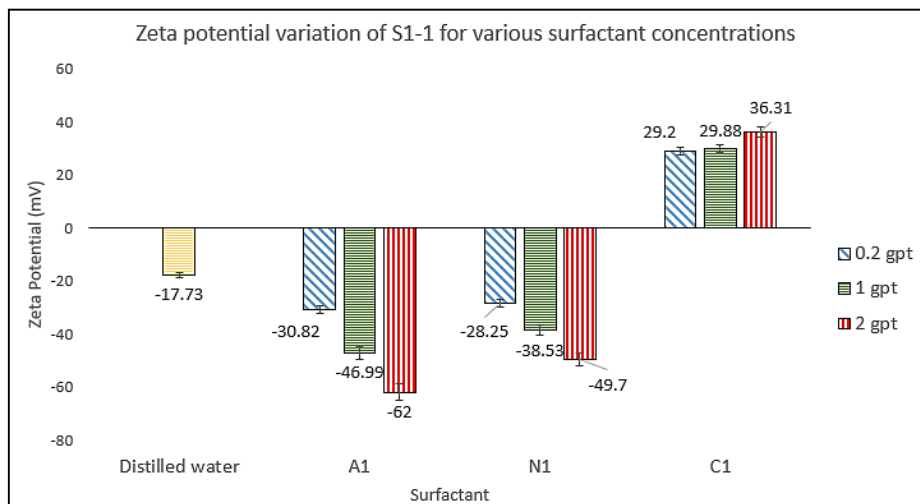


Figure 71. Zeta potential results for S1-1 with various surfactants

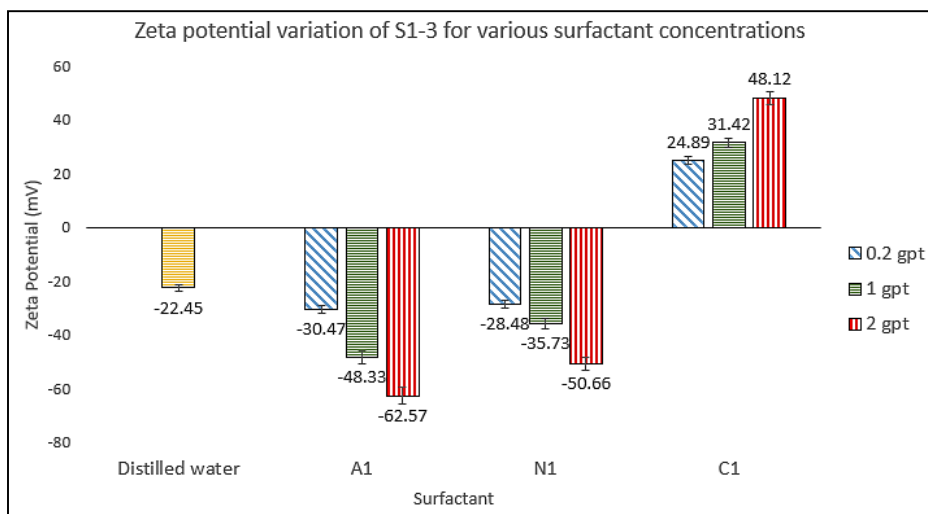


Figure 72. Zeta potential results for S1-3 with various surfactants

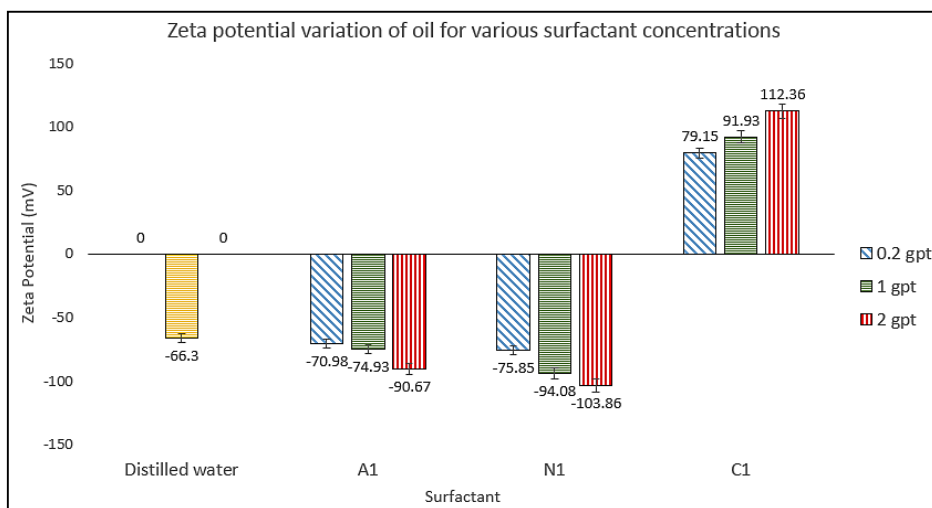


Figure 73. Zeta potential results for the crude oil-surfactant system

One of the major observations from **Figures 71-73** is the higher zeta potential values obtained with surfactants compared to distilled water and brine solutions. These indicated that all the examined surfactants formed films that were more stable than

distilled water for all the concentrations tested. It was also observed that the stability of the film on rock as well as oil droplets increased with increasing surfactant concentration, which further explains the higher reduction in contact angle towards water wet with increasing surfactant concentration. 2 gpt concentration was found to produce very stable films for A1, N1 and C1 as indicated by their zeta potential values as indicated in the above pictographs. It can also be noticed that the zeta potential values for anionic and nonionic surfactants were negative while those for the complex surfactant were positive. Most negative values for rock-surfactant zeta potential were obtained for the predominantly anionic surfactant A1 while the nonionic surfactant N1 produced slightly higher stable films in crude oil-surfactant solutions. Comparing these results with contact angle results, it can be understood that a negative charge at the rock – surfactant interface is preferred over a positive as A1 produced lower contact angles than C1. This can be explained as earlier by double layer repulsion due to negative charges at rock – surfactant and crude oil – surfactant interface.

Before spontaneous imbibition is discussed, it is important to recap the results from contact angle, IFT and zeta potential measurements to better correlate recovery of oil with these factors. The results so far indicate that anionic surfactant A1 produced the most water wet state and stable wetting films besides also reducing IFT the maximum followed by nonionic and complex surfactants respectively. The results for salts were not so straightforward. At their respective optimum salinities, sodium chloride was found to produce more water wet state than calcium chloride. However, IFT was lower for calcium chloride at all the examined salinities. Sodium chloride also produced more stable films

on the rock surface compared to calcium at lower salinities though the strength of these films was much lower than those produced by surfactants. The following graphics should summarize the results so far.

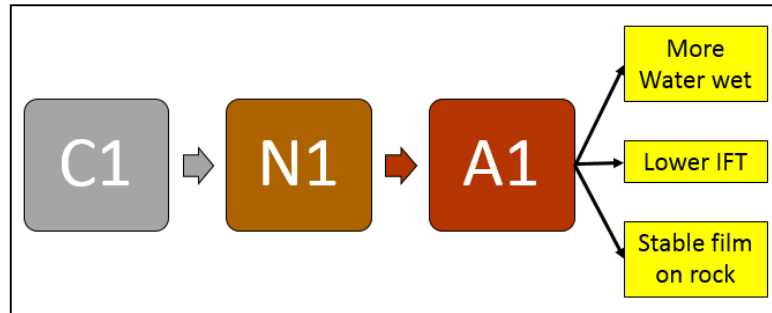


Figure 74. Summary of surfactant tests

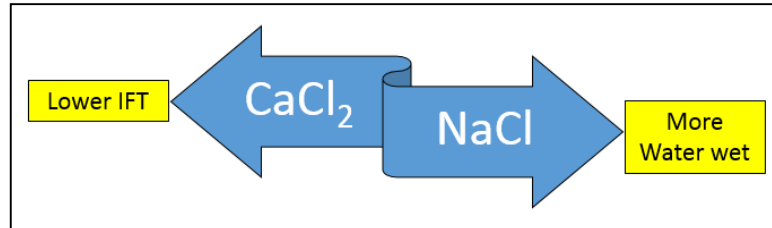


Figure 75. Summary of brine tests

3.6. Spontaneous imbibition experiments

Spontaneous imbibition experiments were conducted to analyze the effect of wettability alteration and IFT reduction by various brines and surfactant formulations on their imbibition into low permeability and low porosity core samples.

3.6.1. *Experimental setup*

Amott Harvey cells (**Figure 76**) were used for carrying out the spontaneous imbibition experiments. The cell consisted of upper and lower chambers made from glass that are held together by aluminum rings with the help of clamping screws. The lower part or the base holds the core sample on a plastic stand designed to hold 2 – 3 inch long cylindrical core samples. The upper part or top has a graduating scale attached which is used to monitor the volume of oil recovered in the process.

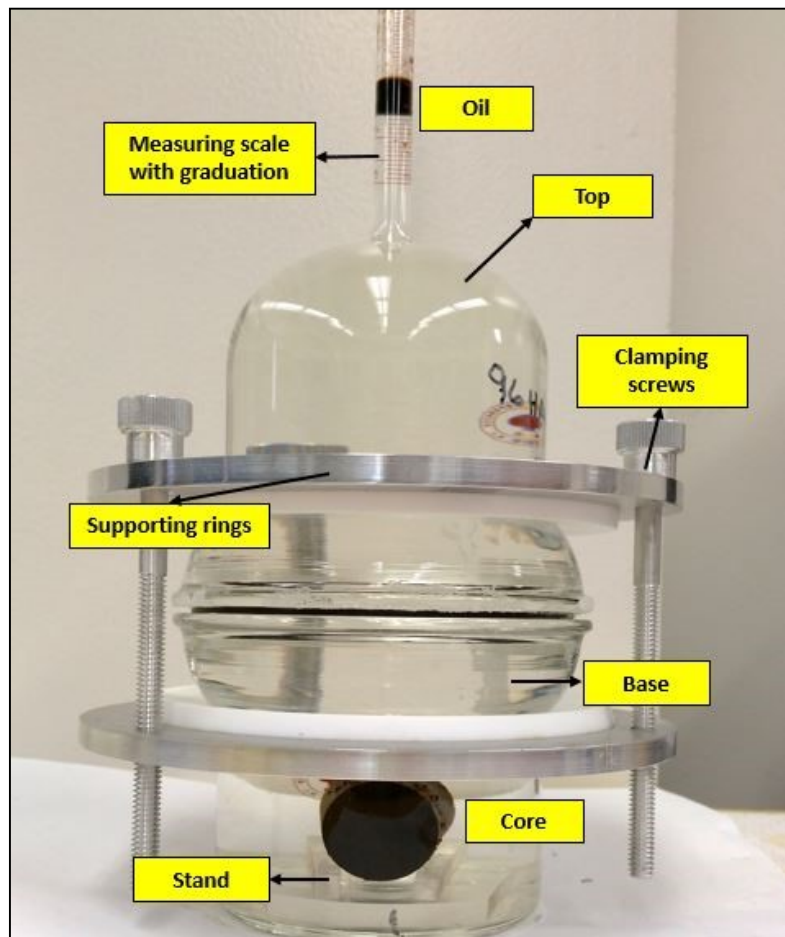


Figure 76. Amott cell for spontaneous imbibition

The Amott Harvey cell setup was placed in a Memmert U1060 oven and maintained at a temperature of 180°F. The setup was periodically scanned using a Toshiba Aquilion TSX – 101A CT scanner at the Chevron Petrophysical Laboratory at Texas A&M University. Images obtained from the CT scanner were analyzed using ImageJ, an open source image processing software.



Figure 77. Amott cells placed in the oven at a fixed temperature of 180°F

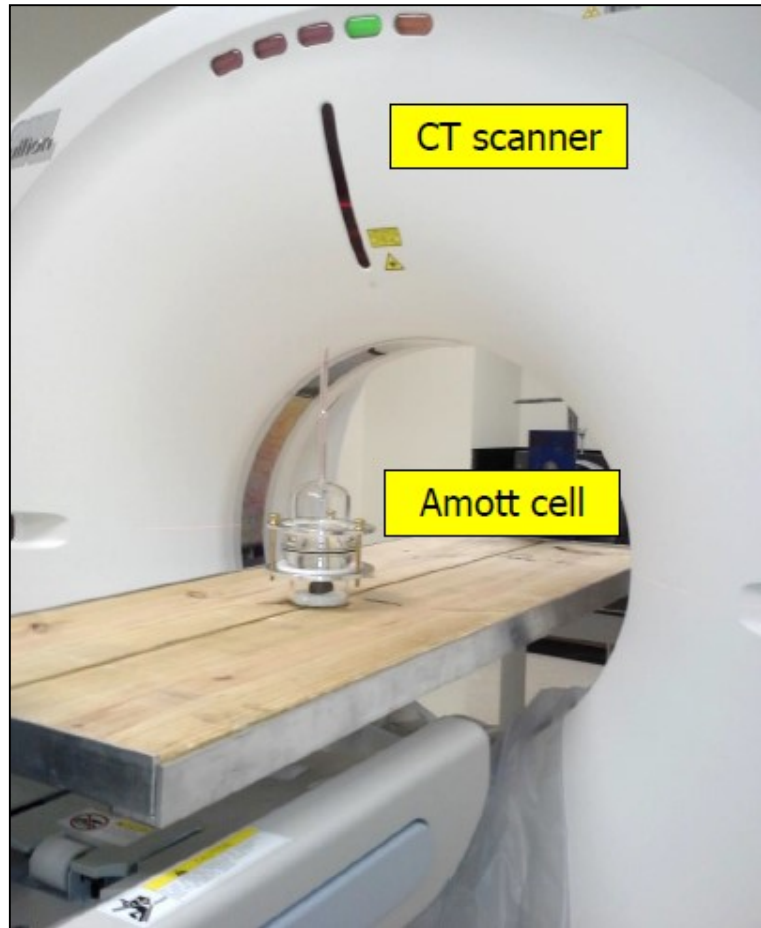


Figure 78. CT scanner with the Amott cell to be scanned

3.6.2. Measurement method

Spontaneous imbibition was carried out at elevated temperature without the aid of any pressure support. The major forces dominating the process were capillary and gravity forces as discussed in the literature review. The cores were placed horizontally and the imbibing fluid had access to the complete core barring minor area that was in contact with the plastic holder placed beneath the core. The oil leaves the cores from the sides or from

the top depending on the dominant mode of imbibition. If the process is capillary driven, the oil is produced from the sides whereas if the process is gravity driven, it is produced from the top. This depends on the vertical permeability of the cores. Those with high vertical permeability tend to favor gravity segregation. Since the samples this study deals with are characterized by ultra-low porosities, it is estimated that capillary imbibition has a more dominant effect than gravity segregation, which would require moderate to high interfacial tension between the oil and the aqueous phase.

The oil which leaves the core migrates upward into a graduating column and is measured to yield a quantitative recovery with the progression of time. The idea behind scanning the setup periodically was to observe changes in fluid saturations inside the core as affected by the movement of fluids in and out of the rock sample. A change in CT number is indicative of fluid movement. An increase in CT number implies an increase in the overall density of the sample which means a portion of low density fluid is replaced by a high density fluid and vice versa. However, it is important to note that the method is subject to experimental inaccuracies such as over cooling of the Amott cell setup which might affect the densities of fluids in situ as it decreases with increasing temperature and lead to inconsistent CT numbers with the progression of time. Hence it is important to maintain a standard protocol to minimize inconsistencies while CT scanning.

3.6.3. Measurement procedure

There were three major phases of the experimental procedure namely:

- Core preparation

- Amott cell setup
- CT scanning and data acquisition

3.6.3.1. Core sample preparation

Core plugs from well S-1 were aged for a period of three months at a temperature of 180°F. The air/gas in the containers had to be occasionally bled off to make sure the containers remained intact. Once the sample was taken out from the oil for the imbibition experiments the following procedure was adopted:

1. The plug was faintly wiped using Kim wipes to remove excess oil from the surface and weighed using a Mettler Toledo XA 105 analytical balance with a readability of 0.01 mg (0.00001g).
2. The length and diameter of the core were measured using a pair of Vernier calipers.
3. The plug is now scanned and placed in an air tight bag to minimize loss of fluids.
4. The contact angle of the core was measured at ambient conditions using distilled water using one of the flat faces of the cylindrical plug.
5. The core was re-weighed before being placed into the Amott cell.

The properties thus measured for all the samples are provided in **Table 10**.

Table 10. Properties of core samples used for spontaneous imbibition experiments

Fluid	Core sample properties					
	Depth (ft)	Diameter (in)	Length (in)	Porosity	Weight (g)	
					Pre-aging	Post-aging
Water	1	0.997	2.288	12.26	67.4886	68.5248
A1	2	0.9935	1.953	13.17	56.8222	57.9611
N1	3	0.955	2.0695	13.17	58.9438	60.1004
C1	4	0.991	1.819	13.17	52.5952	53.6934
2.5% NaCl	5	0.997	2.004	13	58.988	60.0358
5% CaCl ₂	6	1.0015	1.723	13	50.7895	51.6132
2.5% NaCl (no dopant)	7	0.994	1.028	13.17	29.984	30.435
5% CaCl ₂ (no dopant)	8	0.9975	1.8955	13	55.9605	56.9278

Samples for both brine and surfactant tests were chosen such that they did not vary significantly in terms of lithology and petro physical properties. Samples 2, 3 and 4 had a different of 0.20 feet which was also the case for samples 5, 6, 7 and 8.

3.6.3.2. Amott cell setup

Having the core dimensions, weight and contact angle measured and a pre experiment scan taken, the Amott cell setup is the next step in the experiment. The Amott cells used were manufactured by Ace Glass Inc.

1. Solutions as shown in **Table 11** were prepared by and placed in the oven for equilibration.
2. A clean Amott cell base was taken and the core from the air tight bag was placed in it on top of a plastic stand.

3. The base is now filled with the previously prepared surfactant/salt solution to its brim. An O-ring was placed on the rim of the base.
4. A clean Amott cell top was then inserted over the base with the O-ring fitting into the slot along the rim of the top and base parts.
5. Aluminum and plastic clamps held together by aluminum screws were used to hold the top and bottom parts together. It was important to ensure the fluids did not leak at the intersection of the top and bottom parts. This was ensured by the two supporting rings were parallel to each other.
6. The cell was filled with more imbibing fluid up to the neck of the top and enough room was made available for thermal expansion of the fluid.
7. The top was then plugged using a stopper and the setup was scanned with the scan labelled at $t = 0$.
8. The cells were then placed in the oven which was pre-heated to 180°F.

Table 11. Solutions prepared for spontaneous imbibition experiments

Surfactant/salt	Concentration	Amount added	Amount of dopant added	Distilled water (mL)
A1	3 gpt	3 ml	40 g	960 ml
N1	3 gpt	3 ml	40 g	960 ml
C1	3 gpt	3 ml	40 g	960 ml
NaCl ₂	2.5 wt%	25 g	40 g	935 ml
CaCl ₂ .2H ₂ O	5 wt%	50 g	40 g	910 ml

3.6.3.3. CT scanning and data acquisition

CT scanning is an equally important part of this experiment as core sample preparation or Amott cell setup. Once the Amott cell is set up without any leaks or thermal expansion and placed in the oven, periodic CT scans were conducted by adopting the following procedure:

1. The setup was taken from the oven and pictures of the core sample and oil recovered and collected in the graduating column were taken.
2. The setup was now placed on the plank of the CT scanner whose tube was pre heated. The setup was placed in such a way that the direction of scanning w.r.t. the core sample is consistent with all the previous scans.
3. The sample was then scanned using a predetermined protocol and placed back in the oven.
4. Caution was exercised to ensure the least effect of movement on the core sample.
5. Then scans taken were retrieved and processed using ImageJ to analyze the changes in CT number and fluids profile in the core sample.
6. A parameter called penetration magnitude was then calculated to quantify the movement of fluid into the core sample with the progression of time based on the initial CT number and the CT number at a time 't' from equation 5.
7. Oil recovery is calculated by dividing the measured oil volume at any instant by the product of pore volume and oil saturation of the core sample:

$$\text{Oil recovery (\%OOIP)} = \{V_{\text{oil recovered}} / (S_{\text{oi}} * V_{\text{pore}})\} * 100 \text{ (Eq. 10)}$$

3.6.4. Results and discussion

3.6.4.1. Impact of aging process

Before the results of spontaneous imbibition could be discussed, it is important to understand the effect of aging process on the core samples and the resulting changes in oil saturations. **Table 12** provides data on imbibition volumes of oil into different core samples during the aging process. The density of oil used to convert the weight to volume of oil imbibed was 0.7176 g/cc, which is the density measured at 180°F. Pore volume and change in oil saturation were calculated using equations 11-15:

$$V_{\text{core}} = \pi d^2 L / 4 \quad (\text{Eq. 11})$$

$$V_{\text{pore}} = V_{\text{core}} * \varphi \quad (\text{Eq. 12})$$

$$W_{\text{post-aging}} - W_{\text{pre-aging}} = W_{\text{oil,im}} \quad (\text{Eq. 13})$$

$$V_{\text{oil,im}} = W_{\text{oil,im}} / \rho_{\text{oil @ 180F}} \quad (\text{Eq. 14})$$

$$\Delta S_o = V_{\text{oil,im}} / V_{\text{pore}} \quad (\text{Eq. 15})$$

where

d = Diameter of the core

L = Length of the core

φ = Porosity

$W_{\text{post-aging}}$ = Weight of the rock after aging

$W_{\text{pre-aging}}$ = Weight of the rock before aging

$W_{\text{oil,im}}$ = Weight of oil imbibed into core during aging

$V_{\text{oil,im}}$ = Volume of oil imbibed into core during aging

$\rho_{\text{oil @ 180F}}$ = Density of oil at 180°F (aging temperature)

ΔS_o = Change in oil saturation due to aging

Table 12. Effect of aging process on core samples used for spontaneous imbibition

Sample	$W_{oil,im}$ (g)	$V_{oil,im}$ (ml)	V_{pore} (ml)	ΔS_o
1	1.04	1.44	3.59	40.3%
2	1.14	1.59	3.27	48.6%
3	1.16	1.61	3.19	50.4%
4	1.09	1.53	3.03	50.6%
5	1.05	1.46	3.33	43.9%
6	0.82	1.15	2.89	39.8%
7	0.45	0.63	1.60	39.3%
8	0.97	1.35	3.15	42.8%

The oil saturation of all samples changed by 40-50% indicating the oil could penetrate the cores and displace a gaseous phase as observed from the aging process. The nature of this gaseous phase could not be concluded upon as the mechanism for preserving the core samples was not known. The data provided for this well suggests that the reservoir rock had an initial oil saturation of 45.8%. This is added to the change in oil saturation due to aging to yield the initial oil saturation in the sample prior to conducting the spontaneous imbibition tests, S_{oi} , which is presented in **Table 13**. The assumption here is that the change in saturation is due to the replacement of trapped air/gas in core sample, which might have been a result of the coring and preservation process, by oil. This was also observed during the aging process when there was constant bubbling through the oil.



Figure 79. Release of air/gas bubbles during aging process

Table 13. Initial oil saturations of the core samples prior to imbibition

Sample	S _{oi}
1	86.1%
2	94.4%
3	96.2%
4	96.4%
5	89.6%
6	85.5%
7	85.05%
8	88.55%

3.6.4.2. Imbibition results

This section presents the imbibition results for brines and surfactants which include wettability changes, penetration of the fluids into cores and the associated oil recovery. The order of discussion of results same as listed before with wettability and IFT changes used to understand the penetration of fluids and oil recovery. Initial tests conducted with distilled water are also presented and discussed.

3.6.4.2.1. Distilled water

Distilled water was used as to serve as a reference point for imbibition studies. The results for water without any additives are presented in the following table. Water slightly altered the wettability of the rock though the final state remained intermediate wet.

Table 14. Results for imbibition test with distilled water

Fluid	IFT (mN/m)	Final contact angle (o)	Final penetration magnitude (Hounsfield Units)	Oil Recovery (%OOIP)
Water	34.03	85.3	8	1.9

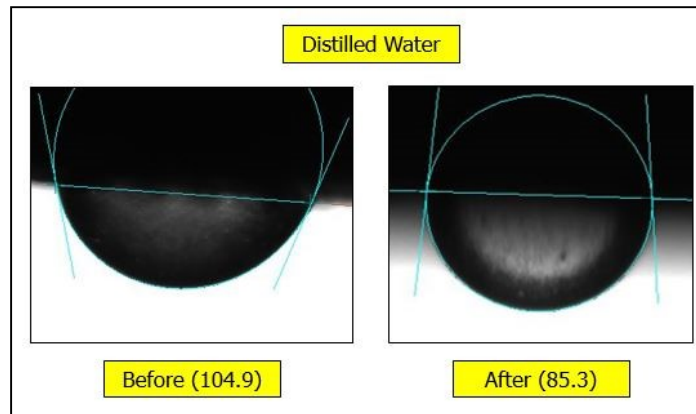


Figure 80. Contact angles measured before and after imbibition with water (values in the braces are the contact angles in degrees)

Penetration of distilled water into the rock water quantified by calculating the penetration magnitude based on the CT number data obtained from post processing as discussed in the procedure for these experiments. The penetration curve thus plotted is shown in the **Figure 81**. It can be observed that the penetration was steady over the course of the experiment though the magnitude was low. The ultimate penetration magnitude was found to be 8 HU meaning the overall CT number of the sample increased by 8 HU as the lower density oil phase was replaced by high density aqueous phase.

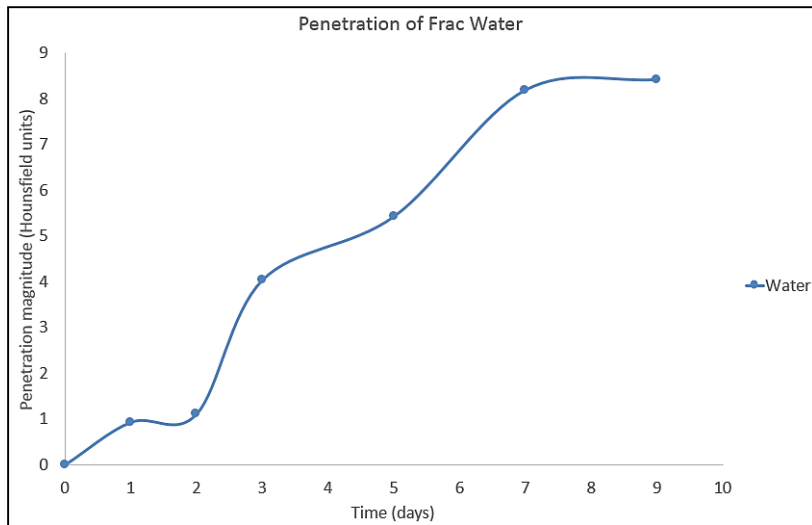


Figure 81. Penetration curve for distilled water

Movement of the imbibing fluid, i.e., distilled water was studied using the CT scans taken at various times as shown below. The purple portions in the circled region are the bedding planes along which the most noticeable changes occur. Hence it is safe to say the distilled water imbibed along the bedding planes to displace oil although the change between initial and final states is not significant.

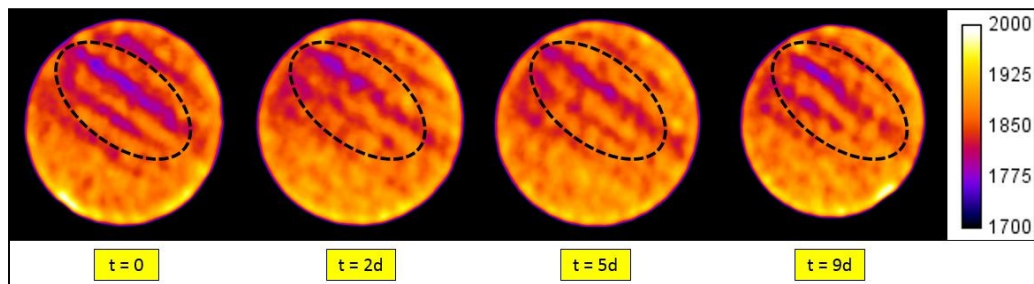


Figure 82. CT scans for distilled water imbibition (color scale for CT number shown to the right)

The oil recovery for distilled water is as shown in **Figure 83**. Oil was recovered over a period of 1 day beyond which no additional oil could be recovered. This is an indication that water distilled water was not able to penetrate deeper into the matrix thus recovering only oil from the periphery. Though penetration was increasing over time, the change in density is low implying the imbibing fluid could not displace the oil from pore throats due to high IFT and intermediate wet state. The ultimate recovery was 1.9% of the oil originally in place.

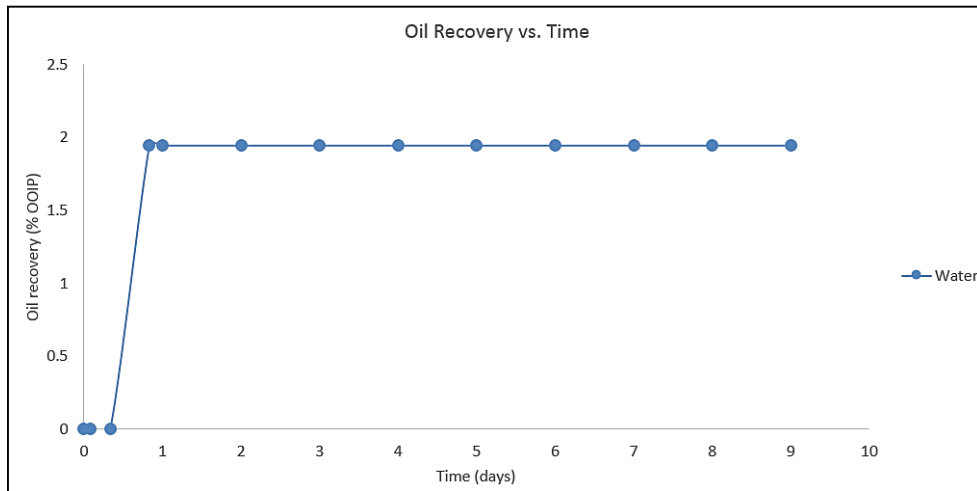


Figure 83. Oil recovery from distilled water imbibition

3.6.4.2.2. Brines

The objective of these experiments was to understand effectiveness of two brine solutions, 2.5 wt% sodium chloride and 5 wt% calcium chloride on imbibing into the rock matrix and displacing oil. These concentrations were chosen to be the optimum concentrations for promoting the maximum water wetness from contact angle experiments

as discussed earlier. Sodium chloride produced a more water wet state while calcium chloride produced a lower IFT compared to sodium chloride brine as also observed earlier. Thus the imbibition results from these experiments were intended to determine the dominant mechanism that aids fluid penetration into the samples. The results for imbibition experiments are summarized in **Table 15**.

Table 15. Results for brine imbibition tests

Fluid	IFT (mN/m)	Final contact angle (θ)	Final penetration magnitude (Hounsfield Units)	Oil Recovery (%OOIP)
2.5 wt% NaCl	31.57	41.1	14	8.1
5 wt% CaCl ₂ .2H ₂ O	29.33	44.8	12	7.3

84 and 85 show the contact angle measured on the flat side the core sample used for imbibition tests. Two readings were taken before and after the experiment and as can be observed, both the salts, altered the wettability from an initial intermediate wet to a water wet. Sodium chloride produced a slightly lower contact angle meaning more water wetness.

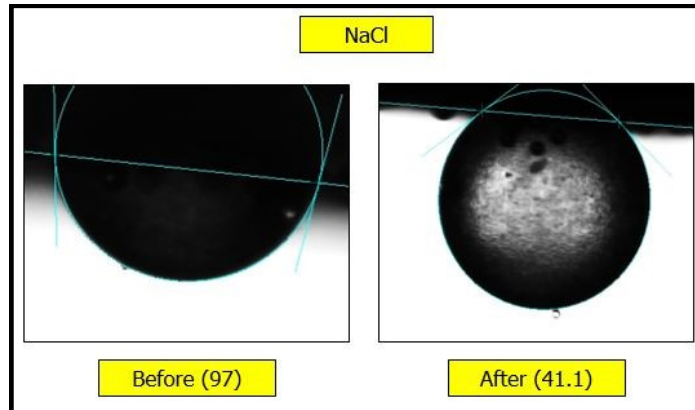


Figure 84. Contact angles measured before and after imbibition with sodium chloride (values in the braces are the contact angles in degrees)

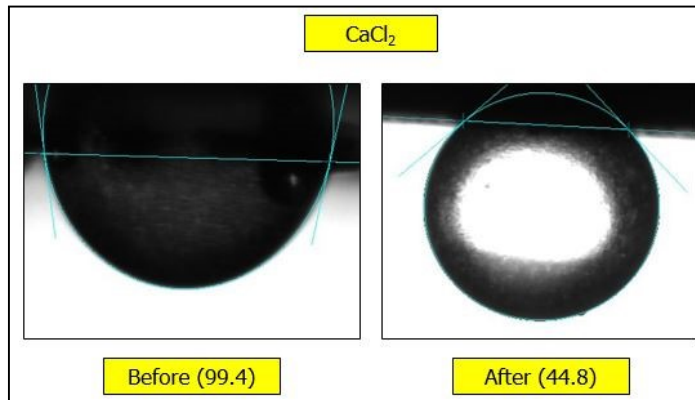


Figure 85. Contact angles measured before and after imbibition with calcium chloride (values in the braces are the contact angles in degrees)

The following graphics depict the penetration magnitude and oil recovery. As is evident from these curves, sodium chloride penetrated the most into the rock followed by calcium chloride. The final penetration for sodium chloride was almost twice as that of water. It is clearly evident that brines penetrated much better than water implying alteration of wettability plays a major role in improving the penetration of fluid into the rock matrix.

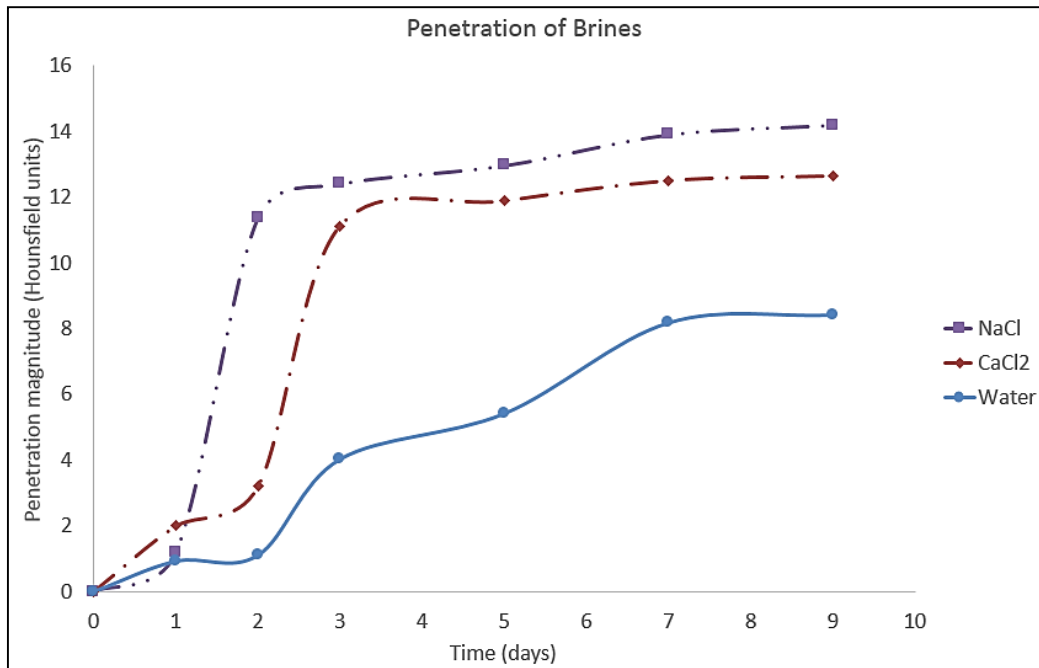


Figure 86. Penetration curves for brine and distilled water

As can be seen in **Figure 86**, calcium chloride penetrated faster initially compared to sodium chloride. This is probably due to the lower oil/brine IFT values produced by calcium chloride which help the fluid to penetrate faster into the rock matrix. However, as time progressed, sodium chloride penetrated faster implying capillary forces started to dominate. The low penetration of water at the same time signifies the importance of altering wettability for improved penetration.

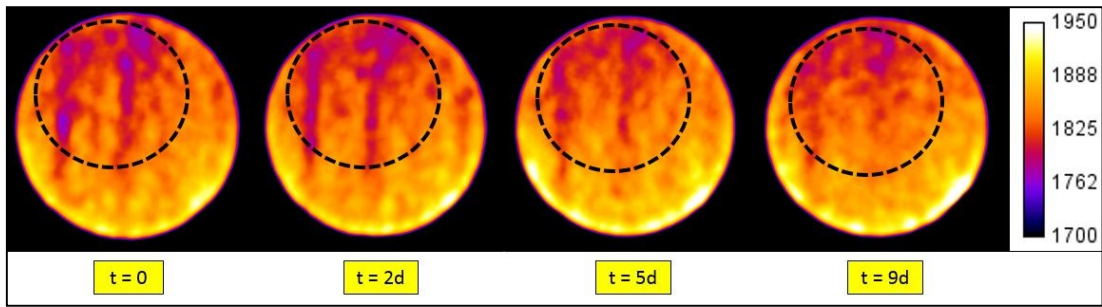


Figure 87. CT scans for sodium chloride brine imbibition (color scale for CT number shown to the right)

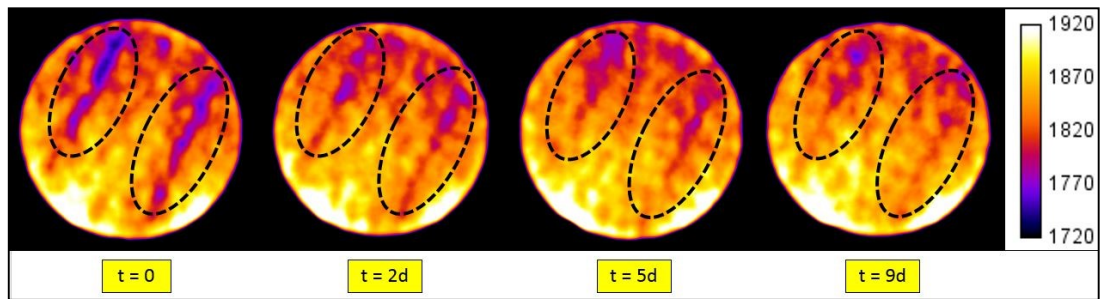


Figure 88. CT scans for calcium chloride brine imbibition (color scale for CT number shown to the right)

As indicated from the CT scans in **Figures 87-88**, imbibition occurred along the bedding planes shown in the circled regions similar to distilled water. However, salts were able to alter the wetting nature of the rock thereby imbibing better along these planes and displacing more oil as low density purple zones are replaced by higher density orange and yellow zones. However, it is also important to note that these images do not completely reflect the imbibition profiles of fluids as the assigned color is an average value calculated for a pixel while many mechanisms such as clay swelling and rock dissolution take place at the micro level that may not be captured by the CT scanner.

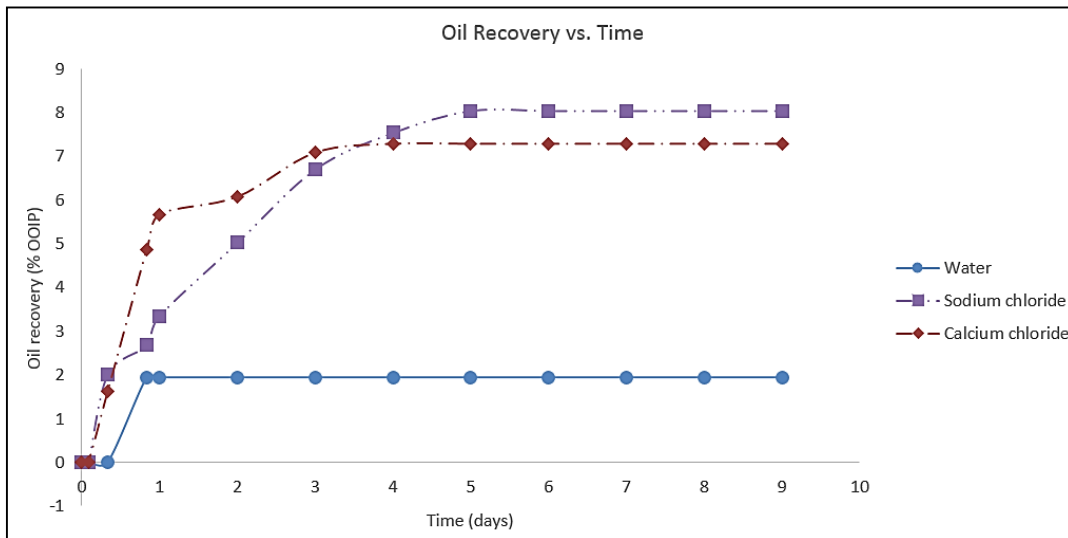


Figure 89. Oil recovery for brine and distilled water from imbibition experiments

Recovery curves (**Figure 89**) suggest both the salts were able to recover more oil than distilled water. Besides, the recovery curves for the salts did not flatten out as fast as the curve for water implying the brine were able to penetrate deeper into the rock matrix and drive more oil out as time progressed. Thus as the wettability of the rock is altered, the fluid penetrates deeper into the rock and displaces the oil in place. Reduction in oil/brine IFT seems to improve the penetration in the early stages while capillary imbibition seems to dominate the ultimate recovery. This is understandable as moderate to high IFT values improve the recovery from ultra-low permeability reservoirs where capillary imbibition plays a significant role. The nature of oil recovered from both the experiments seems to vary as observed from their color (as shown below) as well as gas

chromatography results. The gas chromatographic analysis was performed on Agilent 6890A GC device with an attached 5972 HP Mass Selective Detector (MSD) probe. Chemstation software was used to process the results. The oil sample was diluted using dichloromethane and 1 μ L of this diluted solution was added to the gas chromatography device. Lighter components in oil could not be captured while recovering the samples for chromatographic analysis.

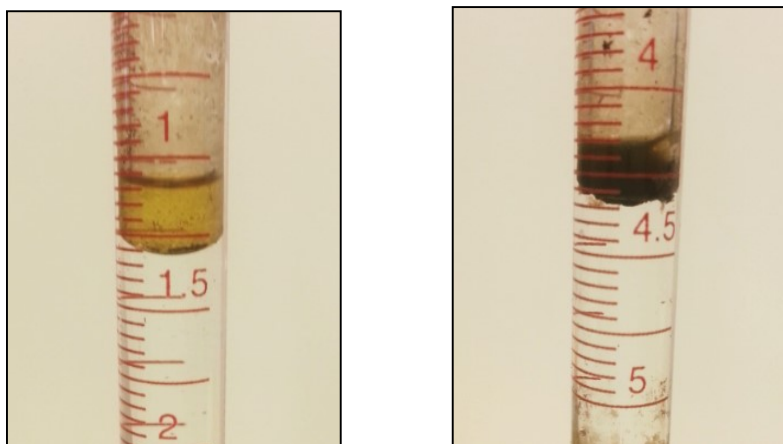


Figure 90. Oil recovered from sodium chloride (left) and calcium chloride (right) brine imbibition

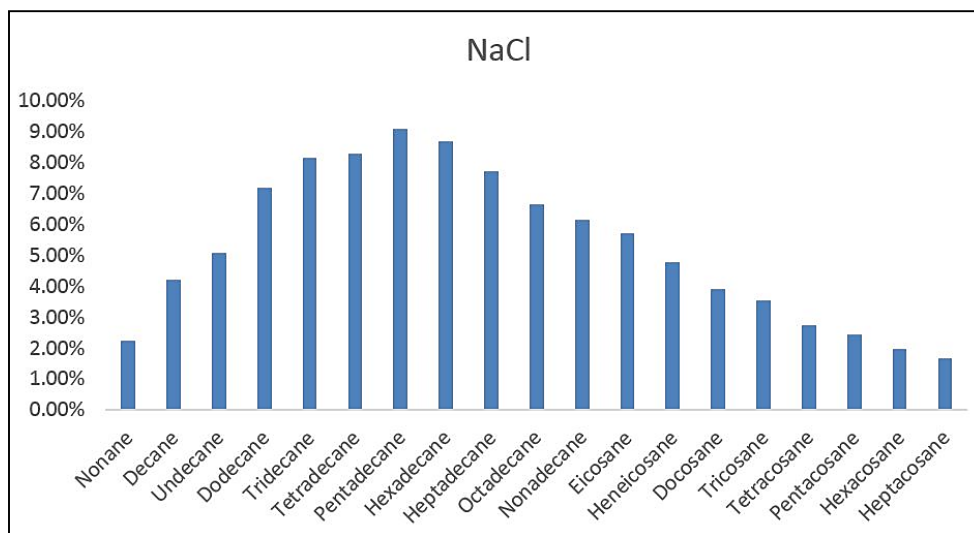


Figure 91. Gas chromatograph of oil recovered from sodium chloride brine imbibition

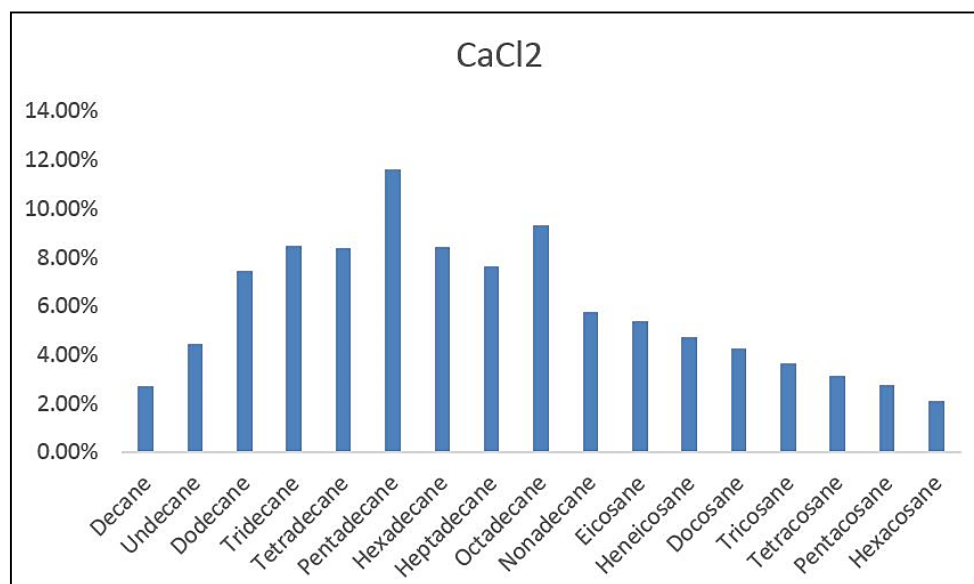


Figure 92. Gas chromatograph of oil recovered from calcium chloride brine imbibition

The gas chromatograph (**Figure 92**) implies sodium chloride brine could recover a wider range of hydrocarbon groups (C9 – C27) compared to calcium chloride brine (C10 – C26). The dark color of oil obtained from calcium chloride is probably due to the tendency of calcium ion to form complexes with negatively charged surface active agents in crude though further experimentation may be needed to verify this.

Hence the experiments with brines helped conclude wettability alteration did play a major role in improving the fluid penetration and the resultant oil recovery from the shale samples examined. Lowering IFT led to faster imbibition in the early stages where the fluid has to overcome the boundary capillary effects which was followed by dominance of capillary imbibition as more oil was recovered for sodium chloride which promoted higher water wetness but higher IFT compared to calcium chloride.

Another set of imbibition studies was conducted using brines (2.5 wt% NaCl and 5 wt% CaCl₂.2H₂O) prepared without the dopant to verify the results obtained. The recovery curves obtained are shown in **Figure 93**. As observed, the results verify the superior performance of brines compared to distilled water. However, the difference in recoveries between sodium and calcium chloride brines was higher as sodium chloride recovered 11% and calcium chloride recovered 4.7% oil originally in place.

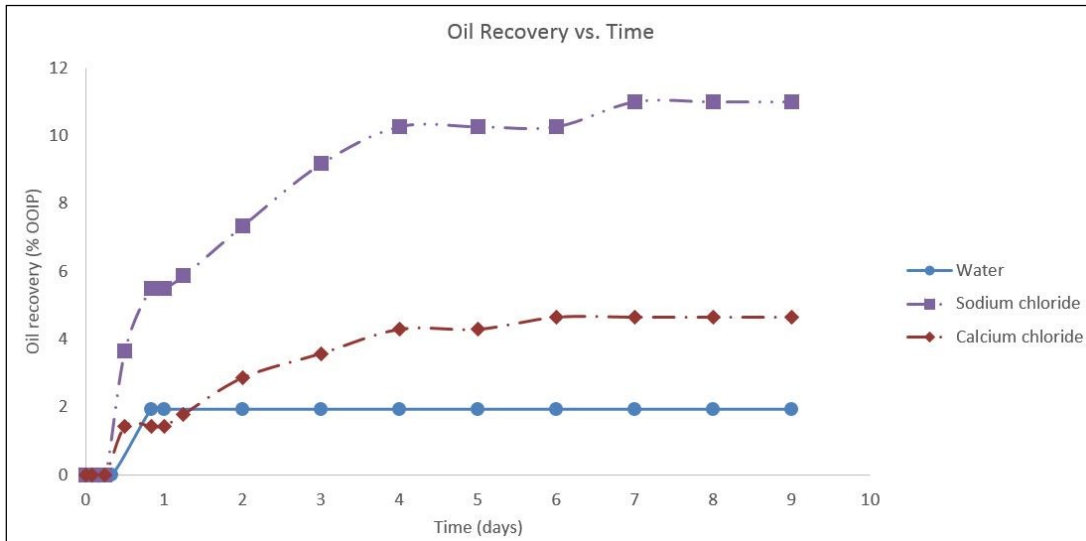


Figure 93. Oil recovery curves for brine imbibition without dopant addition

3.6.4.2.3. Surfactants

Three surfactants as mentioned earlier – anionic, nonionic and a complex surfactant were considered for imbibition studies. The surfactant concentration used was 3 gpt (3 ml per liter of solution) as it was established earlier that increasing surfactant concentration reduced the contact angle and decreased oil/water IFT. Besides, these concentration were found to be below the critical micellar concentrations, implying an increase in concentration leads to higher effect on contact angle and oil/water IFT. Solutions were prepared as shown in **Table 11**. Summary of results is provided in **Table 16**.

Table 16. Results for surfactant imbibition tests.

Fluid	IFT (mN/m)	Final contact angle (o)	Final penetration magnitude (Hounsfield Units)	Oil Recovery (%OOIP)
A1	2.89	39.2	13	3.3
N1	4.48	41.2	17	4.1
C1	7.25	77.5	11	2.8

Figures 94 and 95 depict the contact angle measured on the flat side the core sample used for imbibition tests. Two readings were taken before and after the experiment and as can be observed, all the surfactants altered the wettability from an initial oil/intermediate wet to a water wet. A1 produced a slightly lower contact angle meaning more water wetness followed by N1 and C1. The results for N1 and A1 are comparable but C1 performed poorly compared to anionic and nonionic counterparts as also indicated by contact angle experiments discussed earlier.

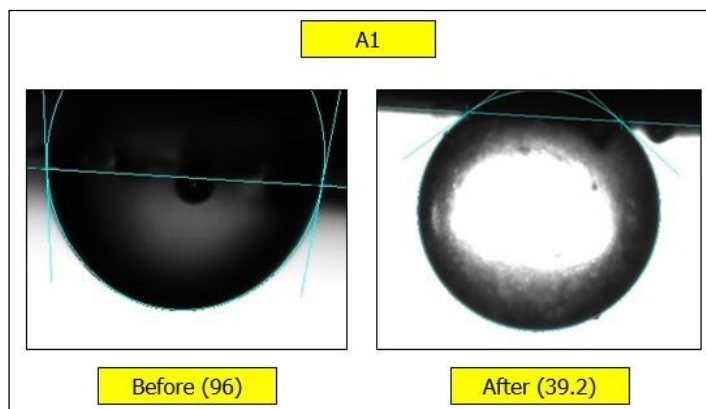


Figure 94. Contact angles measured before and after imbibition with surfactant A1 (values in the braces are the contact angles in degrees)

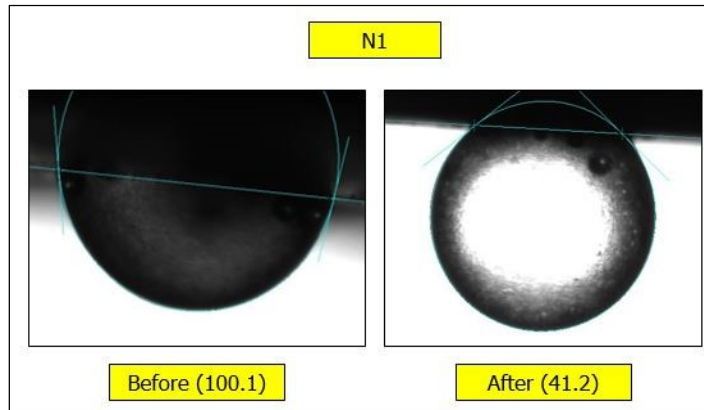


Figure 95. Contact angles measured before and after imbibition with surfactant N1 (values in the braces are the contact angles in degrees)

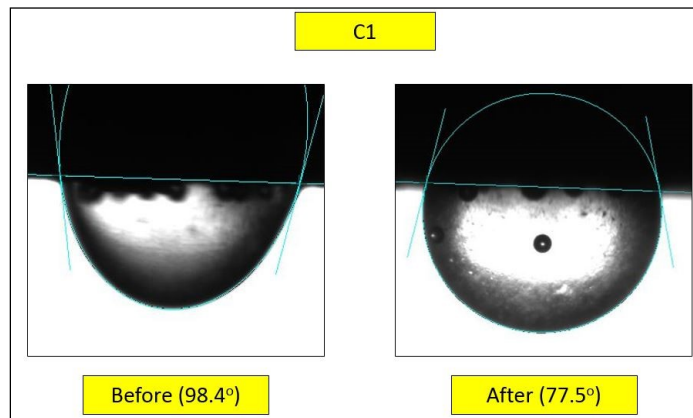


Figure 96. Contact angles measured before and after imbibition with surfactant C1 (values in the braces are the contact angles in degrees)

Penetration magnitude was calculated and plotted as a function of time as shown in **Figure 97**. The anionic surfactant showed higher initial penetration owing to the lower IFT but the ultimate penetration was more nonionic surfactant with a higher IFT signifying the importance of capillary forces in imbibition. Besides, the charge of the surfactant is also estimated to have played a key role as negatively charged anionic surfactant faces

more repulsion from the host rock surface compared to the nonionic surfactant. The complex surfactant performed better than water but poorly compared to the other two surfactants as is expected due to its lesser capacity to promote a water wet state on the rock considered.

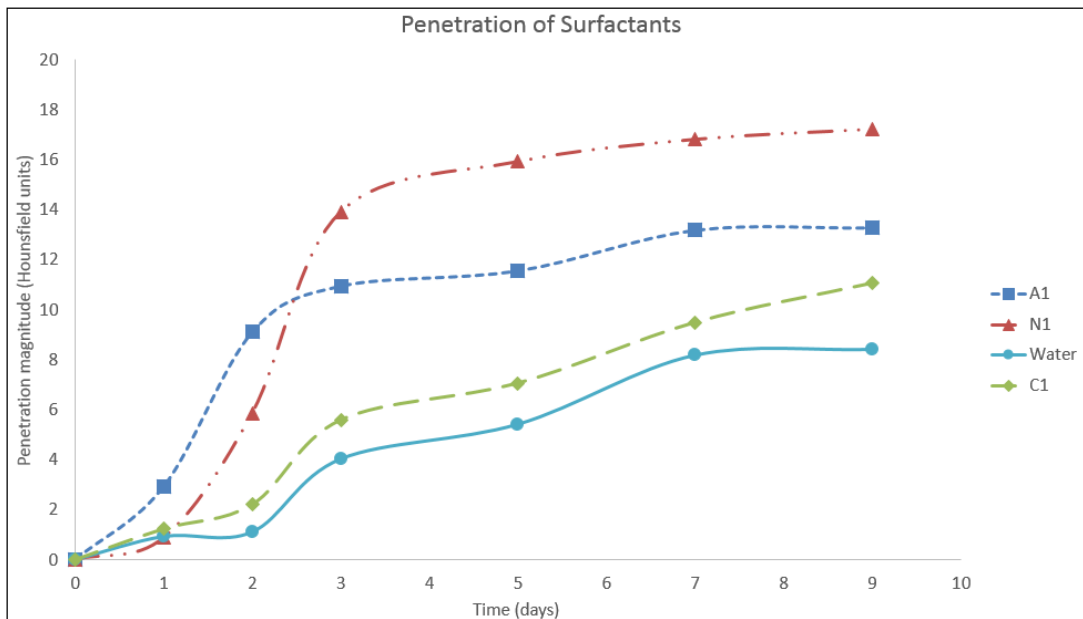


Figure 97. Penetration curves for surfactants and distilled water

CT scans were taken at various time intervals and the images were processed to observe changes in the bulk density and fluid distribution profiles. The following figures show CT images for anionic, nonionic and complex surfactants at various time intervals.

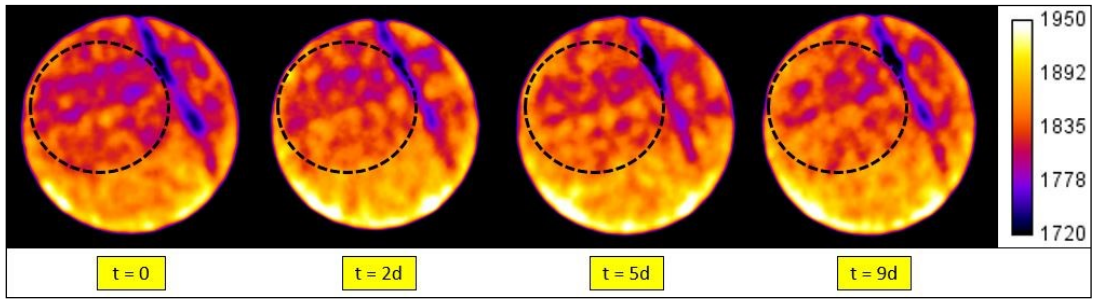


Figure 98. CT scans for surfactant A1 imbibition (color scale for CT number shown to the right)

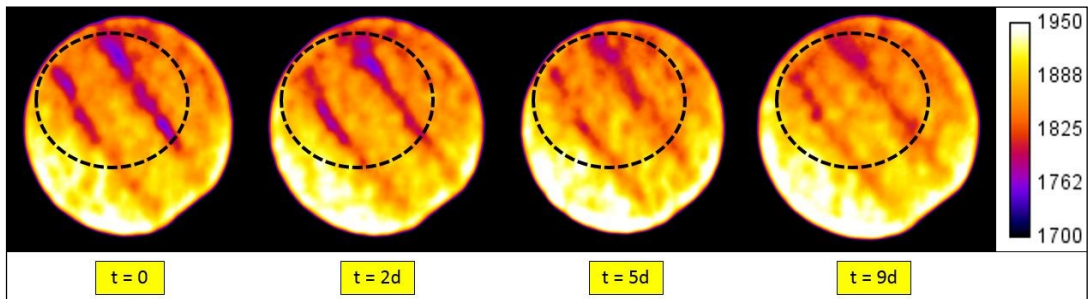


Figure 99. CT scans for surfactant N1 imbibition (color scale for CT number shown to the right)

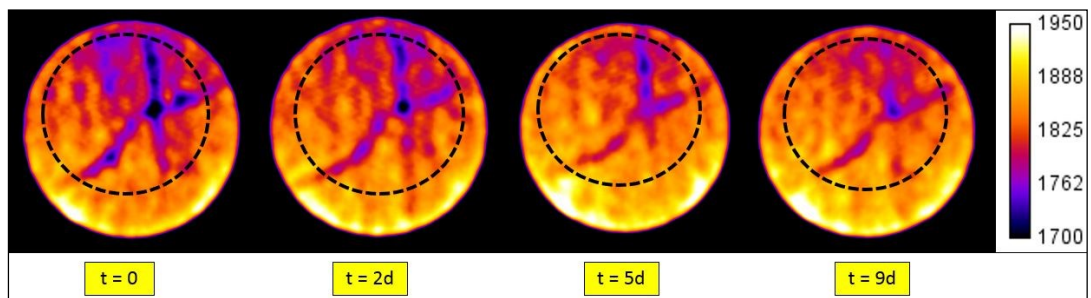


Figure 100. CT scans for surfactant C1 imbibition (color scale for CT number shown to the right)

Observing the circled regions of the scans in all the three cases, visible changes are evident going from 0 to 9 days as dark purple regions transform into yellowish orange

implying the increase in density of the sample. This is due to the replacement of high density surfactant solution with lower density oil. In some cases, the increase in density may also be due to formation of an in situ emulsion which does not necessarily mean recovery of oil from the sample. Such is estimated to be the case with the complex surfactant C1 which produces noticeable change in the circled region but produces less oil compared to the other two surfactants. Besides, various other factors like clay swelling and micro fractures opening may decrease the overall CT number but increase oil recovery. Thus penetration magnitude may not directly be related to oil recovery.

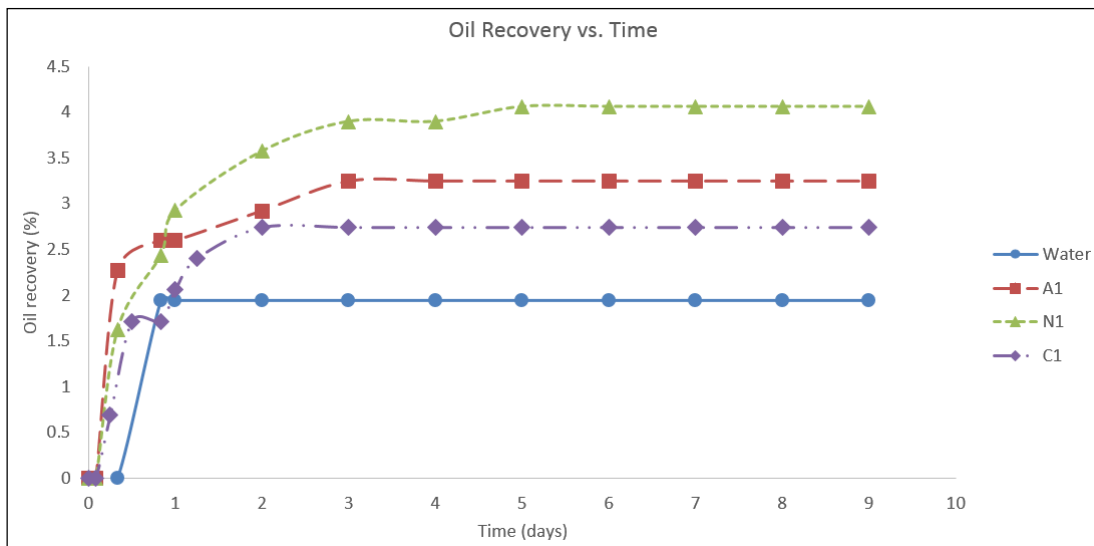


Figure 101. Oil recovery for surfactants and distilled water from imbibition experiments

Figure 101 shows the recovery curves obtained from spontaneous imbibition experiments conducted with surfactants and water. As is evident from the graph, surfactants showed superior performance compared to distilled water as expected due to

their higher penetration into the rock matrix as verified by CT scans. Hence altering the wettability of the rock played a key role in improving the imbibing fluid performance and led to higher oil recovery. Anionic surfactant A1 produced faster initially due to the low IFT and higher penetration as capillary imbibition started to dominate and N1 started producing more oil after 1 day. The production fell flat beyond 5 days suggesting that the most of the penetration takes place in the first few days beyond which the imbibition effect is significantly lower. Comparing the performance of the surfactants, it can be understood lowering the IFT too much does not guarantee higher recovery as nonionic surfactant produced more oil compared to anionic and complex surfactants. The poor performance of complex surfactant is due to its inability to promote a strong water wet state as the other two surfactants. However, all the surfactants could alter the nature of the rock towards more water wet which improved oil recovery compared to the base distilled water case.

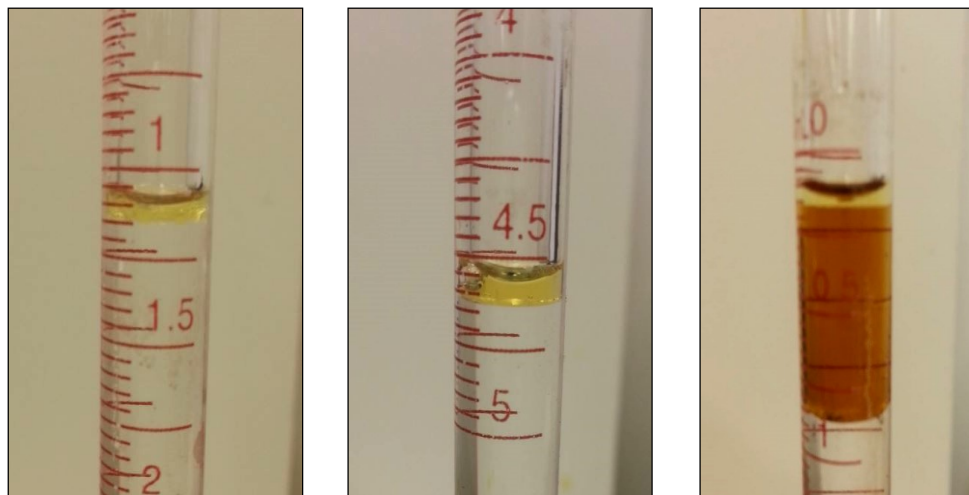


Figure 102. Oil recovered from surfactant A1 (left), N1 (middle) and C1 (right) brine imbibition

4. CONCLUSIONS AND RECOMMENDATIONS

4.1. Conclusions

This work aimed at analyzing the effectiveness of a monovalent sodium chloride and a divalent calcium chloride salt as well as three surfactants – anionic, nonionic and a complex surfactant in altering the surface characteristics of an organic liquid rich shale rock in addition to evaluating their potential as fracture fluid additives to improve oil recovery from these unconventional reservoirs. This study began with measuring the contact angles of rock chips to assess wettability changes followed by interfacial tension measurements at the crude oil/brine interface. These were followed by zeta potential measurements to gather insights on the stability of wetting films on the rock and oil surfaces that helped understand the mechanism of wetting changes and surface interactions. Finally, the work concluded with conducting spontaneous imbibition experiments to measure oil recovery and analyze penetration of the imbibing fluids into the rock matrix. Based on the experimental evidence and understanding, the following conclusions were reached:

- a) Measuring contact angle of the rock samples using distilled water, which is assumed to be base stimulation fluid in this study, suggested the rock is intermediate wet before any additives were added.
- b) Both sodium and calcium chloride were effective in altering the wettability towards more water wet with the water wetness reaching a maximum at an optimum salinity. At this optimum salinity, sodium chloride was found to promote a more water wet state than calcium chloride. However, with increasing

concentration, the rock surface behavior tends to shift towards preferably oil wet. This is probably due to salting out effect which promotes the movement of polar surface active agents in crude towards the rock/brine interface.

- c) Increasing salt concentration decreased the interfacial tension at the crude oil/brine interface for both the salts as calcium chloride produced lower IFT values than sodium chloride at all the tested concentrations.
- d) Zeta potential measurements suggest the rock surface was initially negatively charged. Addition of salts reduces this negativity and alters the stability of thin films on the rock. Sodium chloride formed stable films at low salinities while calcium chloride forms weak brine films compared to sodium chloride and distilled water.
- e) Double layer expansion does not completely explain the changes in wettability due to salt addition as the brine films were weaker than distilled water films. This led to the conclusion that other factors such as multicomponent ion exchange, ion substitution with clays and desorption of polar crude components from the rock due to the alteration of surface charge of rock or oil also play a defining role in shaping the wettability of the host rock surface.
- f) All the surfactants were effective in altering the wettability of the rock towards more water wet and reducing oil/water IFT at the three concentrations tested. Water wetness improved with increasing surfactant concentration except for the complex surfactant.

- g) Anionic surfactant A1 was found to be more effective in terms of wettability alteration and IFT reduction followed by N1 and finally C1. Zeta potential results also verify this observation as A1 formed the most stable films on rock surface followed by N1 and C1. The film stability also increased with increasing surfactant concentration. However, C1 formed the most stable films on oil droplets which implies the hydrophilic part of this surfactant may be positive as opposed to the other two that have negatively and neutrally charged heads.
- h) Spontaneous imbibition experiments with brines suggested that the brines were more effective than distilled water in both penetrating as well as recovering more oil from the unconventional rock samples used. Visible changes were observed from the CT images which suggested higher penetration for brines compared to distilled water. Hence wettability alteration was found to be beneficial in improving the oil recovery.
- i) Sodium chloride brine was found to be more effective in penetrating the rock and improving the oil recovery compared to calcium chloride brine suggesting wettability alteration played a more significant role than IFT reduction in the tight shale samples which is probably due to the dominance of capillary force driven imbibition.
- j) Surfactants were able to penetrate the rock better than distilled water and improve the oil recovery. Initial penetration was higher for the anionic surfactant which is due to the low IFT it produced. However, as time progressed, capillary forces played a dominating role in penetration of surfactant fluid into the rock matrix.

- k) Nonionic surfactant showed highest recovery among the surfactants as it also penetrated the most into the rock matrix. These results verify the importance of maintain a low to moderate IFT in ultra-low permeability rocks where capillary imbibition plays a major role in deciding the ultimate oil recovery.

4.2. Recommendations

The experiments conducted in this study are among the first steps in creating a workflow to tailor high performance stimulating fluids that alter the rock surface to produce more oil. As with every study involving unconventional rocks, the uncertainty is high and hence a robust understanding of rock/fluid and oil/fluid interactions is paramount. The following recommendations are thus put forward to improve this workflow as well as upscale it to pilot/field scale:

- a) Dean Stark procedure can be followed to obtain a clear picture of initial saturations in the core samples as shale being very heterogeneous, the sample saturations may vary from depth to depth.
- b) Oil-surfactant emulsion stability can be studied in further detail to analyze the effect of emulsions forming in situ on the rheological behavior of the imbibing fluid and thus the ultimate oil recovery.
- c) Pressure support could be utilized to reach higher temperatures while measuring surface changes and during spontaneous imbibition.

- d) CT number of the rock can be measured using dry core, which could further be used to track changes in oil and water saturations to obtain imbibition curves for relative permeability models.
- e) Coreflooding at reservoir temperature and pressure could be carried out to test the effectiveness of salts and surfactants in recovering additional oil and reflect conditions closer to the field case.
- f) Reservoir simulation can be carried out using the relative permeabilities obtained from imbibition tests as well as micro fracture propagation models. Huff and puff schemes can be tested to account for and analyze the imbibition of fluid from fractures into the rock matrix.
- g) Various formations with different lithology can be tested using a similar workflow to understand the effectiveness of monovalent/divalent brines as well as surfactants on altering rock wettability and improving oil recovery.

REFERENCES

- Abdel-Wali, A.A., 1996. Effect of Simple Polar Compounds and Salinity on Interfacial Tension and Wettability of Rock/Oil/Brine System. *Journal of King Saud University, Engineering Science* (2), Vol. **8**: 153 – 163.
- Abdallah, W. *et al*, 2007. Fundamentals of Wettability. *Schlumberger Oilfield Review*, summer 2007.
- Abe, A.A., 2005. Relative Permeability and Wettability Implications of Dilute Surfactants at Reservoir Conditions. MS Thesis, Idaho State University, Idaho, USA, May 2004.
- Adams, W.T. and Schievelbein, V.H., 1987. Surfactant Flooding Carbonate Reservoirs. *SPE Reservoir Engineering*, November 1987, pp. 619 – 626.
- Adejare, O.O, Nasralla, R.A. and Nasr-El-Din, H.A., 2012. A Procedure for Measuring Contact Angles When Surfactants Reduce the Interfacial Tension and Cause Oil Droplets to Spread. Paper SPE 160876 presented at the SPE Saudi Arabia Section Technical Symposium and Exhibition, Al-Khobar, Saudi Arabia, 6 – 11 April.
- Akin, S. and Kovscek, A.R., 2003. Computed Tomography in Petroleum Engineering Research. Applications of Computerized X-Ray Tomography in Geology and Related Domains **215**: 23 – 38.
- AlShaikh, M and Mahadevan, J., 2014. Impact of Brine Composition on Carbonate Wettability: A Sensitivity Study. Paper SPE 172187-MS presented at the SPE Saudi

Arabia Section Annual Technical Symposium and Exhibition, Al-Khobar, Saudi Arabia, 21 – 24 April.

Alotaibi, M.B. and Nasr-El-Din, H.A., 2009. Effect of Brine Salinity on Reservoir Fluids Interfacial Tension. Paper SPE 121569 presented at the 2009 SPE EUROPEC/EAGE Annual Conference and Exhibition, Amsterdam, The Netherlands, 8 – 11 June.

Alvarez, J.O. *et al*, 2014. Impact of Surfactants for Wettability Alteration in stimulation Fluids and the Potential for Surfactant EOR in Unconventional Liquid Reservoirs. Paper SPE 169001-MS presented at the SPE Unconventional Resources Conference, Woodlands, Texas, USA, 1 – 3 April.

Anderson, W.G., 1986. Wettability Literature Survey – Part 1: Rock/Oil/Brine Interactions and the Effect of Core Handling on Wettability. *Journal of Petroleum Technology*, November 1986, pp 1125 – 1144.

Austad, T., Matre, B. and Milner, J., 1998. Chemical Flooding of Oil Reservoirs 8: Spontaneous Oil Expulsion from Oil and Water Wet low Permeability Chalk Material by Aqueous Surfactant Solutions. *Colloids and Surfaces A: Physicochemical and Engineering Aspects* **137** (1 – 3): 117 – 129.

Babadagli, T., 2003. Analysis of Oil Recovery by Spontaneous Imbibition of Surfactant Solution. Paper SPE 84866 presented at SPE International Improved Oil Recovery Conference in Asia Pacific, Kuala Lumpur, Malaysia, 20 – 21 October.

Bai, J. *et al*, 2010. Influence of Interaction between Heavy Oil Components and Petroleum Sulfonate on the Oil – Water Interfacial Tension. *Journal of Dispersion Science and Technology*, **2010**, **31**: 551 – 556.

- Brady, P.V., Krumhansi, J.L. and Mariner, P.E., 2012. Surface Complexation Modeling for Improved Oil Recovery. Paper SPE 153744 presented at The Eighteenth SPE Improved Oil Recovery Symposium, Tulsa, Oklahoma, USA, April 14 – 18.
- Brown, C.E. and Neustadter, E.L., 1980. The Wettability of Oil/Water/Silica Systems with Reference to Oil Recovery. *Canadian Journal of Petroleum Technology* **19** (3): 100 – 110.
- Buckley, J.S., 2001. Effective wettability of minerals exposed to crude oil. *Current Opinion in Colloid and Interfacial Science* **6** (3): 191 – 196.
- Cai, B., Yang, J. and Guo, T., 1996. Interfacial Tension of Hydrocarbon + Water/Brine Systems under High Pressure. *Journal of Chemical and Engineering Data* **41**(3): 493 – 496.
- Chen, H.L. *et al*, 2000. Laboratory Monitoring of Surfactant Imbibition Using Computerized Tomography. Paper presented at the SPE International Petroleum Conference and Exhibition, Villahermosa, Mexico. DOI: 10.2118/59006-MS.
- Chen, L. *et al*, 2014. Zeta potential of limenstone in a large range of salinity. *Colloids and Surfaces A: Pysiochemal and Engineering Aspects*, **450**: 1 – 8.
- Craig, F.F., 1971. *The Reservoir Engineering Aspects of Waterflooding* **3** (1971).
- Cuie, L., 1984. Rock/Crude Oil Interactions and Wettability: An Attempt to Understand their Interrelation. Paper SPE 13211 presented at the 1984 SPE Annual Technical Conference and Exhibition, Houston, 16 – 19 September.
- Denekas, M.O., Mattax, C.C. and Davis, G.T., 1959. Effects of Crude Oil Components on Rock Wettability. *AIME* **216**: 330 – 333.

- Dong, H., Yong, Y and Rui, W., 2006. The Effect of Wettability on Oil Recovery of Alkaline/Surfactant/Polymer Flooding. Paper SPE 102564 presented at the SPE 2006 Annual Technical Conference and Exhibition, San Antonio, Texas, USA, 24 – 27 September.
- Fitzgerald, T., 2013. Frackonomics: Some Economics of Hydraulic Fracturing. *Case Western Reserve Law Review* **63** (4): 1337 – 1362.
- Glover, P., 2001. Wettability. Formation Evaluation MSc. Course Notes. Quebec, Canada.
- Gupta, R. and Mohanty, K.K., 2008. Wettability Alteration of Fractured Carbonate Reservoirs. Paper SPE 113407 presented at the SPE/DOE Symposium on Improved Oil Recovery, Tulsa, Oklahoma, USA, 19 – 23 April.
- Hirasaki, G.J., 1991. Wettability Fundamentals and Surface Forces. *SPE Formation Evaluation*, **June 1991**: 217 – 226.
- Jennings, H.Y., 1957. Surface Properties of Natural and Synthetic Porous Media. *Producers Monthly* **21**(5): 20 – 24.
- Johansen, R.T. and Dunning, H.N., 1961. Relative Wetting Tendencies of Crude Oil by Capillarimetric Method. *Producers Monthly* **23**(11): 20 – 22.
- Kathel, P and Mohanty, K.K., 2013. EOR in Tight Oil Reservoirs through Wettability Alteration. Paper SPE 166281 presented at the SPE Annual Technical Conference and Exhibition, New Orleans, Louisiana, 30 September – 2 October.
- Kwak, H.T., Yousef, A.A and Al-Saleh, S, 2014. New Insights on the Role of Multivalent Ions in Water – Carbonate Rock Interactions. Paper SPE 169112-MS

presented at the SPE Improved Oil Recovery Symposium, Tulsa, Oklahoma, 12 – 15 April.

Lager, A. *et al*, 2008. Low salinity oil recovery – an experimental investigation. *Petrophysics Journal* **49**: 28 – 35.

Lashkarboloki, M, Ayatollahi, S. and Riazi, M., 2014. The Impacts of Aqueous Ions on Interfacial Tension and Wettability of an Asphaltenic – Acidic Crude Oil Reservoir during Smart Water Injection. *Journal of Chemical and Engineering Data*, **2014**, **59**: 3624 – 3634.

Lohne, A and Fjelde, I., 2012. Surfactant Flooding in Heterogeneous Formations. Paper SPE 154178 presented at the Eighteenth SPE Improved Oil Recovery Symposium, Tulsa, Oklahoma, 14 – 18 April.

Martavaltzi, C. *et al*, 2012. Wettability Alteration of Carbonates by Optimizing the Brine and Surfactant Composition. Paper SPE 163348 presented at the SPE Kuwait International Petroleum Conference and Exhibition, Kuwait City, Kuwait, 10 – 12 December.

Mattax, C.C. and KYTE, J.R., 1962. Imbibition Oil Recovery from Fractured, Water – Driven Reservoirs. *SPEJ* **2**: 177 – 184.

Minssieux, L., 1987. Surfactant Flooding with Hard Water: A Case Study Solved by HLB Gradient. *SPE Reservoir Engineering* **2**(4): 605 – 612.

Moeini, F. *et al*, 2014. Towards mechanistic understanding of heavy crude oil/brine interfacial tension: The roles of salinity, temperature and pressure. *Fluid Phase Equilibria*, **2014**, **375**: 191 – 200.

Morrow, N.R., Cram, P.J. and McCaffery, F.G., 1973. Displacement Studies in Dolomite with Wettability Control by Octanoic Acid. *SPEJ* **13**(4): 221 – 232.

Morsy, S, Sheng, J.J and Soliman, M.Y., 2013. Waterflooding in the Eagle Ford Shale Formation: Experimental and Simulation Study. Paper SPE 167056 presented at the SPE Unconventional Resources Conference and Exhibition – Asia Pacific, Brisbane, Australia, 11 – 13 November.

Morsy, S and Sheng, J.J., 2014. Effect of Water Salinity on Shale reservoir Productivity. *Advances in Petroleum Exploration and Development* **8**(1): 9 – 14.

Myint, P.C. and Firoozabadi, A., 2015. Thin liquid films in improved oil recovery from low – salinity brine. *Current Opinion in Colloid and Interfacial Science*, 2015, in press.

Nasralla, R.A., Bataweel, M.A. and Nasr-El-Din, H.A., 2011. Investigation of Wettability Alteration by Low Salinity Water in Sandstone Rock. Paper SPE 146322 presented at the SPE Offshore Europe Oil and Gas Conference and Exhibition, Aberdeen, Scotland, UK, 6 – 8 September.

Nasralla, R.A. and Nasr-El-Din, H.A., 2012. Double – Layer Expansion: Is it a Primary Mechanism of Improved Oil Recovery by Low Salinity Waterflooding? Paper SPE 154334 presented at the SPE Improved Oil Recovery Symposium, Tulsa, Oklahoma, 14 – 18 April.

Nasralla, R.A. *et al*, 2014. Demonstrating the Ability of Low – Salinity Waterflood to Improve Oil Recovery in Carbonate Reservoirs by Qualitative Waterflood. Paper SPE 172010-MS presented at the Abu Dhabi International Petroleum Exhibition and Conference, Abu Dhabi, UAE, 10 – 13 November.

Neog, A., 2014. Investigating the Potential of Surfactants in Improving the Performance of Stimulation Fluids in Ultra – Tight Shales. MS Thesis, Texas A&M University, College Station, Texas, May 2014.

Nguyen, P., 2010. Regulatory Options & Challenges in Hydraulic Fracturing. A report prepared for ASME, Fort Worth, TX: Texas Christian University.

Odusina, E., Sondergeld, C. and Rai, C., 2011. An NMR Study on Shale Wettability. Paper SPE 147371 presented at the Canadian Unconventional Resources Conference, Calgary, Alberta, Canada, 15 – 17 November.

Okasha, M.T. and Abdul-Jalil, A., 2010. Effect of Temperature and Pressure on Interfacial Tension and Contact Angle of Khuff Gas Reservoir, Saudi Arabia. Paper SPE 136934 presented at the SPE/DGS Annual Technical Symposium and Exhibition, Al-Khobar, Saudi Arabia, 4 – 7 April.

Price, L.C., 1976. Aqueous Solubility of Petroleum as Applied to its Origin and Primary Migration. AAPG bulletin, **1976**, **60**: 213 – 244.

Passey, Q.R. *et al*, 2010. From oil-prone source rock to gas-producing shale reservoir – Geologic and petrophysical characterization of unconventional shale-gas reservoirs. Paper SPE 13150 presented at the CPS/SPE International Oil & Gas Conference and Exhibition, Beijing, China, 6 – 10 June.

Quan, X. *et al*, 2012. Investigation of Electrical Surface Charges and Wettability Alteration by Ions Matching Waterflooding. Paper presented at the International Symposium of the Society of Core Analysts, Aberdeen, Scotland, UK, 27 – 30 August.

- Salehi, M., Johnson, S.J. and Liang, J.T., 2008. Mechanistic Study of Wettability Alteration Using Surfactants with Applications in Naturally Fractured Reservoirs. *Langmuir* **24**(24): 14099 – 14107.
- Schechter, D.S., Zhou, D. and Orr, F.M., 1994. Low IFT drainage and imbibition. *Journal of Petroleum Science and Engineering* **11**(4): 283 – 300.
- Seethepalli, A., Adibhatla, B. and Mohanty, K.K., 2004. Wettability Alteration during Surfactant Flooding of Carbonate Reservoirs. Paper SPE 89423 presented at the SPE/DOE Symposium on Improved Oil Recovery, Tulsa, Oklahoma, 17 – 21 April.
- Seifert, W.K. and Howels, W.G., 1969. Interfacially Active Acids in California Crude Oil. *Analytical Chemistry* **41**(4): 554 – 562.
- Serrano Seldana, E., *et al*, 2004. Wettability of Solid/Brine/n-dodecane Systems: Experimental Study of the Effects of ionic Strength and Surfactant Concentration. *Colloids and Surfaces A: Physicochemical and Engineering Aspects* **241**: 343 – 349.
- Shuler, P. and Tang, Y.C., 2010. Chemical EOR Process for Bakken Shale. Paper presented at AAPG Annual Convention and Exhibition, New Orleans, Louisiana, April 11 – 14.
- Somasundaran, P. and Agar, G.E., 1967. The Zero Point of Charge of Calcite. *Colloid Interfacial Science* **24**(4): 433 – 440.
- Somasundaran, P., 1975. Interfacial Chemistry of Particulate Flotation. *Advances in Interfacial Phenomena of Particulate/Solution/gas Systems: Application to Flotation Research*, AIChE Symposium Series **71**(150): 1 – 15.

Stadness, D.C. and Austad, T., 2000. Wettability Alteration in Chalk 2: Mechanism for Wettability Alteration from Oil-Wet to Water-Wet Using Surfactants. *Journal of Petroleum Science and Engineering* **2000**: 123 – 143.

Standal, S. *et al*, 1999. Effect of polar organic components on wettability as studied by adsorption and contact angles. *Journal of Petroleum Science and Engineering* **24**: 131 – 144.

Staufer, C.E., 1965. The measurement of surface tension by the pendant drop technique. *The Journal of Physical Chemistry*, volume 69, pages 1933 – 1938.

Andreas, J.M., Hauser, E.A., Tucker, W.B., 1938. Boundary Tension by Pendant Drops. *The Journal of Physical Chemistry*, volume 42, pages 1001 – 1019.

Strumm, W. and Morgan, J.J., 1970. *Aquatic Chemistry*. New York City: J. Wiley and Sons.

Thyne, G., 2013. A review of the Measurement of Wettability in Shales. A report prepared for Sandia National Laboratory, Science based Solutions LLC.

Treiber, L.E., Archer, D.L. and Owens, W.W., 1972. A Laboratory Investigation of the Wettability of Fifty Oil Producing Reservoirs, *SPEJ* **6**: 531 – 540.

Vijapurapu, C.S. and Rao, D.N., 2003. Compositional Effects of Fluids Spreading, Adhesion and Wettability in Porous Media. *Colloids and Surfaces A: Physicochemical and Engineering Aspects* **241**: 335 – 342.

Wang, W. and Gupta, A., 1995. Investigation of the Effect of Temperature and Pressure on Wettability Using Modified Pendant Drop method. Paper SPE 30544 presented at the SPE Annual technical Conference and Exhibition, Dallas, U.S.A., 22 – 25 October.

Wang, D. *et al*, 2010. Flow Rate Behavior and Imbibition in Shale. Paper SPE 138521 presented at the SPE Eastern Regional Meeting, Morgantown, West Virginia, USA, 12 – 14 October.

Wang, D. *et al*, 2011. Surfactant Formulation Study for Bakken Shale Imbibition. Paper SPE 145510 presented at the SPE Annual technical Conference and Exhibition, Denver, Colorado, USA, 30 October – 2 November.

Wang, D. *et al*, 2012. Wettability Survey in Bakken Shale Using Surfactant Imbibition. Paper SPE 153853 presented at the eighteenth SPE Improved Oil Recovery Symposium, Tulsa, Oklahoma, USA, 14 – 18 April.

Weiss, W.W. and Xie, X., 2007. Oilfield Surfactants Improve Recovery by Imbibition. Paper SPE 106402 presented at the SPE International Symposium on Oilfield Chemistry, Houston, Texas, U.S.A., 28 February – 2 March.

Zekhri, A.Y., Ghannam, M.T. and Almehaideb, R.A., 2003. Carbonate Rocks Wettability Changes Induced by Microbial Solution. Paper SPE 80527 presented at the SPE Asia Pacific Oil and Gas Conference and Exhibition, Jakarta, Indonesia, 15 – 17 April.

Zhang, D., 2005. Surfactant-Enhanced Oil Recovery Process for a Fractured, Oil-Wet Carbonate Reservoir. PhD dissertation, Rice University, Houston, Texas, November 2005.

Zhang, P. and Austad, T., 2005. Waterflooding in Chalk – Relationship between Oil Recovery, New Wettability Index, Brine Composition and Cationic Wettability

Modifier. Paper SPE 94209 presented at the SPE EUROPEC/EAGE Annual conference, Madrid, Spain, 13 – 16 June.

Zhou, X., Morrow, N.R. and Ma, S., 2000. Interrelationship of Wettability, Initial Water Saturation, Aging Time and Oil Recovery by Spontaneous Imbibition and Waterflooding. *SPEJ* 5(2): 199 – 207.